A national laboratory of the U.S. Department of Energy
Office of Energy Efficiency & Renewable Energy

National Renewable Energy Laboratory

Innovation for Our Energy Future

Development of New Low-Cost, High-Performance, PV Module Encapsulant/Packaging Materials

Final Technical Progress Report
22 October 2002 – 15 November 2007

R. Tucker
Specialized Technology Resources, Inc.
Enfield, Connecticut

Subcontract Report
NREL/SR-520-43019
April 2008

NREL is operated by Midwest Research Institute • Battelle Contract No. DE-AC36-99-GO10337

Development of New Low-Cost, High-Performance, PV Module Encapsulant/Packaging Materials

Final Technical Progress Report
22 October 2002 – 15 November 2007

R. Tucker
Specialized Technology Resources, Inc.
Enfield, Connecticut

NREL Technical Monitor: Brian Keyes

Prepared under Subcontract No. ZDO-2-30628-10

Subcontract Report
NREL/SR-520-43019
April 2008

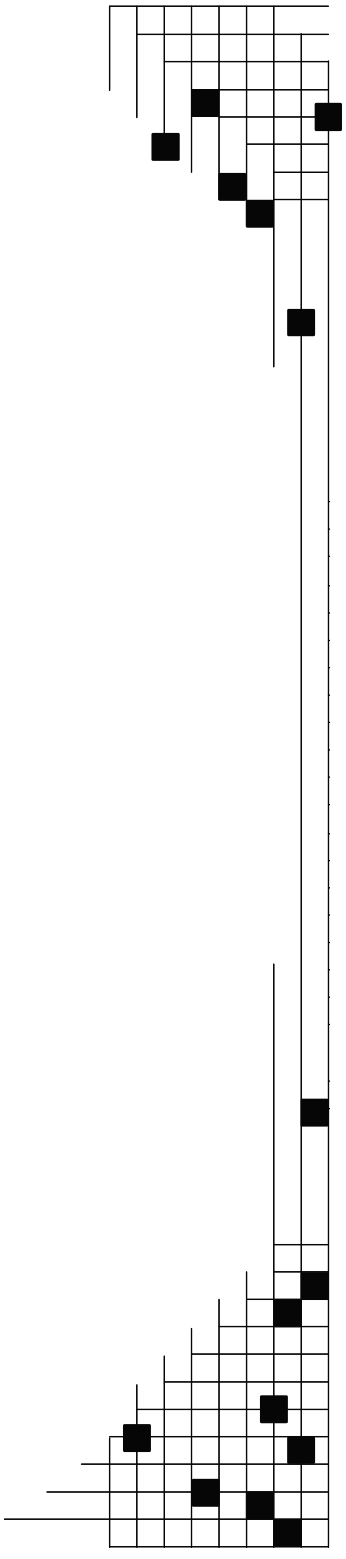

National Renewable Energy Laboratory
1617 Cole Boulevard, Golden, Colorado 80401-3393
303-275-3000 • www.nrel.gov

Operated for the U.S. Department of Energy
Office of Energy Efficiency and Renewable Energy
by Midwest Research Institute • Battelle

Contract No. DE-AC36-99-GO10337

PREFACE

The primary objectives of this subcontract were to work with US-based photovoltaic (PV) module manufacturers representing crystalline silicon, amorphous silicon, copper indium diselenide (CIS), and other state-of-the-art thin-film technologies to develop and qualify new low-cost, high-performance PV module encapsulant/packaging materials, as well as the module production processes that utilize the packaging materials. The manufacturers assisted in the identification of candidate materials' deficiencies while undergoing development, and then ultimately in the qualification of the final, optimized materials designed to specifically meet their requirements. Upon completion of this program, new low-cost, high-performance PV module encapsulant/packaging materials will be qualified, by one or more end-users, for their specific application. This document reports on progress toward these objectives and goals for the second phase of the three-phase subcontract.

ACKNOWLEDGMENTS

Specialized Technology Resources wishes to acknowledge the contributions of the following people and organizations:

- Specialized Technology Resources: S. Agro, D. Chianese, J. Haber, J. Galica, P. Moore, T. Smead, W. Tenero, R. Tucker, and D. Wells.
- University of Connecticut Institute of Material Sciences: H. Dewan and E. Kurz.
- BP Solar
- EPV
- National Renewable Energy Laboratory – Subcontract No. ZDO-2-30628-10
- Shell Solar
- Robert Kasowski, PN Solutions

TABLE OF CONTENTS

FIGURES AND TABLES

PHASE I

INTRODUCTION

The work performed during Phase I focused on three main objectives. The first of these objectives was to gather technical information on topics relevant to the scheduled Phase II encapsulant development work to be initiated under the second year of funding. The second was to gain an understanding of changes in interfacial chemistries within failed thin-film module technologies to hopefully gain insight into the surface chemistry of the interfacial regions of certain commercial modules. The third objective was to optimize both a super fast-cure and flame retardant formulation as a means of improving their processing performance during manufacture and within the overall module construction.

The majority of the first year effort involved optimizing two high performance encapsulant materials that were previously formulated by Specialized Technology Resources Inc. under BP Solarex subcontract ZAX-8-17647-05 awarded by DOE/NREL (1998-2001). The first encapsulant was a faster-curing (super fast-cure) EVA-based encapsulant and the second a flame-retardant (FR) formulation. Photovoltaic modules manufactured with the super fast-cure formulation could be laminated using a six (6) minute process[1,2]. The flame-retardant formulation allowed modules to meet the Class B flammability rating under UL 1703[1]. The Task 3 Effort under this Phase I contract addressed the optimization effort of “faster-curing” and “flame-retardant” EVA-based encapsulant systems with a focus on overcoming process shortcomings for manufacturing scale-up.

TASK 1: INFORMATION SEARCH FOR DEVELOPMENT OF THIN-FILM ENCAPSULANTS

The objective of the Task 1 information search was to identify research or technology pertinent to encapsulation. The following summary will identify issues and practices appearing in the literature that may prove instrumental to the development of new and improved encapsulant/packaging materials for thin film devices. The information search was implemented by the following two surveys.

- Module Manufacturers Survey
- Literature Survey

Significant findings from each of the two surveys are organized by survey type, then information category

Module Manufacturer Survey

STR made individual site visits and conducted interviews of the module manufacturer technical staff to understand the current reliability issues associated with the specific thin film technologies. BP Solar, Shell Solar, and Energy Photovoltaics, Inc. were participating team members. The visits contained an exchange in some cases of proprietary information. Following is a summary of the major unclassified findings of all of the team members on the following topics: Module Attributes, Encapsulant Attributes, Edge Deletion, Process, and Testing.

– Module Attributes

- Most thin film devices are sensitive to moisture exposure
- Most manufacturing processes avoid acid and water exposure
- Module efficiencies are reduced after exposure to 85°C/85%RH
- Special edge seals sometimes help to maintain device efficiency over the duration of qualification testing

– Encapsulant Attributes

- Encapsulant adhesion has not been characterized
- Desire low moisture vapor permeability
- Ideally would like low adhesion to device, high adhesion to glass
- Good electrical insulation
- Optical clarity required for some, not for all
- Thermoplastic OK – must have creep resistance at use temperature
- Upper process temperature is 200°C
- Process friendly – eliminate vacuum laminator or cure times

– Edge Deletion

- Required to isolate device from ground
- Sandblast and laser methods used

- Edge deleted surfaces air cleaned prior to laminating
- Avoid moisture or acidic substances during process

– Process
  - Process highly proprietary to each manufacturer
  - Device packaging represents approximately one half of module production costs
  - Desire lower cost packaging
  - Desire faster process through put
  - Need to keep process temperatures below 200°C

– Testing
  - High humidity produces reduction in module efficiency
  - Failure mechanisms not well understood
  - Glass corrosion appears to be a factor
  - 85°C/85%RH testing sometime produces erroneous pass/fail information
  - Better aging tests required but not yet defined

Literature Survey

A literature review was conducted to identify technical research related to thin film module reliability, conceptual ideas that may be used as a platform for new encapsulation technology, and materials that have potential as new encapsulants or additives of interest in the development of new encapsulants. The search strategy involved a series of approaches that are summarized and organized by Photovoltaic Industry, Patent, and General Literature search strategies.

Photovoltaic Search Strategy

The NREL, Sandia, IEEE, and JPL databases were searched for journal and conference proceeding articles describing research pertinent to the reliability and failure analysis of thin film modules. This search identified papers and presentations with respect to thin film module reliability and provided contacts for NREL and other government employed scientists involved in the study of thin film module reliability. Topics of interest included failure analysis of thin film modules, accelerated testing methods, and reduction of moisture ingression.

The topics covered by NREL publications indicate researchers Joe del Cueto, Gary Jorgensen, Tom McMahon, Carl Osterwald, and Joel Pankow as having conducted substantial research involving the reliability of thin film modules. They have been targeted as having special insight into the reliability issues pertaining to thin film modules, and will be utilized as resources going forward for the encapsulant development.

- Failure Analysis

Module reliability issues have been documented by studying thin film modules in system grids by following performance changes over time versus the Begin of Life (BOL) performance[1, 2, 3]. The mechanisms and environmental influences that cause module performance degradation are poorly understood[4], but sodium migration from the soda lime glass, water vapor, and internal electric fields have all been implicated in the loss of module performance[5].

The NREL and Sandia literature review identified issues of glass instability in the thin film modules relative to the adhesion of the glass TCO layer and its contribution to the failure or efficiency of the device.[6] There is an overall emphasis on the role of moisture and adhesion difficulties between the glass and the encapsulant[7,8,9] as well as various module interfaces after damp heat exposure[10].

Leakage currents between the device and the glass and at the interface of the glass and the encapsulant appear to be the most significant factors with respect to the corrosion of the thin film modules[11]. Additionally, there are electrochemical and galvanic corrosion properties inherent in the devices themselves because of the dissimilar material conductors in contact with each other[12]. Contributors to electrochemical corrosion include sodium migration from the soda-lime glass, water vapor, and internal electric fields[13]. Sodium migration can be induced at 85°C when 100 volts are applied across 500cm^2 of glass[14]. Water vapor greatly accelerates the damage rate, but its absence or near-absence does not completely eliminate the corrosion effect[15]. A high voltage test bed at Florida Solar Energy Center demonstrated that electrical leakage currents vary with ambient humidity[16].

A paper from Florida Solar Energy Center indicated that corrosion of a-Si:H PV modules has occurred in an array operating at 300 V DC in Orlando Florida as well as accelerated testing under high voltage bias in damp heat at NREL[17]. This FSEC work presented a general XPS analysis of EVA on the backing glass indicating the presence of tin, oxygen, silicon, carbon and fluorine at the glass encapsulant surface without mention of sodium. First Solar has indicated that their thin film array performance has been stable over a 5- year period with little incidence of delamination, edge corrosion, or arching problems[18].

Overall, the industry recognizes that damp heat should be a component of qualification testing since this type of testing exposure appears to create a failure response that is similar to that found in fielded modules[19]. However, there is indication in the literature that modules that have demonstrated field stability at NREL do not pass standard accelerated environmental tests[20]. An analysis performed by NREL has suggested that the 85°C/85%RH is unrealistic from the perspective of both temperature and humidity of fielded modules[21].

Other experiments indicate that when permeable back sheets were part of the module construction, peel strengths between glass and EVA were not appreciably affected until

exposures of 800 hours where the moisture ingress occurs primarily through the back sheet when tested at 85°C/85% RH [22].

- Module Moisture Ingression

The literature talks about two main routes of moisture ingression into the module through the polymer back sheet or through the edge of the module[23]. For glass/glass type constructions, an edge seal has been used in addition to the pottant as a means of creating a moisture barrier for the module[24]. Using high moisture barrier encapsulants is one methodology of interest to module manufacturers for reducing moisture ingression and improving the reliability of thin film modules. Global Solar believes that the encapsulant's moisture vapor transmission rate needs to be 5 x 10^{-3} g/m^2/day at 25°C or less for the module to pass the current 1000-hour 85°C/85%RH qualification testing[25].

There has been much analysis of the moisture vapor permeability of EVA and other potential encapsulants[26,27]. The current commercial encapsulants do not adequately protect the module from moisture ingression and the encapsulation parameters appear to be unrelated to the water vapor transmission properties of the cured EVA[28].

With respect to potential moisture barrier encapsulation strategies, films are favored over coatings because of their inherent physical attributes including continuity, mechanical strength, adhesion, and cost[29]. A composite design for the encapsulant is desirable[30]. One view on moisture barrier technology is that it is improbable that industry is going to find a perfect polymer-based moisture barrier, and, therefore, cells, components, and the adhesion of the system must be made more tolerant to moisture[31].

Patent Search Strategy

The US patent literature was searched for patented technology and/or ideas on the following topics.

- Encapsulation and Glass Passivation

The patent search indicated technology for packaging LED's that may potentially cross-over to photovoltaic technology[32, 33]. Materials including vapor deposited silicon oxide, silicon nitride, spin-on glass, or spin-on polyimide are noted as being used to protect devices from moisture or other contaminants in addition to electron beam deposited glass[34, 35, 36, 37]. Many of the spin-on glass inventions appear to require fusion temperatures about 400°C.

- Moisture Vapor Barriers

Much of the patented innovations identified deal with synthetic routes for preparing higher moisture barrier resin[38, 39, 40, 41]. One patent described a composite material that may have utility in improving the moisture resistance of encapsulants not requiring optical properties[42]. There were no patents identified that addressed the strict moisture barrier properties that were indicated by the module manufacturers. However, it may be

possible to use additives to improve barrier properties. For example, wax has been patented as a corrosion inhibitor in epoxy thermosetting compositions[43].

- Packaging, Food Packaging

The prevalent innovation with respect to food packaging appears to be with composite layered structures[44] and alloys[45, 46]. No significant patents were found pertaining to single polymeric material systems or filled composite structures.

- Coupling Agents

The patent literature discusses the utility of silicone oligomers as coupling agents and improving moisture resistance in coatings, curable adhesives and coatings[47]. Patent literature revealing chemistries that may be more hydrolytically stable than the current state of the art was not located.

General Literature Search Strategy

A general literature search was implemented via internet search engines, Infotrieve.com and Dialog.com for information relating to the following general topics.

- Organic Light Emitting Diodes (OLED), Light Emitting Diodes (LED)

The OLED industry is currently using glass ceramic films as conformal barriers on the electrical components of the devices to protect them from moisture[48]. One such invention that has been developed to prevent moisture exposure is to employ the Barix™ process of depositing metal or ceramic oxide layers to provide moisture barrier properties[49]. Another feature of some OLED constructions are desiccant layers that are isolated from the OLED device by a membrane[50].

- Glass

Literature was sought pertaining to soda lime glass chemistry and water transport of ions within the glass. One reference indicated that the XPS analysis can change the surface chemistry of soda lime glass and the amount of sodium detected increases continuously with time[51]. Borosilicate glasses appear to be much better suited with respect to their chemistry and electrical resistance than soda lime glass[52]. AFG Industries has improved the moisture sensitivity of its TCO glass product by reducing the sodium content of the glass and adding a thicker dielectric silica barrier layer[53]. AFG indicates that trapped moisture causes glass corrosion and recommends the following production parameters: glass-to-glass module structure, dry EVA, avoid lamination pinch out or other lamination stress, use acidic detergents to prepare glass for bonding, and to use an edge seal to prevent moisture ingression[54].

Sodium and phosphorus at the interface of the encapsulant and the glass has been found to correlate with a loss of adhesion strength in the encapsulant[55]. Methods of passivating the sodium in the glass were investigated through the literature. It appears that the electrical currents are able to mobilize sodium ions through passivating coatings

including oxidized phosphorous and doped silicon dioxide lattices[56, 57] or silicon nitride/ silicon oxide barriers[58].

A laboratory technique has been developed by Energy Photovoltaics, Inc. wherein an electric field is applied to heated glass to test the TCO delamination[59]. According to this reference, the sodium ions in the glass increased the amount of current that passed through the glass and subsequently was a factor in TCO delamination. The electrical biasing appeared to make the glass more susceptible to TCO delamination. Furthermore, the effects of voltage biasing lie dormant in the absence of moisture. When moisture is later introduced, the TCO begins to delaminate from the glass. The electrical current did not appear to have a similar effect on borosilicate glass having approximately 25% of the sodium of standard soda-lime glass.

- Electronic Devices

General literature on the failure mechanisms of electronic devices indicates ion contamination to be problematic. It has been documented that moisture and other contaminants can enter encapsulants both along the interface between the device leads and the plastic or through the bulk of the plastic [60]. The literature discusses the use of high purity components as well as passivation to protect electronic devices from ion migration. The microelectronic industry has experimented with utilizing inorganic glassy and/or organic polymeric protective insulation layers to provide mechanical and chemical protection of devices. The protective layers often have their own issues with respect to localized structural defects that rendered the metal vulnerable to corrosive attack. Trapped moisture and contaminants in cracks and pin- holes accelerated the corrosion mechanisms[61].

- Moisture Vapor Transmission, Moisture Barrier

A general survey was conducted to locate physical data relative to the moisture barrier properties of polymeric materials to identify candidate materials that might have superior moisture vapor barrier properties compared to EVA, butyl, and silicone rubbers. Literature and information was procured on True Seal PIB insulating glass sealant for comparison with properties of EVA or other alternative encapsulant materials. The PIB is used as a main moisture vapor seal between the glass and metal spacer in insulating glass units[62]. Data was sought to determine the relative moisture vapor transmission rates of candidate polymers for the encapsulant development. A number of sources provided limited data on generic materials[63, 64, 65, 66].

Water vapor barriers are of interest to the pharmaceutical blister packaging industry. The best current moisture-barrier film is PTCFE which has a water vapor transmission rate of 0.03 at 100°F and 90% RH[67].

- Encapsulants

There has been some work in crystalline silicon modules with an alternative encapsulant that does not require vacuum lamination to process[68]. Other European manufacturers are interested in using PVB as thin film module encapsulants[69].

The literature search did not locate documents that define the optimum encapsulant requirements with respect to adhesion strength, dielectric properties, elongation, modulus, or coefficient of linear thermal expansion. However, a calcium test has been used in the OLED industry to accelerate screening of potential encapsulants[70].

TASK 2: INTERFACIAL CHARACTERIZATION OF ENCAPSULANT BONDING

Failure mechanisms in current thin film devices are often attributed throughout the industry to moisture penetration into the module through the bulk of the encapsulant. The emphasis of Task 2 was to characterize the interfacial regions of thin film devices, both new and fielded, to develop a better understanding of the interfacial surface chemistry and to look for changes that may impact adhesion of the encapsulant to the various device substrates. The interfacial regions of the edge delete perimeter of thin film modules are of primary interest in this analysis since the commercial grades of EVA encapsulants have exhibited lower adhesion within the edge-deleted regions. One major objective of this research was to determine the role of the edge-deleted region in moisture transport into the thin-film module and subsequent corrosion of the thin-film device.

The instrumented analysis was performed under subcontract by the University of Connecticut Institute of Materials Science (UCONN-IMS) as a means of better understanding the relationship between the encapsulant and device reliability. Early stages of this effort focused on developing meaningful analytical test procedures to be used in the module characterization. The procedures were established on individual component specimens supplied by the manufacturing team member participants. The procedures were then used in the baseline analysis of unaged thin-film devices and will be later used to analyze aged failed thin film modules. Concurrent work was also performed by STR to assist in development of the testing procedures and also to develop and validate potential accelerated aging protocols that will be utilized under the Phase II, “Task 4: Thin-film Encapsulants – Initial Development.”

The conclusions based on the UCONN-IMS literature study have mirrored the industry belief that moisture is a large contributor to the premature failure of the thin-film devices. UCONN-IMS postulates the following probable failure mechanism:

1. Water migrates through EVA to glass/EVA interface.
2. Water rapidly degrades soda-lime glass surface (both the EVA and glass corrosion product also probably swell) leading to delamination.
3. Water must be prevented from reaching the EVA/glass interface.

The UCONN-IMS analysis of unaged interfaces is nearing completion at this end of the first year funding. Techniques utilized in this evaluation are X-ray photoelectron spectroscopy (XPS), scanning electron microscopy coupled with energy dispersive X-

ray analysis (SEM/EDX), and optical profilometry. Major findings and conclusions are still pending at this time (to be addressed in contract deliverable D-1.5 target date October 1, 2003).

Modules available to the UCONN-IMS analysis of failed fielded modules so far include one failed a-Silicon module supplied by BP Solar as well as four purchased fielded modules from Arizona State University. NREL is in the process of securing examples of modules from PowerLight Corporation. The objective of this analysis will be to identify interfacial chemistries at both visible defects and other regions of the fielded modules. The analysis will attempt to compare the interfacial regions of fielded failed modules with those that have no prior fielding history.

Additional characterization of physical properties is scheduled to develop a better understanding of moisture ingression through the EVA encapsulant and its effect on adhesive strength and interfacial chemistry. A testing protocol involving Karl Fisher determination of moisture concentration relative to adhesive strength, migration into the module, and interfacial chemistry is in design stage for this purpose for implementation in mid October. Additional activities involve the design and validation of accelerated aging protocols for candidate encapsulant materials. One such proposed method for screening encapsulants is to involve applying a voltage bias to test coupons before exposure to high temperature and humidity. The interfacial chemistry of specimens aged in this manner will be validated by the testing protocol developed by UCONN-IMS based on their findings on aged failed modules.

Indications

The major indications at this point in the Task 2 analysis is that soda lime glass that has been utilized in the fabrication of thin film devices appears poorly suited to fabrication of photovoltaic modules from the perspective that the it is not especially stable when exposed to voltage and moisture. The literature indicated a migration of sodium ions to the TCO surface of the modules and, inevitably, delamination of the TCO layer from the glass. This problem appears to be delayed if moisture can be eliminated at the surface of the glass.

Given the instability in the glass, it appears that enhancing EVA adhesion to the glass likely will not play a substantial role in improving the reliability of the photovoltaic modules. It appears that the moisture vapor transmission through the bulk encapsulant must be minimized in order to extend the service life of the modules.

TASK 3: MANUFACTURING SCALE-UP OF EVA BASED ENCAPSLANT SYSTEMS

Super Fast-cure (SFC) and Flame-retardant (FR) encapsulants were optimized as a means of improving observable process shortcomings noted from their initial extrusion trials. The SFC encapsulant required additional formulation optimization to correct a cumbersome, time-intensive compounding procedure, screw slippage, premature

crosslinking during extrusion, and failure of the IEC 61215 qualification test for wet hi-potential. The FR EVA required optimization to correct its unsatisfactory level of crosslinking and to substitute a non halogen-based additive for its current halogen-based additive. Halogenated chemicals are considered environmental risks, particularly in Europe where a non-halogenated FR formulation may prove to be more acceptable and practical.

Experimental Design

Based on the nature and make-up of the curative package in the SFC formulation, it appears that one of the curative's constituents was responsible for the observed screw slippage. It was surmised further that this same constituent was part of the mechanism that reduced the encapsulant's ability to prevent current leakage during the wet hi-pot evaluation. Therefore, reducing and/or minimizing this specific curative additive was the goal, while maintaining the fast and efficient curing properties of the overall curative package.

Moving Die Rheometry (MDR)

MDR, a standard test method that analyzes crosslinking efficiency in rubber and plastic materials, was used to measure curing kinetics to access the impact of modifications to curing packages or evaluate new curing systems. The rheometer measures the shear modulus (i.e. torque) as a function of time at a set temperature during the crosslinking of a polymer. Torque development is a function of crosslink density; as the polymer crosslinks, the resistance to shear (measured as torque) increases. All MDR measurements were carried out in accordance with ASTM D 6204-97.

Mooney Scorch Analysis

The Mooney viscometer is an instrument that compares the processability and stability characteristics of polymer materials. The viscosity is measured as a function of time at constant temperature. Like MDR, the viscosity is related to the curing activity of the polymer. A material that has a strong tendency to crosslink prematurely (i.e. scorch) during processing will have a higher Mooney viscosity per unit of time compared to a material that is not subject to scorching. Mooney Scorch analysis was performed at 104°C.

Mixing Bowl

The mixing bowl measures crosslinking level at constant temperature like the Mooney viscometer, but a shear component is introduced that simulates more accurately the conditions within an extruder. Evaluations with the mixing bowl were accomplished using a Brabender Plasticorder/Rheometer fitted with an oil-heated mixing bowl and high-shear blade mixers. The bowl was maintained at three temperatures, 99°C. 103°C, and 107°C, and formulations were sheared at 100 rpm.

Strand-die Extrusion

A single-screw pilot extruder with 1/16- inch diameter strand-die was used to simulate production processing of each of the experimental compositions. The extrusions were run at a 107°C melt temperature and 3000-PSI backpressure so that the effect of flow restrictions on stability of the experimental compositions could be evaluated.

Flame Impingement

To evaluate the flame-retarding and flammability performance of candidate FR EVA formulations, a test method was modeled after 16CFR Part 1610. Experimental materials were exposed directly to a butane flame at 1,895°C for 15 minutes. During flame impingement, the material was observed for burning, charring, and/or dripping characteristics, as well as the ability of the flame to penetrate through the sample material.

Results and Discussion

Super Fast-Cure Formulation: Formulation Development

To address the issues with this formulation, the overall liquid content in the curative package was systematically reduced and the curing kinetics measured. Figures 1 and 2 show MDR curves for various SFC formulations as a function of liquid content at 150°C, 155°C, and 160°C. The maximum torque achieved (S'_{Max}), which is directly proportional to the crosslinking efficiency, decreased with the reduction of liquid content.

Table 1 compares the peak curing rates of the various SFC formulations to the original SFC encapsulant, X34643-4P, and 15295P. The SFC reformulations had slightly greater curing rates than the original SFC material. Out of the four SFC reformulations, X0045-4 (39% liquid content) had the most similar curing kinetics to X34643-4P.

Additional reformulation of the SFC was done following the MDR results on the 0045 formulation series. Figures 3 and 4 show MDR curves of the 122-61 SFC series as a function of LC at 150°C, 155°C, and 160°C. Based on the reformulated SFC formulation series (0045 and 122-61), a 39% liquid content appears to be the optimum level for maximizing curing performance and minimizing liquid content.

X0045-4, X34643-4P, and 15295P were evaluated with the Mooney viscometer in order to compare the processability of each material. Figure 5 shows the Mooney Scorch data for all three formulations at 104°C. The data surprisingly showed that both SFC formulations had similar process stability compared to the control 15295P formulation, although scorching was noted to occur with the original SFC formulation during its extrusion trials.

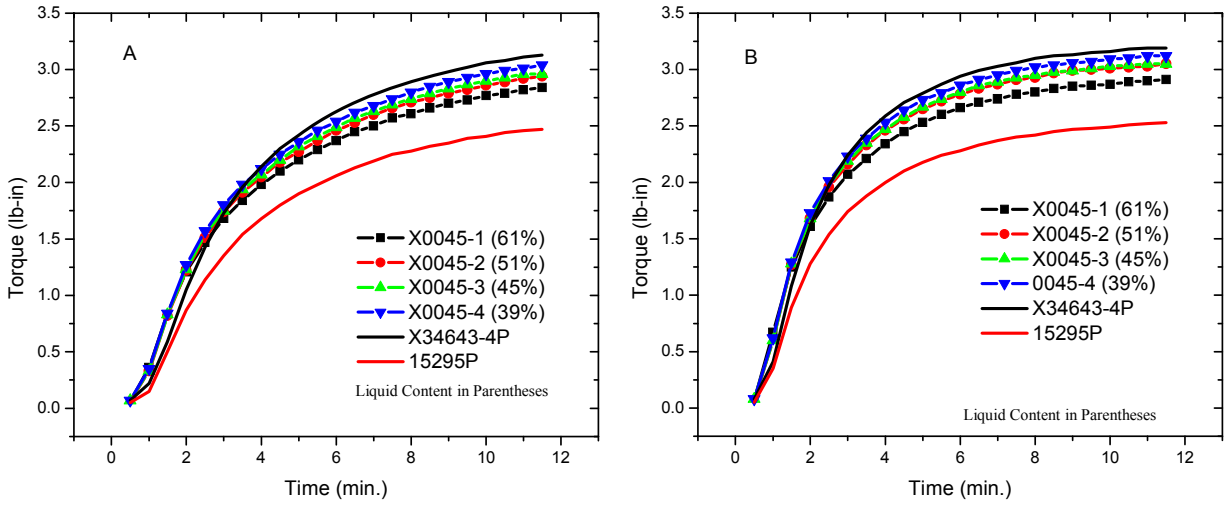

Figure 1. MDR Curves for SFC Formulations and 15295P at A) 150°C and B) 155°C.

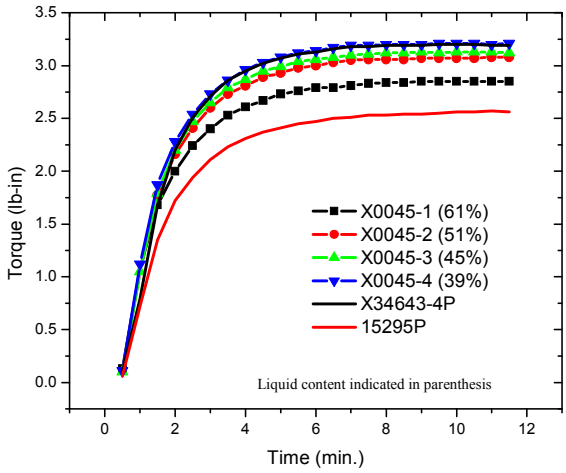

Figure 2. MDR Curves for SFC Formulations and 15295P at 160°C.

	X34643P	15295P	X0045-1
150°C	0.99	0.8	1.03
155°C	1.43	1.22	1.55
160°C	2.09	1.77	2.25

	X0045-2	X0045-3	X0045-4
150°C	1.06	1.06	1.06
155°C	1.61	1.56	1.59
160°C	2.38	2.37	2.52

Table 1. Peak Curing Rates (S'/min.) as a Function of Temperature for SFC Formulations.

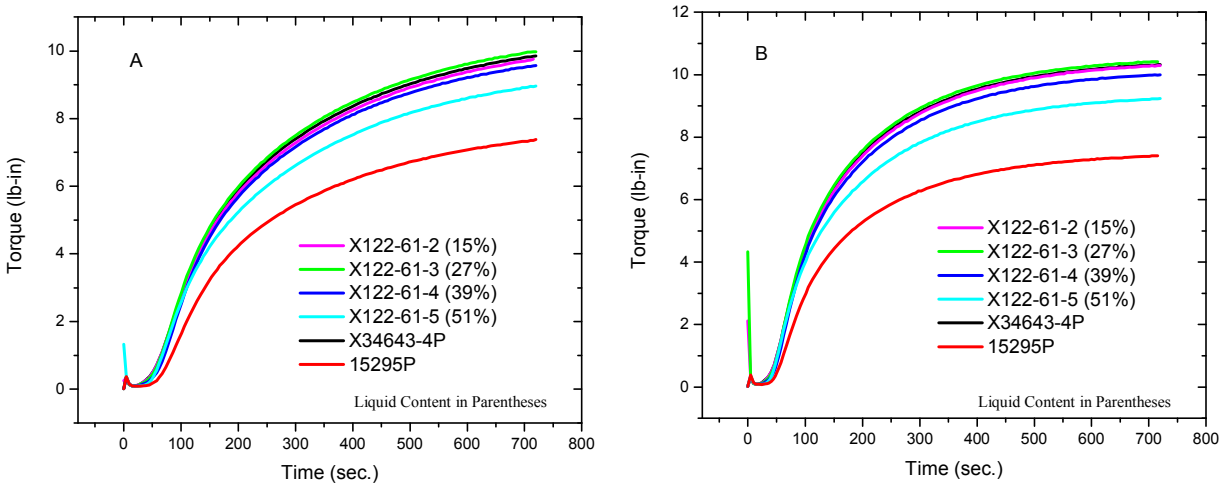

Figure 3. MDR Curves for SFC Formulations and 15295P at A) 150°C and B) 155°C

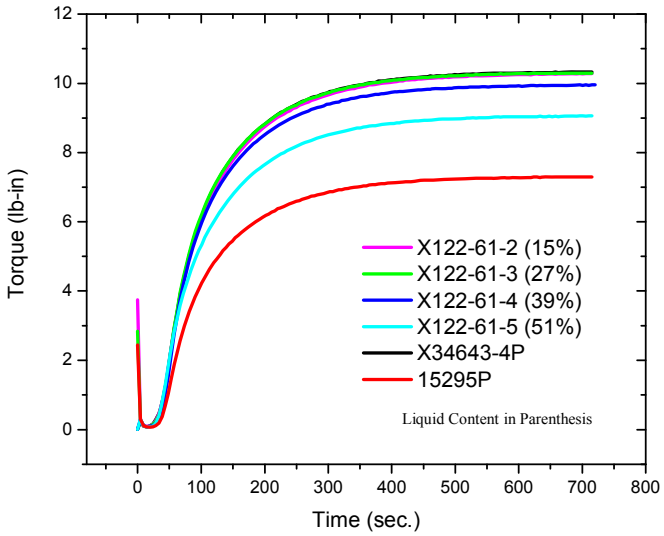

Figure 4. MDR curves for SFC formulations and 15295P at 160°C.

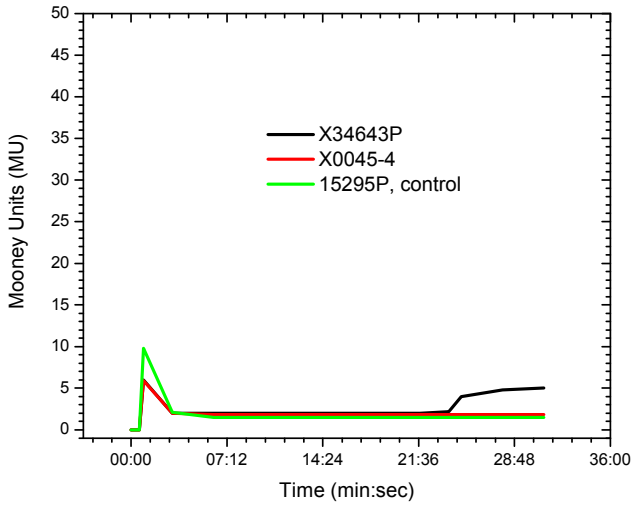

Figure 5. Mooney Scorch data for SFC formulations and 15295P.

To follow-up the Mooney Scorch analysis, a mixing bowl experiment was performed on 15295P and both SFC materials. Because process stability was the focus of this experiment, the critical measurement from the mixing bowl study was the time it takes for the material to initiate crosslinking.

Three formulations were evaluated: a control, the original SFC formulation (-4P), and the reformulated SFC formulation (-XP). Table 2 summarizes the results of the mixing bowl experiment. For 15295P, X34643-4P, and X0045-4, crosslink initiation times were 12.5, 7.5, and 8.5 minutes, respectively. Including the shear component demonstrated a more pronounced difference between the formulations. As expected, the reformulated SFC formulation was slightly more stable (i.e. longer time to initiate crosslinking) compared to the original SFC formulation.

	99 C bowl temp.			103 C bowl temp.			107 C bowl temp.		
Run	1	2	3	4	5	6	7	8	9
Formulation	Control	-4P	-XP	Control	-4P	-XP	Control	-4P	-XP
Minimum Torque	800	900	900	900	900	900	900	850	850
Time at min. torque (min.)	11	10	9	7	6	6	5	5	5
Crosslink Torque	1500	1500	1500	1200	1200	1200	1200	1200	1200
Crosslink Temp (C)	137	126	128	127	122	124	128	123	126
Crosslink Time (sec.)	1140	810	870	750	450	510	570	360	390

Table 2. Summary of results from mixing bowl experiment.

The maximum material dwell time in an encapsulant production extruder was determined to be five (5) minutes. Both SFC formulations had characteristic times (crosslink initiation times) greater than the residence time, suggesting that the SFC formulations should not crosslink during extrusion. Therefore, it appears that material scorching is dependent more on the flow dynamics and operating conditions of the extruder rather than the material formulation.

Super Fast-Cure Formulation: Extrusion Optimization

Extrusion optimization trials were first conducted on the pilot scale using a pilot extruder and strand die to simulate the flow dynamics of the manufacturing extruder. This pilot test was used to compare the original super fast-cure formulation with the new optimized compositions.

The pilot test proved much less severe than the full- scale production, and was not able to fully reproduce the premature crosslinking that was seen with the same composition on the production equipment. These results obviated the need for the extrusion trials of all viable candidates to be performed on manufacturing scale and strongly indicated that it may be necessary to make modifications to the design of the process equipment.

Further experimentation indicated that the extruder design required modification to successfully process the SFC formulations. The extruder barrel was optimized, and a proprietary screw was designed based on EVA flow dynamics. These modifications resulted in significant extrusion performance gains. STR observed at least a 7% decrease in overall extrusion temperatures and a 30% increase in material output compared to pre-modified process conditions.

Two SFC reformulations were extruded on the modified process: X0045-4/122-61-4 and X122-61-3. Both materials ran extremely well during the extrusion trial; the sheet form and overall encapsulant quality were excellent. Product from this trial appeared to laminate and cure effectively.

During extrusion of the original SFC formulation (March 2000 and October 2000), the edges of the encapsulant were wavy; this flow instability was observed within the first 0.375 inches from the edge of the extruded sheet. This edge waviness was not observed for either of the reformulated SFC formulations on the modified extruder. Furthermore, sheet thickness was easily kept constant throughout the trial, unlike the run on the previous manufacturing equipment.

There was no observation of screw slippage during the extrusion trial. Melt pressure remained at expected levels, and when the screw was removed from the barrel for cleaning, there were no pellet deposits and molten resin buildup on the screw. During the 2000 extrusion trials of the original SFC formulation, STR's production personnel noted deposits on the root and trailing flights of the screw.

Production output (measured in pounds of encapsulant extruded per hour) on the improved SFC formulations was increased by 91% over the previous formulation. The near doubling of production output with the current process/formulation is about 80% of STR's normal production output with typical EVA-based formulations and is considered satisfactory for production scale.

Faster extrusion rates without affect on the encapsulant were accomplished, in part, by lower temperature profiles. Die and melt temperatures were 11% and 3% lower, respectively, compared to the previous extrusion conditions with the original SFC formulation.

The temperature profile of the 2003 extrusion trial was also lower, on average, than typical production conditions; die temperatures were approximately 18% lower and melt temperature was 7% lower. The reduced temperatures still did not affect extruding the SFC formulations into sheet form or the overall encapsulant quality. Therefore, there appears to be a lot of room to increase the production rate of the SFC formulations with the current extruder setup.

Flame-Retardant Formulation: Formulation Development

The first generation FR EVA encapsulants did not meet the crosslink density requirements for cured photovoltaic modules. Central to this reformulation effort was a new curing system capable of producing an effective crosslink density with similar or better curing performance compared to the STR fast-cure formulation 15295P.

MDR data in Table 3 and Figures 6 and 7 compares 15295P and the original FR formulation (X33579P-FR) to two (2) experimental FR formulations (X122-11-1P and X122-11-2P). The experimental FR formulations had more robust curing performance (faster cure speed and higher S'_{Max}) versus the other controls. In particular, the curative package in X122-11-2P greatly improved the crosslinking efficiency, resulting in higher S'_{Max} compared to 15295P and the SFC materials. Although the curing kinetics and efficiencies were improved in both FR encapsulants, these materials appeared to have adequate processing stability under Mooney Scorch (Figure. 8).

	15295P	X33579P-FR	X122-11-1P-FR	X122-11-2P-FR
150°C	0.8	0.53	0.65	1.11
155°C	1.22	1.39	0.85	1.34
160°C	1.77	1.37	1.50	2.80

Table 3. Peak curing rates (S'/min.) as a function of temperature for FR EVA formulations.

A non-halogenated FR EVA formulation was evaluated for its flame-retardant effectiveness against the original, halogenated formulation. Each formulation was laminated to 15295P and then cured prior to flammability testing. Table 4 summarizes the results of the flame test. Note that the sample type/orientation describes the

laminate and the layer that is first in contact with the flame. For example, EVA is in contact with the flame, followed by FR-EVA, and scrim for run #1.

When the flame impinged first on the 15295P side, it took less than one (1) minute for the flame to burn through the non-FR layer. The flame and subsequent combustion appeared to increase in intensity 30 seconds into the start of the test, likely due to cleavage of the highly flammable acetate groups.

Once 15295P was effectively burned off, the flame impingement contacted the FR EVA layer. However, for both the halogenated and non-halogenated formulations, the penetration of the flame appeared to stop at this layer. During the rest of the 15-minute exposure period, neither FR formulations burned, nor fueled the butane flame as the 15295P did. When FR EVA was exposed first to the flame (i.e. impingement first started at the FR EVA layer), the FR layer did not burn, and because the flame could not penetrate this layer, the regular EVA layer underneath only darkened but did not ignite.

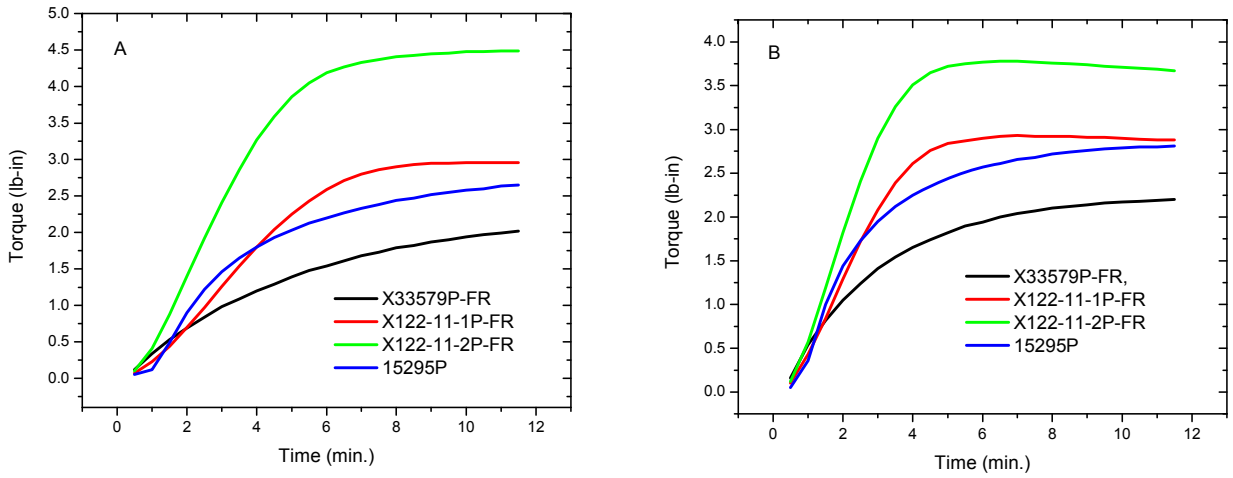

Figure 6. MDR Curves for FR EVA Formulations and 15295P at A) 150°C and B) 155°C.

Depending on the laminate layer exposed to the flame first, the burning patterns on the laminate were nearly identical for both formulations. Figures 9 and 10 show the burning patterns of each FR formulation. The similarity in how the material managed the flame impingement illustrated the flame-retardant effectiveness of the non-halogenated formulation.

Flame Retardant Formulation: Extrusion Optimization

The FR EVA formulation X122-11-2P-FR (non-halogenated) was extruded as part of the overall extrusion trial conducted with the optimized production scale extruder setup. The FR EVA formulation ran extremely well during the extrusion trial without complication from the optimized curing performance. No problems were observed

during processing relative to compounding, screw slippage, or premature crosslinking. The reformulated FR encapsulant was produced at typical production process speeds.

STR's next step with the SFC and FR EVA formulations will be module lamination trials with the encapsulant formulations. Modules made with the SFC materials will be submitted for IEC 61215 qualification testing and fielded on a tracker for continuous monitoring. Modules with the FR EVA encapsulant will first undergo flammability testing.

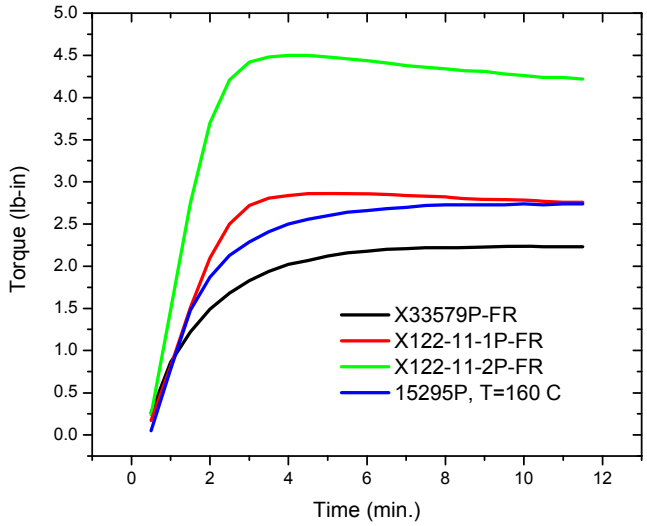

Figure 7. MDR Curves for FR EVA Formulations and 15295P at 160°C.

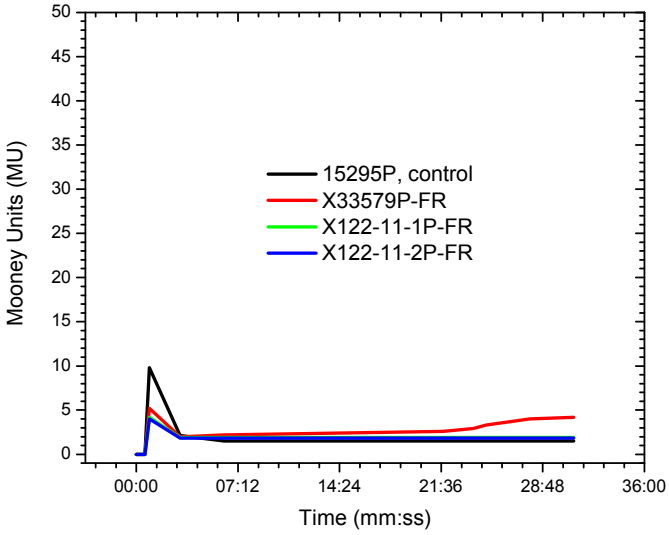

Figure 8. Mooney Scorch Data for FR EVA Formulations and 15295P.

FRONT BACK

Figure 9. Flame-impinged samples of non-halogenated FR formulation.

FRONT BACK

Figure 10. Flame-Impinged samples of halogenated FR formulation.

Run	Sample Type/Orientation[1]	Burn-through (yes/no)	Comments
1	EVA/FR-EVA/S-layer	N	▪ After 5 min., no burn-through or general combustion. ▪ Still good after 10 min. ▪ Looks good after 15 min.
2	EVA/FR-EVA/S-layer	N	▪ Repeat of run #1. ▪ Initial burning of top EVA layer – snap, crackle, pop, smoke – then ceases. ▪ No burn-through after 5, 10, 15 min. ▪ Flame seems to be hitting a “wall”.
3	EVA/FR-EVA (non-halogenated)/S-layer	N	▪ After 5 min., no burn-through, similar to regular FR-EVA. ▪ No combustion due to cleavage of acetate groups. ▪ Same performance as runs 1 and 2.
4	EVA/FR-EVA (non-halogenated)/S-layer	N	▪ Same performance as run #3.
5	FR-EVA/EVA	N	▪ Flame stuck at the FR-EVA layer; no burn-through after 3:15. ▪ Much more puckering behind the laminated compared to previous runs. ▪ No apparent burn-through after 10 min.
6	EVA/FR-EVA	Y	▪ FR-EVA layer fell apart that led to burn-through.

Run	Sample Type/Orientation[1]	Burn-through (yes/no)	Comments
			▪
7	FR-EVA/S-layer/EVA	N	▪ After 1.5 min., flame is stalled at the facing encapsulant layer.
8	EVA/S-layer/FR-EVA	N	▪ Initial bubbling and burning of top EVA layer, then stopped. ▪ Flame penetration stopped.
9	EVA/S-layer	Y	▪ Vicious burning – growth of flame. ▪ EVA is no more; scrim left.
10	FR-EVA (non-halogenated)/S-layer/EVA	N	▪ Looking good after 10 min, ▪ Did fine.
11	EVA/S-layer/FR-EVA (non-halogenated)	N	▪ Top EVA layer burned fast. ▪ A drop of liquid formed during combustion. ▪ Localized burning – sizzling and boiling. ▪ No burn-through.
12	FR-EVA (non-halogenated)/EVA	N	▪ Flame stuck at the FR-EVA layer. ▪ No burn-through.
13	EVA/FR-EVA (non-halogenated)	N	▪ First 5 min., burning of the EVA layer. ▪ Flame and burning stopped at FR-EVA layer. ▪ No burn-through.

Table 4. Summary of results from flame impingement experiment.

Conclusions

Excellent progress has been made towards qualifying two new encapsulants for the crystalline type modules and for understanding the current industry findings, and technical issues surrounding the thin film modules technology.

- Obtained insight into the technical issues, concerns, and obstacles faced by each module- manufacturing team member in improving the reliability of their thin film modules,

- Evaluated research conducted within the thin film module manufacturing industry and by national team members to better understand where additional analysis or further understanding may be required,

- Identified potential formulation strategies for new high performance encapsulants,

- Developed analytical procedures for interfacial characterization of failed thin film modules,

- Scheduled interfacial characterization of failed thin film modules,

- Improved the extrusion performance of Super-fast Cure and Flame-retardant EVA encapsulants, and

- Scheduled commercial lamination trials and subsequent IEC qualification testing for the new improved Super-fast Cure and Flame-retardant EVA.

Future Work

The Task 2 interfacial analysis work will continue into the second year of funding. The analysis will include aged fielded modules that have experienced substantial loss in efficiency.

The Task 3 manufacturing scale up work will continue into the second year of funding so that commercial module lamination trials may be completed. Modules made with the SFC materials will be submitted for IEC 61215 qualification testing and fielded on a tracker for continuous monitoring. Modules with the FR EVA encapsulant will first undergo large-scale flammability testing before qualification testing, assuming they successfully pass flammability testing.

PHASE II

INTRODUCTION

The Phase II work summarized in the following section focuses on five (5) main objectives/tasks.

- Task 4: complete the preliminary formulation development of thin-film candidate encapsulant materials,
- Task 5: processing assessment, manufacturing trials, and module performance testing of candidate thin-film-specific materials,
- Task 6: complete the analytical work performed at the University of Connecticut Institute of Material Science,
- Task 7: complete the pre-commercial testing of flame-retardant (FR) and super fast-cure (SFC) EVA-based encapsulants, and
- Task 8: design of modifications to SFC manufacturing process.

Formulation efforts for thin-film-specific encapsulants have included material and additives selection, characterization, preliminary formulation, and limited performance evaluation. Characterization of prospective materials was accomplished via an STR-developed analytical protocol, and selection of viable encapsulant candidates was completed for the thin-film manufacturer team member. Lamination and qualification testing was done by the thin-film manufacturer on selected encapsulant candidates.

Interfacial characterization of thin-film modules was also completed during Phase II. Analysis has been completed for modules “as manufactured” and after “field exposure” or “laboratory aging.”

The pre-commercialization activities of the high-performance encapsulants for crystalline silicon-type modules have included module fabrication and fielding for the Super-fast cure (SFC) EVA-based encapsulant, as well as module fabrication, fielding, and IEC qualification screening for the Flame-retardant (FR) EVA encapsulant. Testing results on the FR encapsulant found that this formulation had poor wet electrical resistance.

In addition to encapsulant testing, modifications of the manufacturing process that fabricates the SFC has begun. The process modifications have been developed to reduce the overall manufacturing costs of the SFC formulation.

TASK 4: THIN-FILM ENCAPSULANTS – INITIAL DEVELOPMENT

The objective of the Task 4 development effort was to formulate viable, new encapsulant materials specific for thin-film modules, offering higher performance than the current EVA product at a lower cost. As part of this effort, an exhaustive list of starting materials was prepared, and commercial sample materials were solicited from the suppliers. Simultaneously, an experimental approach was designed to help screen the formulated candidate materials for their potential benefits as encapsulant materials. Important performance properties were identified, and screening protocols were developed. Each candidate formulation, once compounded, was then evaluated using the established screening design so that important performance information could be established for each.

Candidate Materials

The selection criteria for the candidate materials included the optical performance of the material, dimensional stability at 90°C, moisture vapor transmission properties, moisture adsorption properties, adhesive properties, particle size distribution, glass transition temperature, modulus, tensile properties, and electrical properties.

Extensive research was conducted to identify potential candidate raw materials for the formulation development effort. Resin and additives manufacturers were solicited for commercial samples according to the materials qualifications presented in Table 5.

Cost	< $2.50 per pound
Elongation	> 450 %
Modulus	< 10 mPa
Electrical Properties	>500 V/mil
Moisture Absorption	< 0.7 %
Density	> 0.9
Process Temperature	Between 80°C and 200°C
Adhesion	Resistance to moisture

Table 5. Material qualifications/criteria.

Approximately 30 “base” resins were procured from seven (7) manufacturers to be used as starting materials in the various formulation strategies; over 50 different additives were also procured from approximately 15 manufacturers. Many of the materials under consideration did not have extensive technical data for electrical and barrier properties and required characterization to establish their baseline performance properties.

Experimental Approach

The experimental approach for the Task 4 effort was broad, encompassing a wide variety of technologies as a means of balancing the expressed needs of the thin-film industry (cost, manufacturability, and performance). Each approach addressed one or

more anticipated benefits to thin-film module technology above and beyond the benefits of the existing, commercially-produced EVA-based encapsulants. As part of the experimental approach, a screening protocol was developed that was capable of evaluating the performance of each candidate formulation. The most promising candidate formulations were selected based on their total contribution to the specific performance goals to be achieved by a new encapsulant; namely those candidate formulations demonstrating improved moisture barrier properties, stable adhesion to glass, lower cost, and improved manufacturability.

The emphasis of the formulation work and experimental design was to establish an understanding of the required physical performance with respect to adhesion versus elasticity and to maximize these properties relative to humidity resistance. Laboratory screening tests were developed as a means of rapidly qualifying the experimental compositions for their potential suitability as encapsulants.

Formulation Strategy

The formulation strategy of encapsulants for thin-film modules involved two main approaches for developing new and improved extruded sheet encapsulants:

- Improve the existing EVA-based formula, and
- Develop EVA-alternative based formulations.

The improved EVA approach focuses in developing an EVA-based encapsulant formulation with improved barrier properties and/or easier process-ability by PV manufacturers.

The EVA-alternative approach focuses on alternative materials that are able to contribute to advances in processing or module performance above that of EVA-based encapsulants. Encapsulants selected under this strategy look beyond the traditional physical performance characteristics of EVA-based materials, so that alternative encapsulants can be developed, which provide considerable performance or process advantages over the existing state-of-the-art EVA-based encapsulants.

Under the Phase II work, the formulation development effort progressed through research, selection, and acquisition of candidate resins and resin modifiers. The materials acquired for this effort included fillers, adhesion promoters, curatives, accelerators, and stabilizers. A performance evaluation protocol was implemented so that the candidates and formulated candidates could be evaluated efficiently for their potential contribution to new, high-performance encapsulants.

Performance Evaluation

A testing methodology was developed so that candidate materials can be effectively evaluated for their potential importance to the performance of the encapsulant. The methodology involved screening base resin materials for critical performance properties

as part of a first level screening process. The data developed under this first level screening process was used to establish a baseline of properties before they are formulated as encapsulants.

Under the first level screening process, each candidate base resin underwent the following performance tests:

1. Tensile properties
2. Peel adhesion to glass
3. Peel adhesion after high humidity at 85°C
4. Moisture vapor transmission
5. Dimensional stability at 90°C
6. Volume resistivity
7. Volume resistivity after high humidity at 85°C

The baseline performance of each resin was then used to establish the formulation methodology developed for each formulated candidate. The formulated candidates were evaluated for peel adhesion to glass after high humidity exposure, followed by moisture vapor transmission, dimensional stability, water absorption testing, and thermal shock testing.

Moisture Ingression Analysis

As part of the performance evaluation, an analysis of the moisture ingression pathway was initiated as a means of providing some basic information regarding the equilibrium state of a thin-film module after exposure to environmental moisture. The procedures developed for this analysis would also become a possible screening tool for understanding the performance of a given encapsulant candidate from the perspective of determining the location-specific percent moisture absorbed by the encapsulant following accelerated aging at high temperature and high humidity conditions.

This research involved the basic study of the moisture content of the encapsulant at numerous locations within a test laminate as a function of time and temperature. This technique was believed to be an alternative method for establishing the suitability of each candidate encapsulant because it measures not only the rate of permeability through the polymer, but also the amount of moisture available at the interfacial surfaces. For example, some materials have very low moisture vapor permeability; however, they have the ability to absorb larger amounts of water.

The moisture ingression analysis was developed using a Metrohm 831 Karl Fisher Coulometer integrated with an EM Sciences EV-6 Aquastar Solid Evaporator. Special test laminates were prepared using a construction of glass, encapsulant, and aluminum backsheet. After accelerated exposure, the encapsulant was removed from specific locations within the test specimen in order to map the relative moisture content of the polymer.

Baseline Characterization

Characterization of each candidate starting material was implemented to identify possible shortcomings with respect to encapsulation. Criteria for further development was based on the overall performance of the material, with special consideration being given to inherent moisture absorption/barrier properties, basic adhesion after humidity and thermal shock and insulation performance. The formulation development process for each candidate was then independently designed based on the physical attributes of each material.

The first level screening process evaluated 30 EVA-alternative resins. Their basic, unmodified physical performance is presented in Figure 11. Data for all the starting materials provide a baseline performance for comparison with the final formulated products.

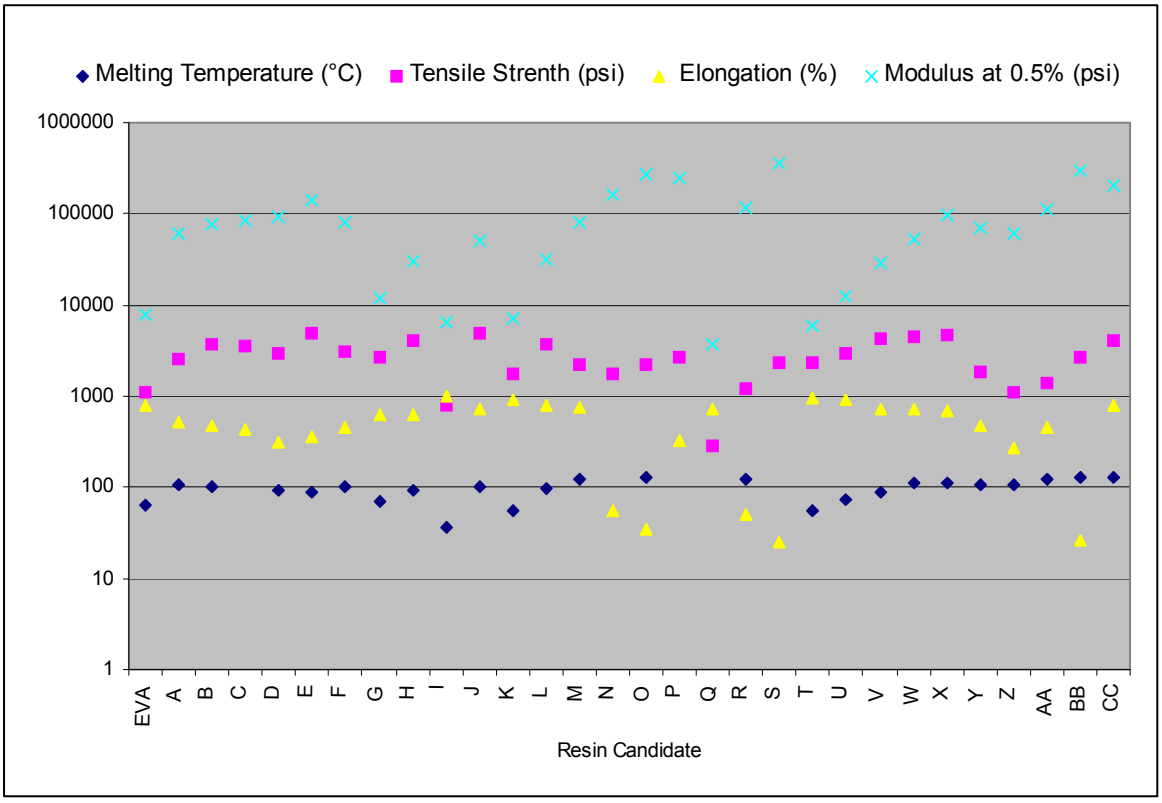

Figure 11. Physical properties of candidate resins.

All candidates had excellent electrical properties after exposure to high humidity conditions based on Volume Resistivity Testing (ASTM D257) shown in Figure 12. Most candidates had better insulation properties than EVA.

In addition to comparable physical and electrical performance properties, many of the candidate resins have baseline barrier properties that are an order of magnitude more efficient moisture barriers than EVA as illustrated in Figure 13 as determined by ASTM

E96. However, the ASTM E 96 test method for water vapor transmission rate was not able to characterize many of the high barrier candidates.

A simultaneous effort to develop a thermogravimetric test procedure for water vapor transmission rate was explored as a means of creating an in-house rapid screening protocol. The advantages to the thermogravimetric procedure were that the films could be characterized at elevated temperatures for a better simulation of the module qualification testing environment, and the test appeared to provide meaningful data after only several hours of testing in contrast to the several weeks required by the ASTM E96 test method. Furthermore, this procedure also appeared more capable of characterizing good barrier films. However, the method yielded inconsistent results when applied to systems of interest and was subsequently scrapped.

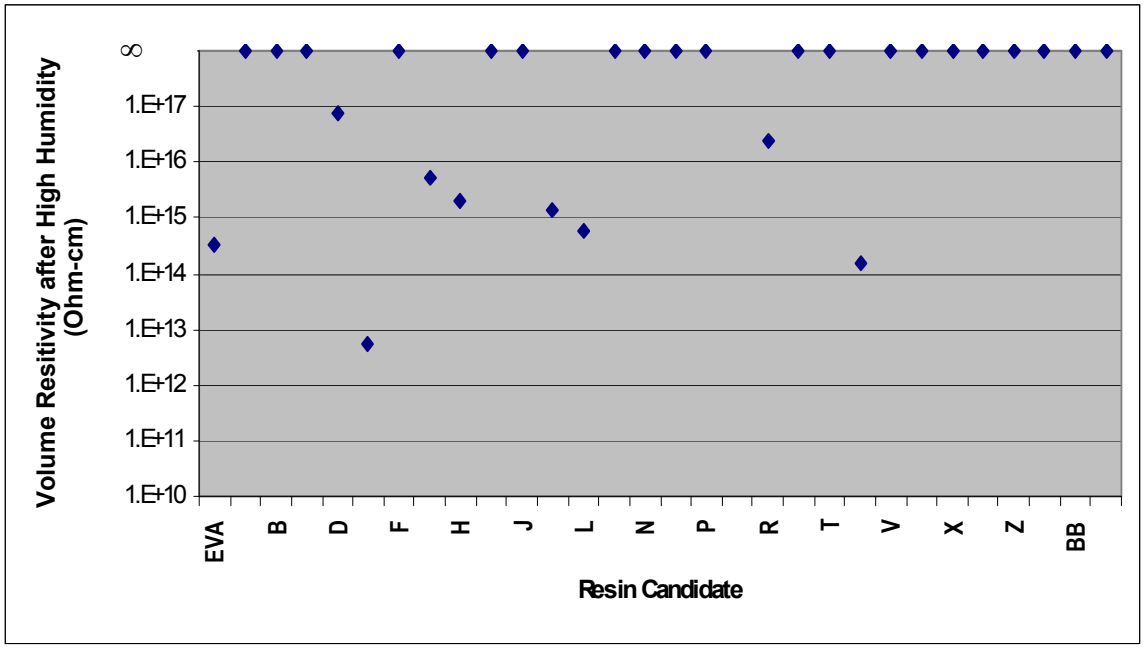

Figure 12. Wet volume resistivity of candidate resins.

The initial formulation development centered around those resin materials and additives having the potential to result in improved moisture barrier performance. The selected candidates were formulated for optimum adhesion to glass after exposure to high temperature and humidity.

Most of the candidate resin products required substantial modification to improve their adhesion to glass. The peel adhesion strengths of the unmodified resins are presented in Figure 14.

Experimental Formulations

The two main strategies for formulation development were done concurrently. The first strategy, the modified EVA strategy, involved adding barrier materials and other

additives to the EVA-based encapsulant as a means of optimizing the performance for barrier performance. This strategy was expected to produce both optically transparent and opaque materials requiring similar processing to the current commercially available EVA-based encapsulant. CIS-based thin-film technology was first and foremost connected with this strategy.

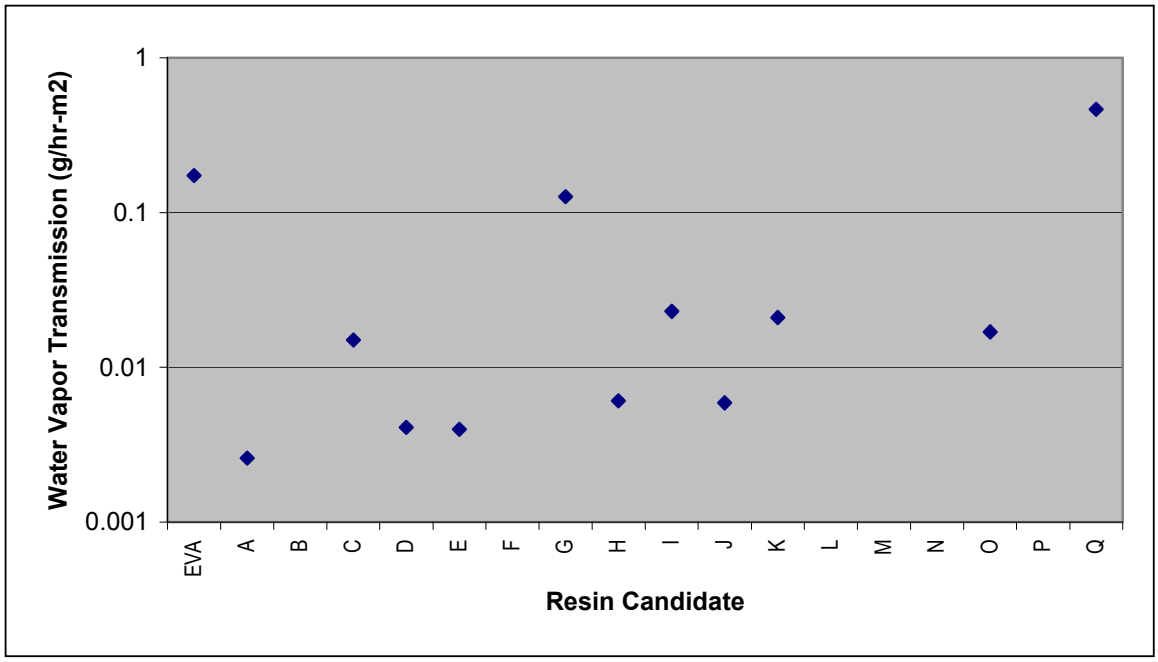

Figure 13. Water vapor transmission rates of candidate resins by ASTM E 96.

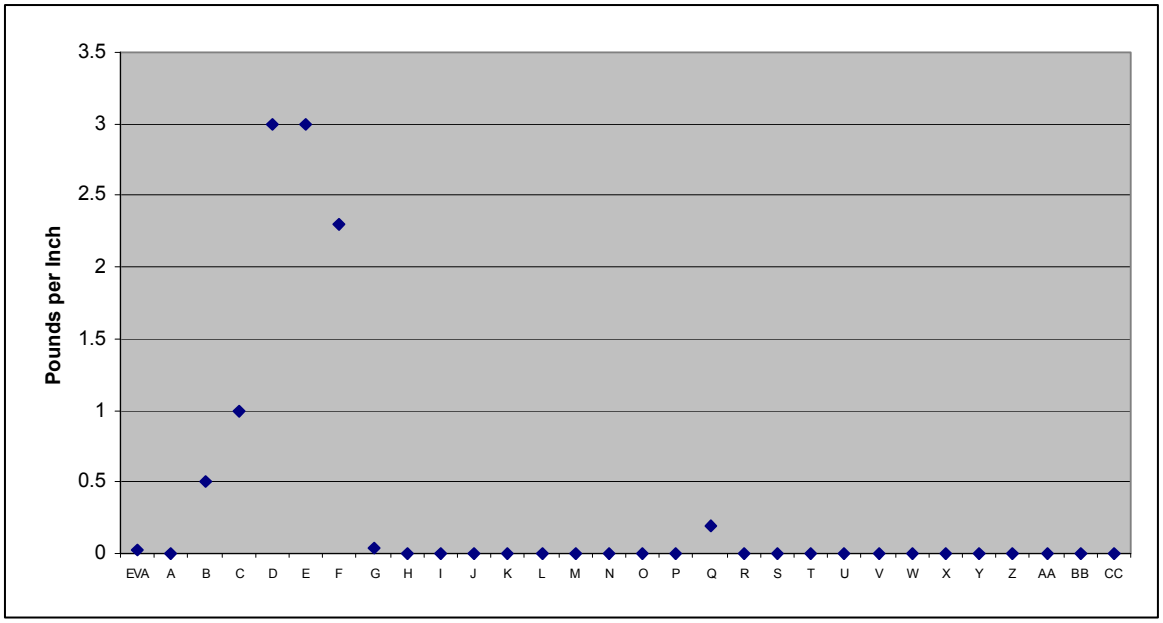

Figure 14. Peel adhesion to glass of unmodified candidate resins.

The non-EVA formulation strategy, primarily related with Amorphous Silicon (a-Si) and Cadmium Telluride (CdTe), held promise for creating a sheet product having both good optical properties and higher vapor barrier properties than the current EVA-based encapsulants. Much of the non-EVA-based formulation strategy promised processing advantages over the state-of-the-art commercial EVA encapsulant products.

Modified EVA Formulations

The modified EVA approach to formulation involved blending the existing encapsulant with barrier additives as a means of minimizing the moisture absorption and water vapor permeability of the polymer. Experiments concentrated on developing optimum processing parameters to maximize dispersion of six different additives. Certain additives were difficult to uniformly disperse, and required substantial process development. Initial experimental results indicated that encapsulants could be formulated with these additives without significant impact on the peel adhesion strength of the EVA based encapsulant. Typical peel adhesion strengths were in the range of 60 pounds per inch and ultimate elongation values of the films were in excess of 500% elongation. This approach also was proven to reduce the moisture vapor transmission rate of the EVA encapsulant. Initial experiments indicated an approximate 40% reduction in water vapor transmission through certain formulated encapsulant films as seen in Figure 15.

The EVA formulations were also modified to contain certain additives that would preserve the optical properties of the material, and possibly minimize the vapor transmission rates of the EVA. These additives were blended with EVA to produce approximately 30 new compositions, which were evaluated for their adhesion to glass. In most cases, the additives did not enhance the EVA's adhesion to glass as illustrated in the Figure 15 comparison of a select few compositions with the formulated EVA encapsulant.

Other EVA-based formulations were considered that allows the material to be processed at lower laminator temperatures. According to one of our manufacturing team members, higher lamination temperatures reduce the device efficiency.

For our CIS manufacturer team member, which has ceased participation as subcontractor, STR recommended that a previously developed low-temperature, faster-cure formulation be evaluated. A summary of this formulation X0140P, was given during the European PV conference in Barcelona in June 2005[71].

Non-EVA Formulations

Physical performance characterization of the 30 non-EVA candidate materials described previously in Figures 11, 12 and 13 suggested that significant modification would be required to create new improved encapsulant products. Within the non-EVA subset of materials, all required formulation to improve their adhesion to glass. A subset of these materials required formulation to improve their dimensional stability at elevated

temperature. Yet another subset of materials required modification to increase their flexibility.

Basic formulation work was initiated with barrier films that had the best polymer structure for modification to affect the desired properties. One resin material, in particular, had very low water vapor transmission rates but provided enough functionality to improve the material's glass adhesion. With an appropriate adhesion additive package, glass adhesion strength was improved from 0.5 pounds per inch width of peel (lb/in) to 45.32 lb/in while maintaining the outstanding water vapor transmission performance (70X less than an EVA-based formulation at 0.0026 g/m^2-hr). This modified resin is designated as X125-37.

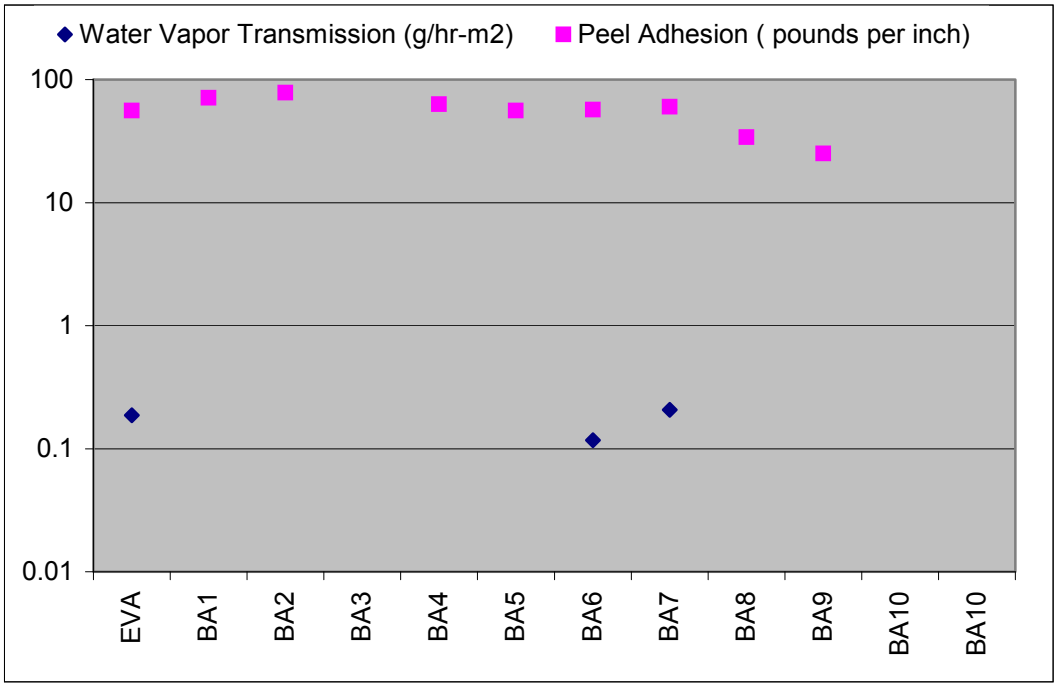

Figure 15. Performance of EVA-based encapsulants with barrier additives.

TASK 5: INITIAL LAMINATION AND QUALIFICATION TRIALS FOR THIN-FILM ENCAPSULANTS

The purpose of this task was to develop candidate encapsulants for each of the thin film manufacturers. One formulation from each strategy in Task 4 was selected for testing by STR's PV manufacturing team members.

For the EVA-based encapsulant, a low-temperature curing material (X0140P) was chosen for CIS-based thin-film devices. Due to the construction of CIS devices, a high light transmission encapsulant is required as it is applied on top of the device. According to our CIS team member, moisture sensitivity is not a major factor; this is

consistent with how the device is constructed within a module and its similarity with crystalline-based module constructions.

As mentioned in the previous section, lamination temperatures can affect the CIS device efficiency. Therefore, the low-temperature-cure encapsulant was selected. Unfortunately, due to the stoppage of activity from the CIS manufacturing partner, X0140P was not evaluated.

a-Si and CdTE thin-film devices are much more sensitive to moisture, probably connected with the fact that the typical PV module construction with these technologies does not fully encapsulate the PV device with a polymer-based, high electrically insulative material. Most a-Si and CdTE PV devices are applied directly to the glass superstrate. Therefore, the encapsulant does not need to be optically transparent.

With the above considerations, a low water vapor transmission rate material with poor optics was chosen ,X125-37, was chosen for lamination and initial qualification testing by the a-Si PV manufacturer team member.

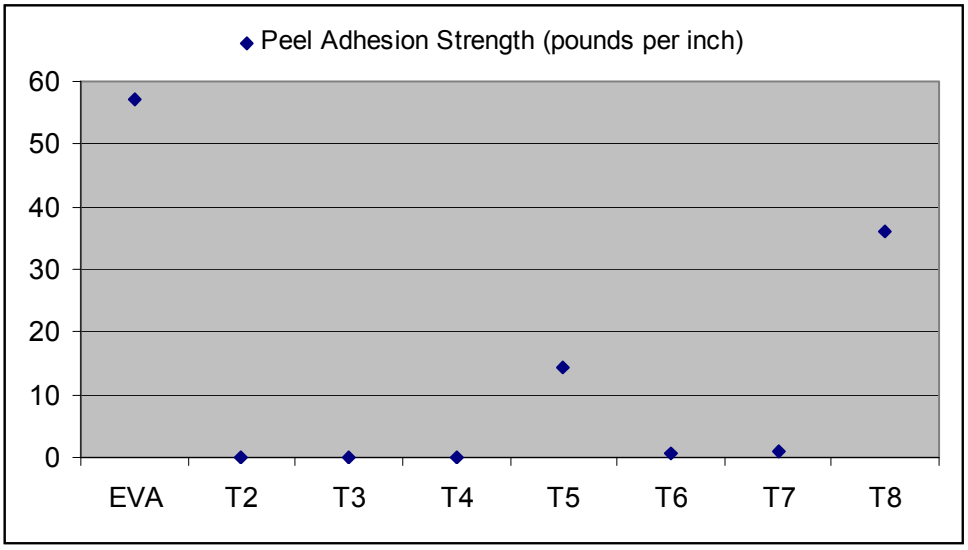

Figure 16. Peel adhesion of transparent modified EVA-based encapsulant candidates.

The current encapsulant material employed by the a-Si PV manufacturer team member requires a lamination cycle of 8 minutes at 160°C. X125-37 has a higher melting point versus the current encapsulant; therefore, some lamination process adjustment was made.

In order to determine a suitable cycle for the X125-37 material, simple glass/glass laminates, sans PV device, were laminated and evaluated for proper melting and adhesion of the encapsulant. In addition to proper melting and adhesion of the encapsulant, visual quality of the laminate was considered.

Glass/glass laminates were carefully inspected for bubbles and void formation (i.e., areas where no encapsulant material is present). For lamination evacuation time of less than 2.5 minutes, bubbles due to entrapped air could be seen.

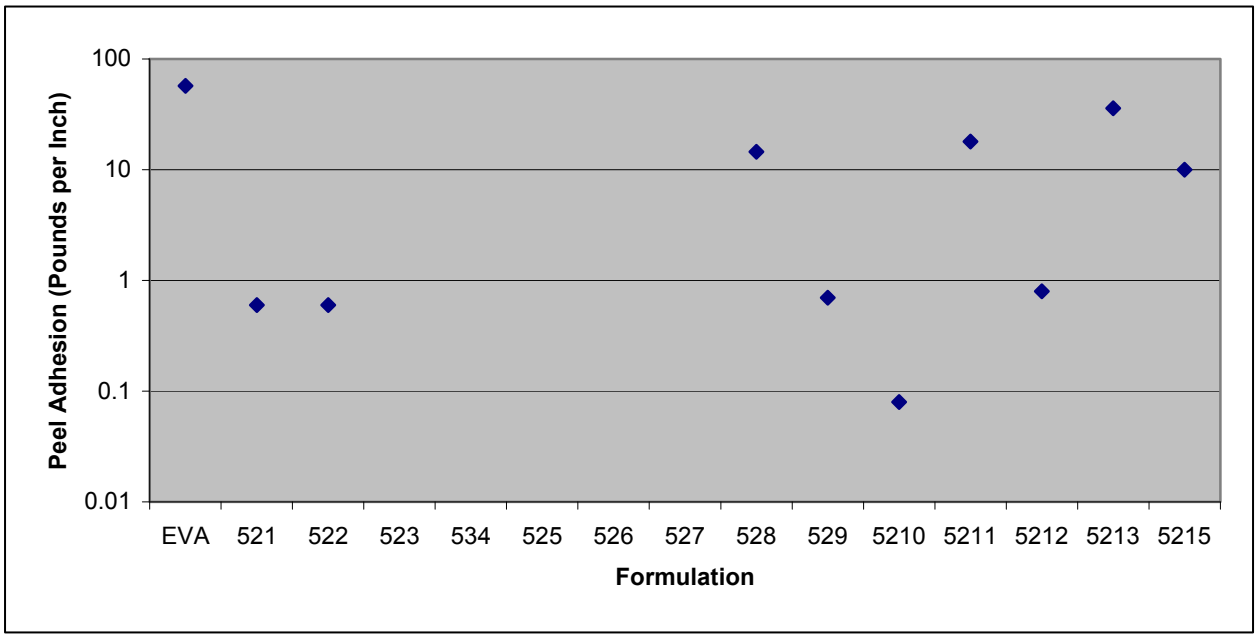

Figure 17. Peel adhesion of additional formulations.

Void formation was not observed during the trials. Voids typical form due to inherent stress in the encapsulant material from the extrusion process. X125-37 was manufactured using a proprietary process that eliminated the residual stress in the encapsulant sheet.

A 12-minute cycle at 150°C was deemed to be satisfactory to consistently produce modules with the required final encapsulant mechanical properties.

a-Si PV modules were made for damp-heat exposure (500 hours at 85°C and 85% relative humidity). Additional sample "plates" with the X125-37 were constructed to measure glass adhesion of the encapsulant during damp-heat exposure (1000 hours). X125-37-laminated a-Si modules appeared satisfactory after damp-heat exposure. No device degradation was observed at the glass/PV device interface or at the device (back)/encapsulant interface. No encapsulant delamination was observed as well.

Although no pictures were taken of the modules prior to exposure; however, the following photographs (Figure 18) show various areas of a module after 500 hours damp-heat.

Figures 19-22 show adhesion results of the encapsulant before and after 1000 hours damp-heat exposure against glass and the backside of the PV device (i.e., cell). X125-37 (E) was compared to other formulations that were derivatives of X125-37. Against glass, X125-37 adhesion strength was so strong before and after damp-heat (average

peel strength was 117 N/cm) that the pulling substrate failed during adhesion testing. Little adhesion degradation was observed for both glass and device backside after 500 hours damp-heat.

The adhesion results confirm that X125-37 shall adequately protect the module and PV device. Furthermore, we expect that modules manufactured with the formulation shall successfully pass a full IEC 61215 qualification testing sequence.

Based on these results, modules will be qualified with the X125-37 formulation.

Figure 18. Pictures of a-Si module after damp heat exposure.

TASK 6: INTERFACIAL CHARACTERIZATION OF ENCAPSULANT BONDING

Failure mechanisms in current thin-film devices are often attributed throughout the industry to moisture penetration into the module through the bulk of the encapsulant. The emphasis of Task 2 and 6 was to characterize the interfacial regions of thin film devices, both new and fielded, to develop a better understanding of the interfacial surface chemistry and to look for changes that may impact adhesion of the encapsulant to the various device substrates. The interfacial regions of the edge delete perimeter of thin-film modules are of primary interest in this analysis since the commercial grades of EVA encapsulants have exhibited lower adhesion within the edge-deleted regions. One major objective of this research was to determine the role of the edge-deleted region in

moisture transport into the thin-film module and subsequent corrosion of the thin-film device.

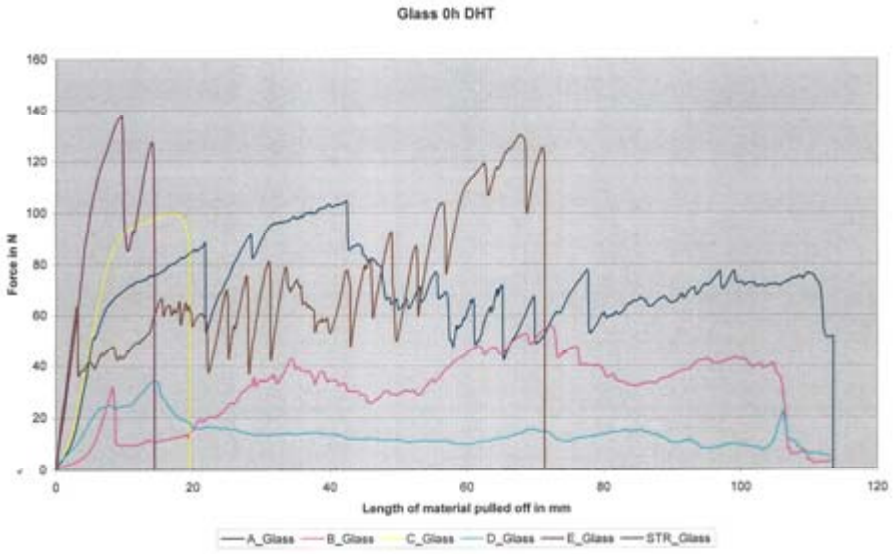

Figure 19. Glass adhesion strength results before damp-heat exposure.

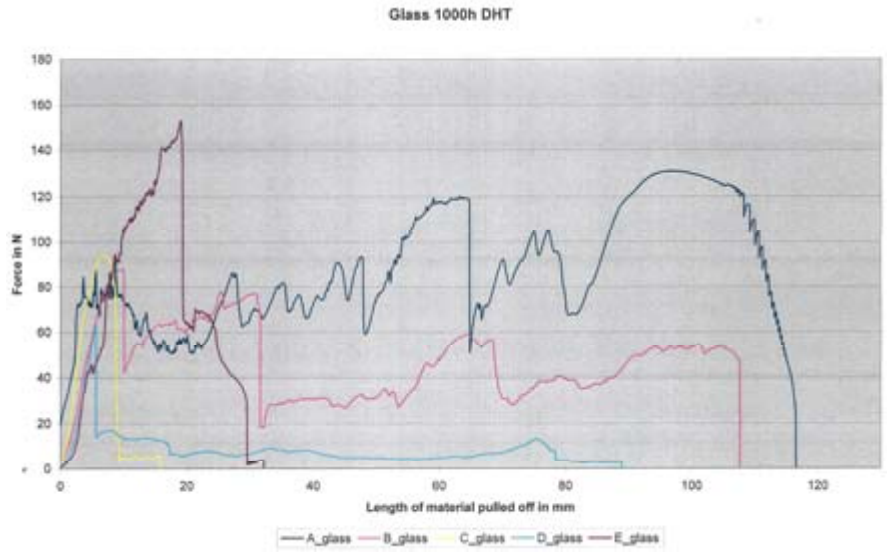

Figure 20. Glass adhesion strength results after damp-heat exposure.

Overview

The University of Connecticut, Institute of Material Science (IMS) has conducted a detailed failure analysis of good and failed amorphous silicon thin film modules and also failed and laboratory aged CdTe thin film modules. The findings from IMS are discussed in three (3) sections according to module type.

The first section of the report describes results for a visibly corroded a-Si module supplied by BP Solar. The a-Si module, identified as STR122-130, was reportedly accelerated aged under bias; the test conditions and final efficiency performance was not documented.

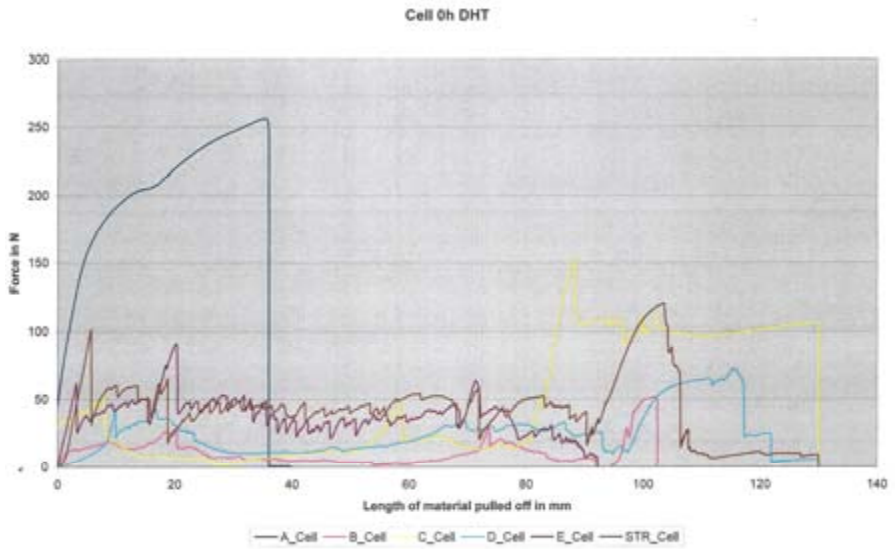

Figure 21. PV device adhesion strength results before damp-heat exposure.

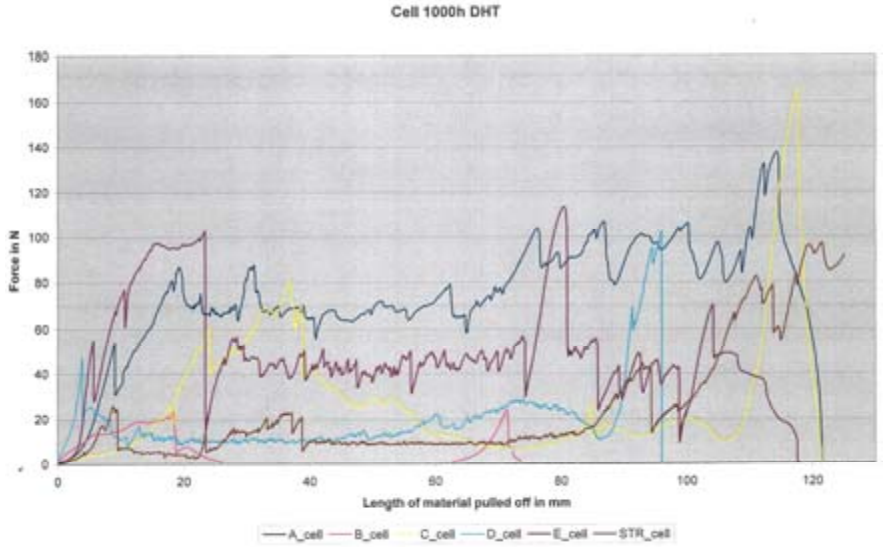

Figure 22. PV device adhesion strength results after damp-heat exposure.

In the second section 2, IMS discussed the analysis of a module provided by APS and labeled as STR 122-131-3. This module is amorphous silicon with a flexible back sheet construction and edge seal. The history for 122-131-3 with respect to fielding, aging, and operating efficiency is largely unknown, but given the designation of “OK” by the manufacturer.

Section 3 detailed findings for the analysis of two types of CdTe thin film modules. The first type was a BP Solar 980 CdTe module that had been fielded for three years as part of a 225 kVA Dublin California installation until gross failure when the cover glass became cracked. The final efficiency of this module was not possible to characterize due to the extensive module damage. The second BP 980 CdTe module was a module that had been laboratory aged for 250 hours at 85°C and 85% relative humidity and had a measured loss in fill factor of 11%.

Section 1: Examination of "FAILED Amorphous Silicon Module" # NREL/STR-122-130

Upon visual examination of the entire photovoltaic panel it appeared highly corroded (bar graph corrosion) on the bottom side but normal from lower middle to top of the module.

Small sections (~1cm square) of the laminated module were cut from the panel's corroded areas and normal appearing regions and named according to where they came from ("Corroded Device Area", "Good device area" etc.).

These still laminated module sections were opened up to give two samples each: the glass bearing the photovoltaic device, and the cover glass (also referred to as "mating-surface").

EVA has been used as a thin layer to laminate the two glass pieces together. This EVA layer adheres well to one of the two glasses, i.e., on separation the EVA would often primarily stay with one of the two surfaces (but not always the same surface). By processing multiple samples material could be obtained with the EVA on either surface.

XPS (X-ray photoelectron spectroscopy) data was obtained from numerous samples, five of which are detailed in the following table. The presence and/or absence of certain elements on these surfaces has been used to arrive at the following:

- Corroded Device Area glass with EVA on top surface (column #1 of Table 5): In addition to the common elements on a glass surface, like: C, Ca, Na, Mg, Si and O, we find that Sn, As and Zn are also present on the EVA surface of the "Corroded Device Area Glass, as seen in Row #1 of the table. These latter elements are most likely a part of the composition of the coated layers of the photovoltaic device on the glass. But here they are found to be present on the top surface of EVA layer covering the Device.

    - Mating Cover Glass, (column #2 of Table 7): These same elements, viz. Sn, As, and Zn are also present on the "Mating Cover-Glass surface". This confirms that these elements have not only diffused/permeated through EVA but have also deposited on the Cover glass.

- Deleted Edge Good Device Area, (column #3 of Table 6):

    - In spite of this being the deleted edge of the device-bearing glass, Sn is present on the surface. It could be the conducting film of Sn compounds that are normally deposited directly on the glass by the glass-sheet manufacturer or later on during the photovoltaic manufacturing process. It appears that this thin film has not been deleted fully, while the components of the PV device above were fully deleted.

    - The presence of a current path provided by the improper deletion of Sn from the deleted area would have given rise to electrolytic plating/deplating action in the areas where the water permeation (bottom side of panel) was sufficient to form an electrolytic path. This would explain the occurrence of heavy corrosion as observed on the bottom side of the module during the wet/hot environment tests.

- Mating Glass of Deleted Edge of Good Device Area (EVA on Top Surface in contact with deleted region), (column #4 of Table 6):

    - No Sn was detected in this regions (as expected) whereas it was detected in a similar sample from the corroded sample – indicated either a locally better delete on the photovoltaic device panel or: the EVA surface in contact with the deleted edge of the good device area, did not get any Sn coating because of absence of water and therefore lack of electrolytic process. Whereas on the bottom side of the module over a longer period of time, water could have collected and permeated sufficiently into the EVA and on the EVA-Glass interfaces to cause the electrolytic plating/deplating action.

- Good Device Area (No EVA on Top Surface), (column #5 of Table 6):

    - It is observed that Mg, K and As are absent from the top surface while Sn is present (as the top conducting layer of the device). It is possible that Mg, K and As are normally present deeper in the device and cannot therefore be detected by XPS while in sample #1 the corrosion process brought them up to the surface and hence through the EVA to its top surface, as seen in row #1 of the table.

High resolution XPS of the C peak in both the regions that appear good and those that appear corroded are similar indicating a relatively consistent C state distribution independent of location. A typical high-resolution spectrum of the C1s peak is shown in Figure 23. Peaks 1-4 are expected for EVA as detailed by Klemchuk et al.[72] for ~33 wt.% VA EVA. A small (0.5-1.5 at. %) fifth peak was noted in all regions indicating slight aging of the EVA.

Visual Observation

The cover glass in a corroded region of the panel bears a mirror image (as can be seen by the naked eye) of the corroded zig-zag lines or islands as present on the corroded device glass indicates that these elements got transported through the EVA by the corrosion process.

Sample Type: / Elements (ev)/At. Percentage	Corroded Device Area Glass-EVA on Top	Mating Cover Glass of Corroded Device Area	Deleted Edge of Good Device Area	Mating Glass of Deleted Edge of Good Device Area (EVA on Top)	Good Device Area (No Visible EVA on Top Surface)
C 1s	284.65 ev	284.48	284.58	284.05	284.33
	65.16 %	46.69	58.64	74.53	65.4
Na 1s	1072.65	1072.48	1072.17		1073.33
	0.44	2.04	2.01		2.14
Mg 2s	90.65	90.48			
	6.03	8.04			
Ca 2p	348.65	349.48	347.20	347.05	350.33
	5.08	1.65	0.61	0.3	0.64
Si 2p	102.65	103.48	102.54	104.05	103.33
	4.78	10.53	10.74	5.94	3.9
O 1s	531.65	532.48	532.56	531.05	533.33
	16.57	28.49	25.99	19.23	24.61
Zn 2p	1022.65	1022.48			1025.33
	0.18	0.46			0.34
K 2p	300.65		304.54		
	3.22		1.43		
As 3p	139.65	142.48			
	0.99	0.57			
Sn 3d	487.65	487.48	487.51		489.33
	2.11	1.54	0.57		2.97

Table 6. Summary of XPS data of failed module NREL/STR –22-130.

FTIR

The various exposed surfaces of EVA (corroded regions, uncorroded, device and delete) were also examined by FTIR (Fourier transform infrared spectroscopy). Typical spectra are shown in Figure 24. No differences were observed.

Although we have only acquired data on one failed module there are several interesting phenomena. We observe mirror image corrosion patterns on mating sections of cover glass and device sides. Where there is visible corrosion there is transport of various elements through the EVA. This indicates that the two surfaces somehow "communicate" with each other possibly by transport/diffusion through the EVA in a wet

(?) environment.

We observe indications that the deletion process may not have been 100% effective and may leave residual Sn in deleted regions where it is not desired.

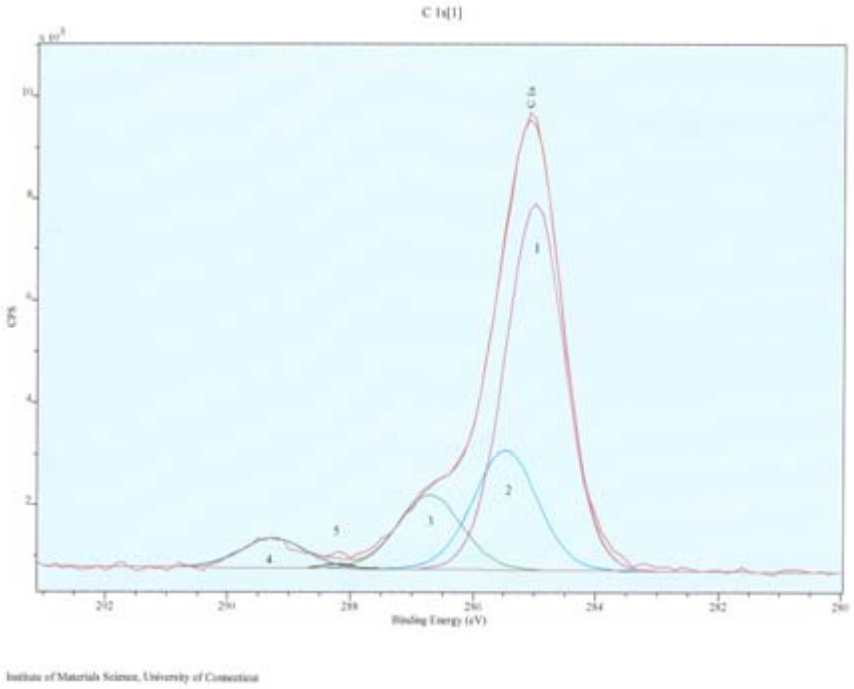

Figure 23. High Resolution XPS C1s in EVA.

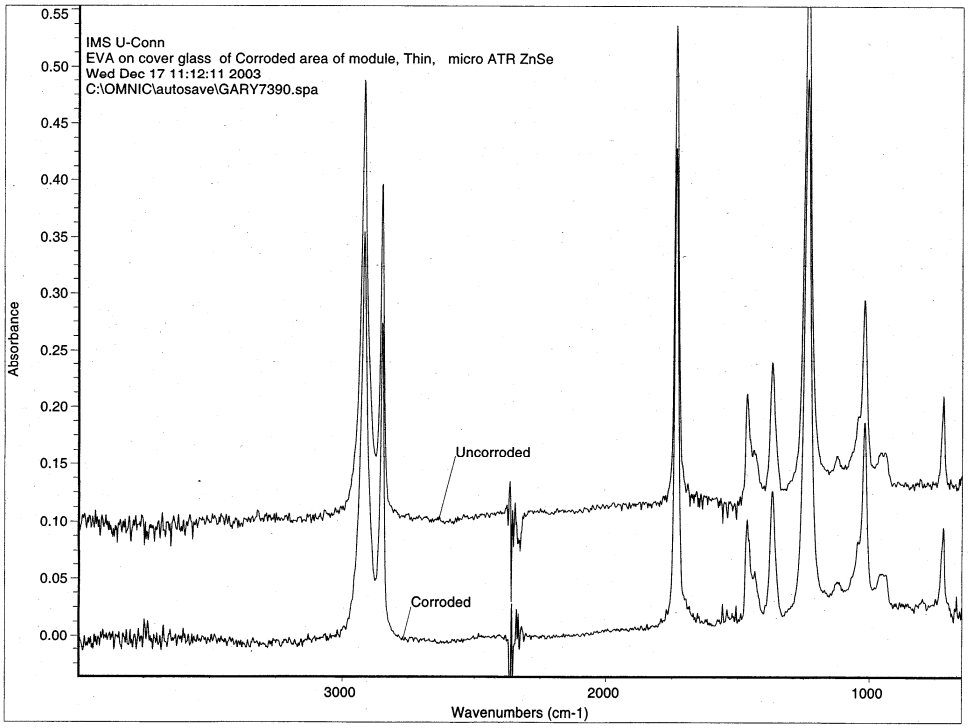

Figure 24. Typical FTIR spectra. These specific spectra are from corroded and uncorroded cover glass in a device area.

To-date all results are consistent with a two-phase degradation of the EVA/Glass region. Initially the glass/EVA bond is weakened by the presence of water. This is a reversible effect. On prolonged exposure to water the glass degrades leading to the corrosion pattern and decreased performance.

Section 2: Examinations of Module # STR122-131-3

We have begun to examine module STR #122-131-3 which was described to us as "OK" – not failed. We do not know its history. However please remember that the construction of this module is quite different from that of the failed module we are in the process of studying extensively. This (OK) module consists of a glass panel on which the photovoltaic device has been coated. The edge-deleted width is only 3 mm wide as compared to the failed module's approximately 10mm delete all around. This (OK) panel has no cover glass; rather it has a thick black polymer covering one entire surface. Further another translucent polymer material exists as a thick bead all around the edge of the device. Both of these materials will be examined as part of our investigation of this device.

We also plan to examine the EVA more completely and compare the used material to new unused material by XPS for examination of the aging peak, FTIR, GC/MS (gas chromatography with mass spectrometry) for any absorbed volatiles, and EDX (energy dispersive X-ray analysis) for further indication of transport of material not expected to be in the EVA.

It was found that EVA films between glass substrates and superstrates in photovoltaic cells could be removed on exposure to low (LN_2) temperatures. The freestanding EVA films were then cryo-fractured so the bulk material was not contaminated and the cross-section examined by SEM (scanning electron microscopy)/EDX. Figure 25 is an EDX spectra of a typical cured EVA used in photovoltaic cells as supplied to IMS by STR.

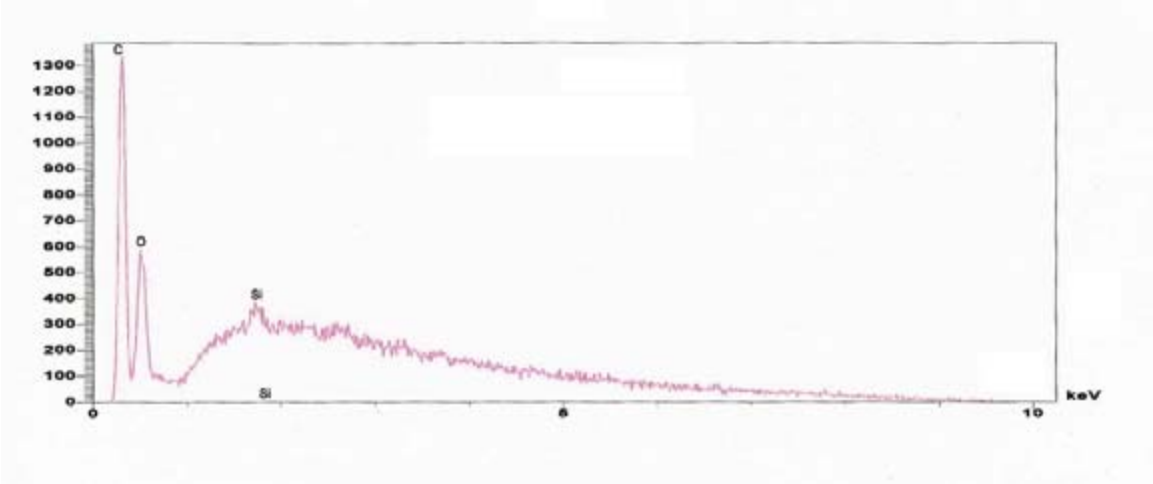

Figure 25. Typical EDX spectrum of virgin cured EVA as supplied by STR.

Although we did not have a “good” module with known history we did have several small sections of various photovoltaic cells that did not show any sign of corrosion or delamination. Numerous cross-sections of EVA extracted from these samples were examined. Most were similar to the spectrum in Figure 25.

However, occasionally foreign materials were detected within the EVA, particularly near the edges of the device. Figure 26 shows a spectrum revealing contamination typically found within the EVA near the edges of this device. Determination of the source of the K and Cl cannot be made with certainty. However, they are common contaminants found in local water supplies.

Examination of a photovoltaic module, which exhibited significant corrosion along one edge, was then undertaken. Freestanding EVA samples were acquired from several regions; good appearing delete region, good appearing device region, corroded appearing device region and corroded appearing deleted region. Multiple cryo-fractured EVA samples were obtained in all of these regions.

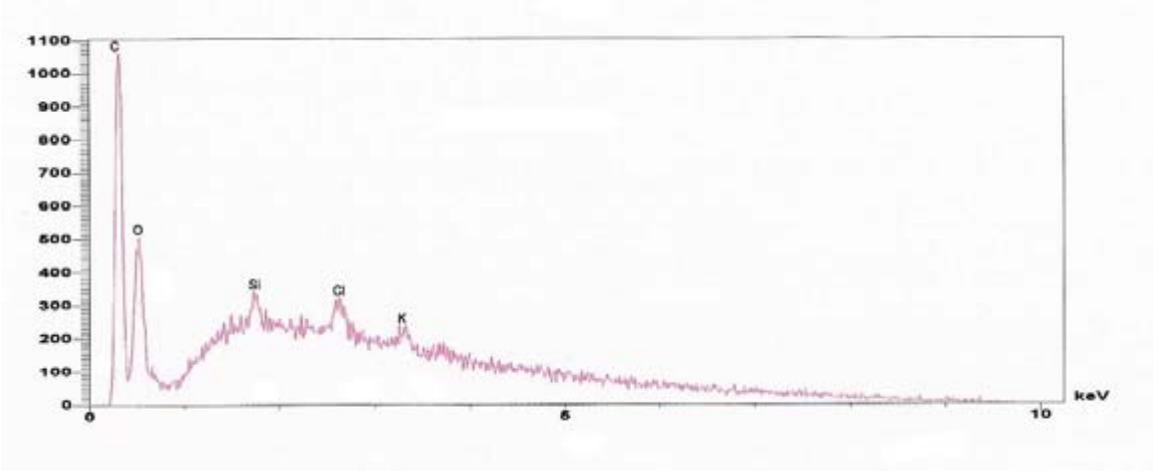

Figure 26. EDX of “good” module near edge.

As shown in Figures 27–32 some contamination within the EVA was found in all locations in this module. However; the contamination within the EVA was heaviest in corroded areas (either device or delete region). Common contaminants in regions that did not appear corroded (Figures 27-29) include Ca, S, K, occasionally Cl, and sometimes an excess of Si. Contamination within the EVA was much heavier in regions where corrosion was visible optically (Figures 28-31). Contaminants in these regions include all of the above contaminants, large excesses of Si (particularly in device region), and occasionally Al, Na and Fe. Without doing controlled experiments it cannot be determined for certain whether these contaminants are due to degradation of the glass/device or are brought in with any water or other material permeating the device.

Our previous analysis of the composition of these glasses (September 2003) indicated that, to some extent, all of these materials, except S and Cl, are components of the glass itself and thus this contamination could be due to glass degradation. Alternatively; we commonly detect K and Cl contamination in local water supplies and occasionally S,

Na and Fe. Without more controlled experiments the source of the contamination within the EVA cannot be unambiguously determined. We believe it is likely that both glass degradation and associated water ingression play a part in the migration of these materials into the EVA.

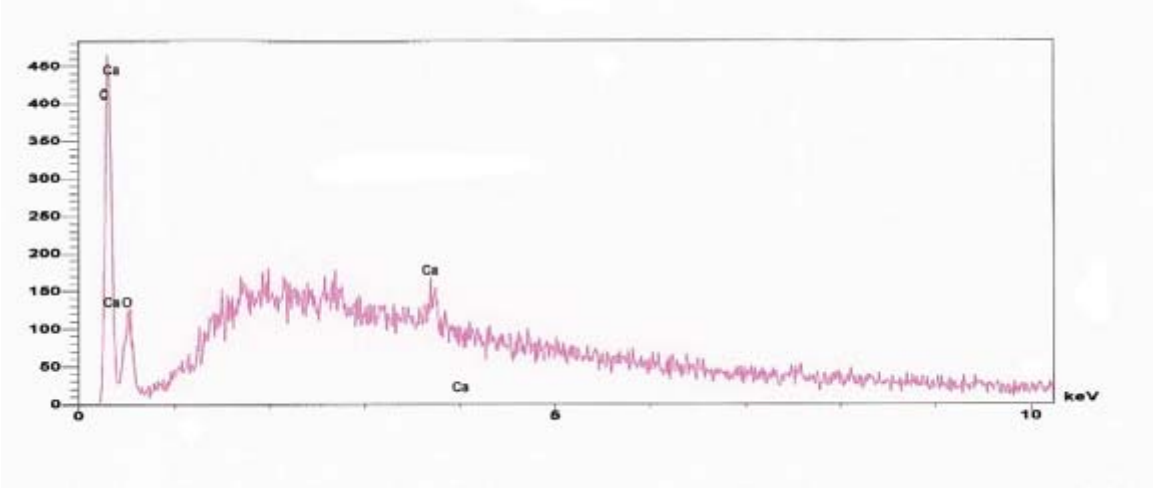

Figure 27. Corroded device – EVA in good device area.

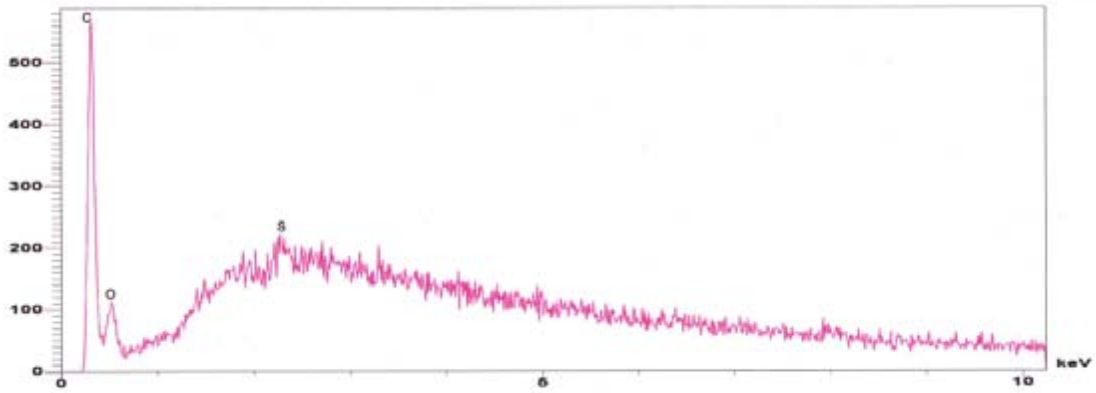

Figure 28: Corroded device - good delete area.

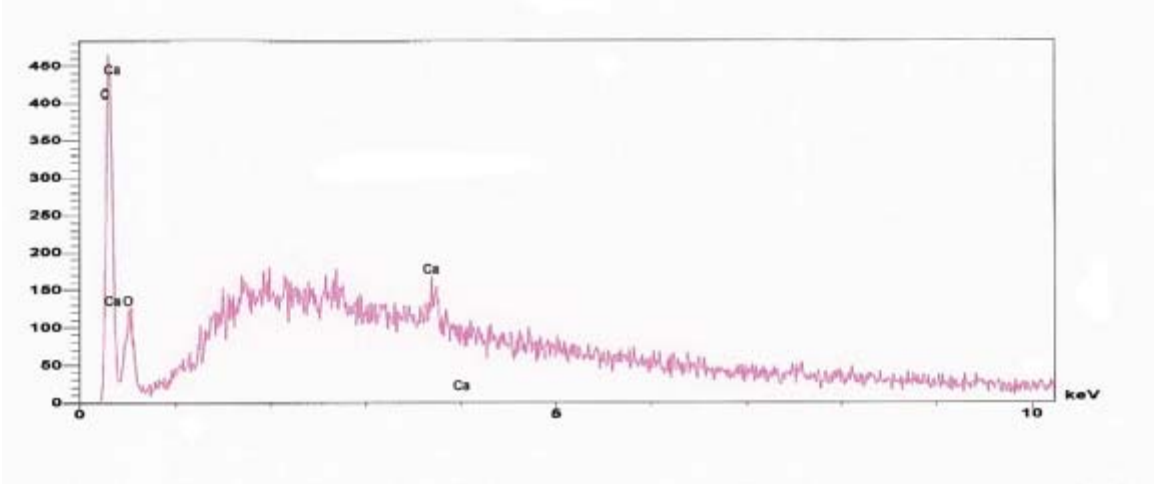

Figure 29. Corroded device – good delete area.

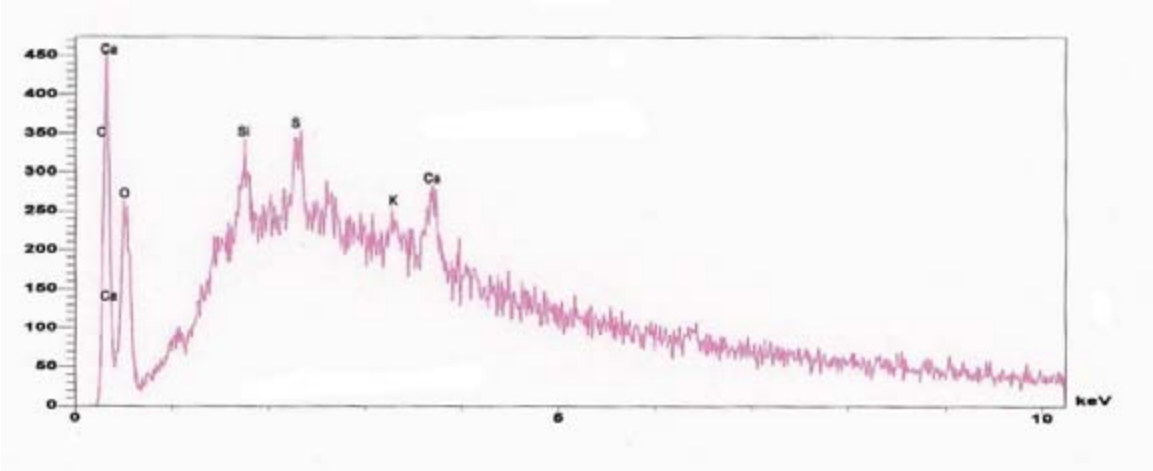

Figure 30. Corroded device – EVA in corroded deleted area.

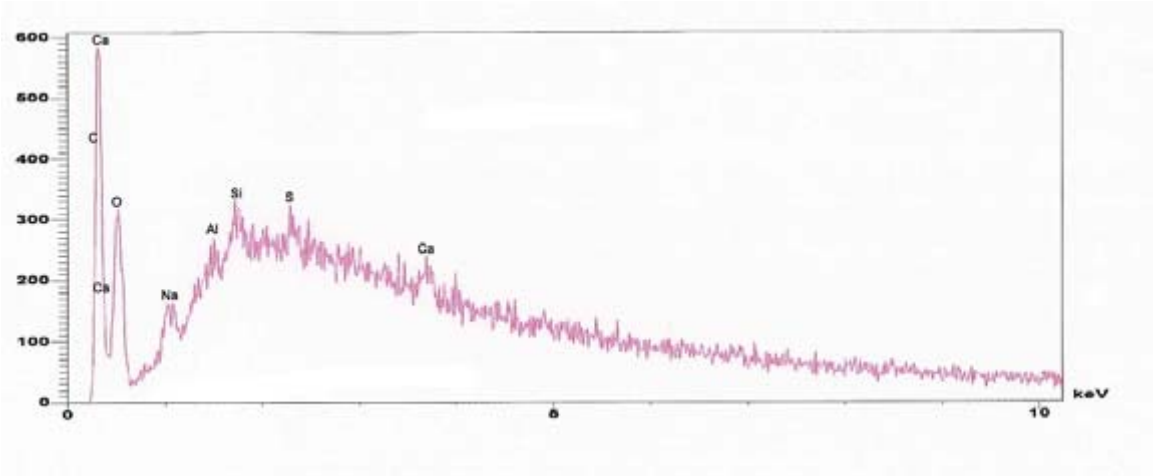

Figure 31. Corroded Device –EVA in corroded deleted area.

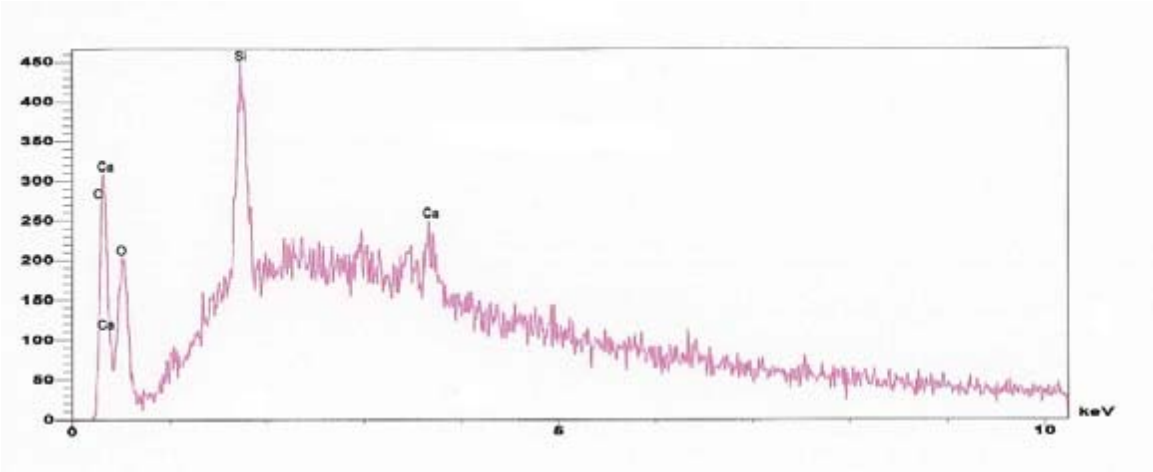

Figure 32. Corroded Device – corroded device area.

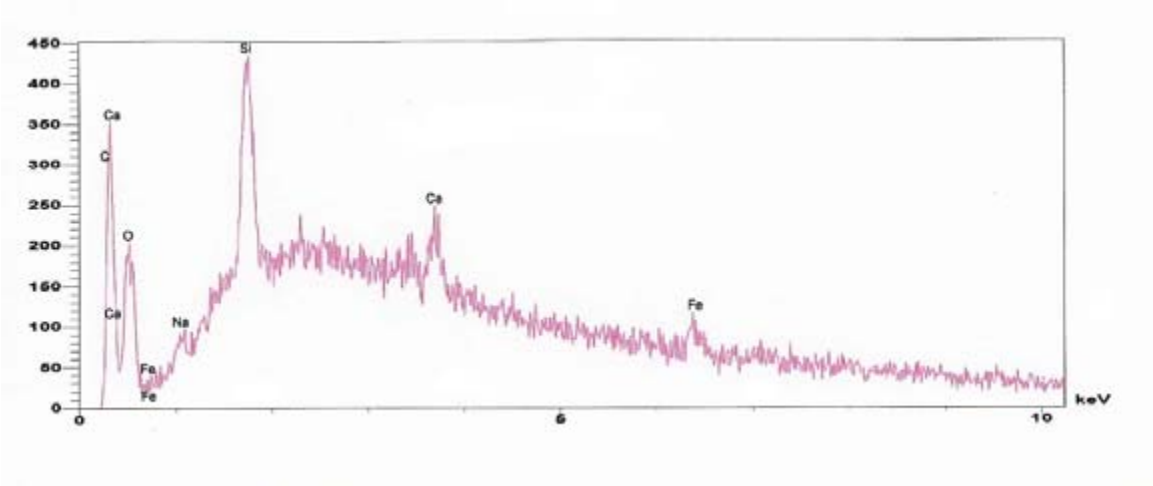

Figure 33. Corroded device – corroded device area.

Section 3: Evaluation of 2 BP Solar CdTe Modules

The EVA, EVA/glass and EVA/device interface have been examined by multiple techniques for two BP Solar CdTe photovoltaic modules. One of the two had cracked in the field after some usage (BP-980). The other (BP-980B) was tested in the lab under accelerated aging conditions (250 hours at 85°C/85% RH). T his unit had a measured loss in fill factor of approximately 11%. Patches of discoloration were observed visually on BP-980B over the junction box and extending a couple of cm from the junction box where the wire leads exit the device. Other than these patches and the crack no other signs of degradation, discoloration, or corrosion were observed visually. Upon disassembly of the modules no discoloration or brittleness was observed in the EVA. On disassembly and sample preparation for XPS and other examinations we did not observe a classical delamination in these discolored regions. Rather, the device appears to fail more cohesively in this discolored region than in other normal colored regions. On separating the device and EVA in a normal colored region most of the device remained with the glass upon which it was deposited. However, in this region of discoloration, the device appears to split more evenly between the glass surface where it was originally deposited and the EVA.

EVA samples from various locations (several in the delete region, several in the device region near the junction box, several in the device region in numerous other locations) in both CdTe samples were examined by FTIR. Figure 34 is a typical FTIR spectrum of EVA from either module at any location. As detailed in Klemchuk[72] various absorbance ratios could be used as a measure of change in EVA composition. However, all spectra were similar and any differences between spectra obtained at different locations were well within experimental error.

The bulk composition of the EVA extracted from many locations was investigated by cryo-fracturing and examining the cross-section by SEM/EDX. In general these samples were much less contaminated than those from the corroded photovoltaic cell. The baseline (virgin cured but unused EVA) has an EDX spectrum as shown in Figure 35.

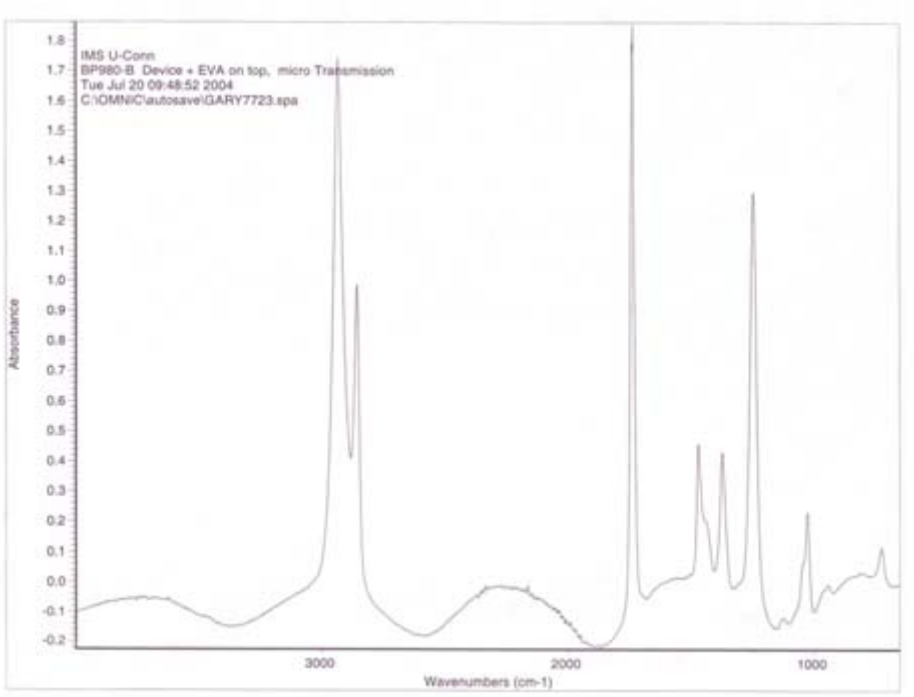

Figure 34. Typical FTIR spectrum of EVA in CdTe solar cells.

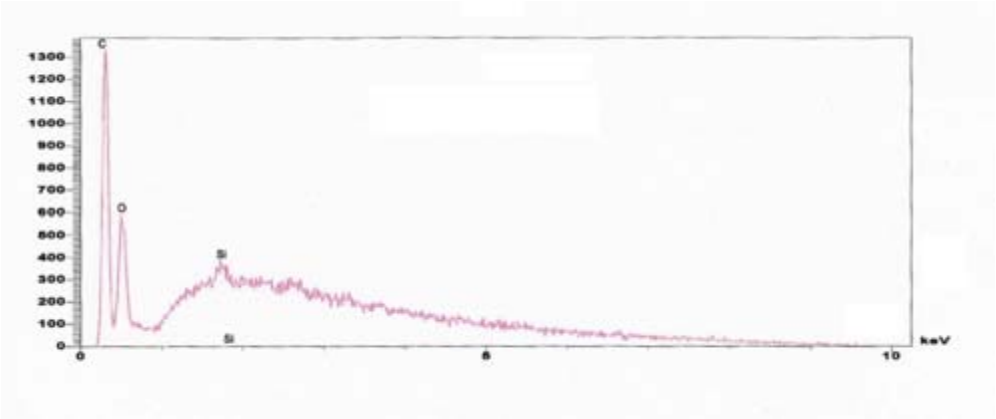

Figure 35. Typical EDX spectrum of virgin cured EVA as supplied by STR.

In general, EDX spectra obtained from samples of EVA from these two modules were very similar to this spectrum. We did occasionally find small amounts of contamination within the EVA as shown by the following spectrum (Figure 36). The most common contamination was an excess of Si. Traces of Ca, Sn, Na and Cl were also found to some extent within the EVA. These were not major contaminations (most were barely detectable by EDX), and there did not, in general, appear to be any preference for one location within the device over another (although as noted below Cl was not detected in the delete region).

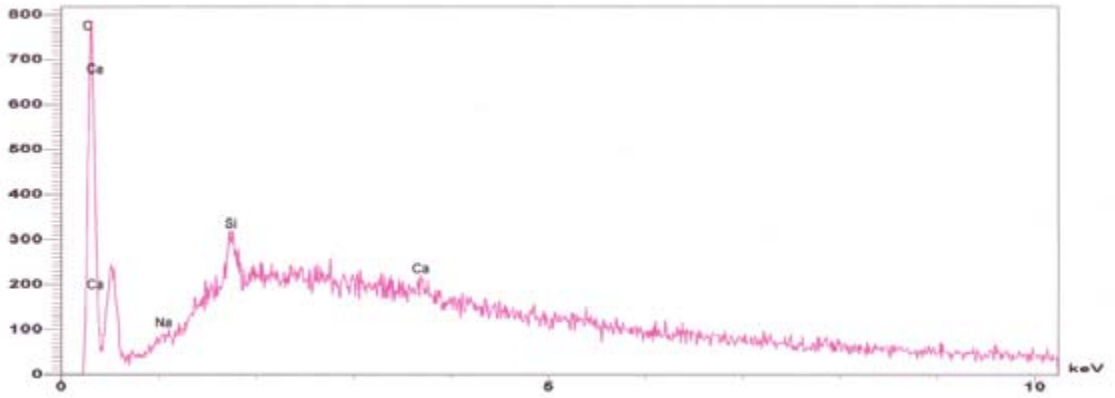

Figure 36. Typical contamination within EVA in CdTe modules.

Numerous locations within both of the CdTe modules were examined in detail through the use of XPS. In order to create a baseline a section of a cover glass in a CdTe device was sandblasted at IMS and examined by XPS (Figure 37). This spectrum has been quantified and the results are contained in column H in both Tables 7 and 8. These tables summarize some of the XPS analysis performed on these two modules.

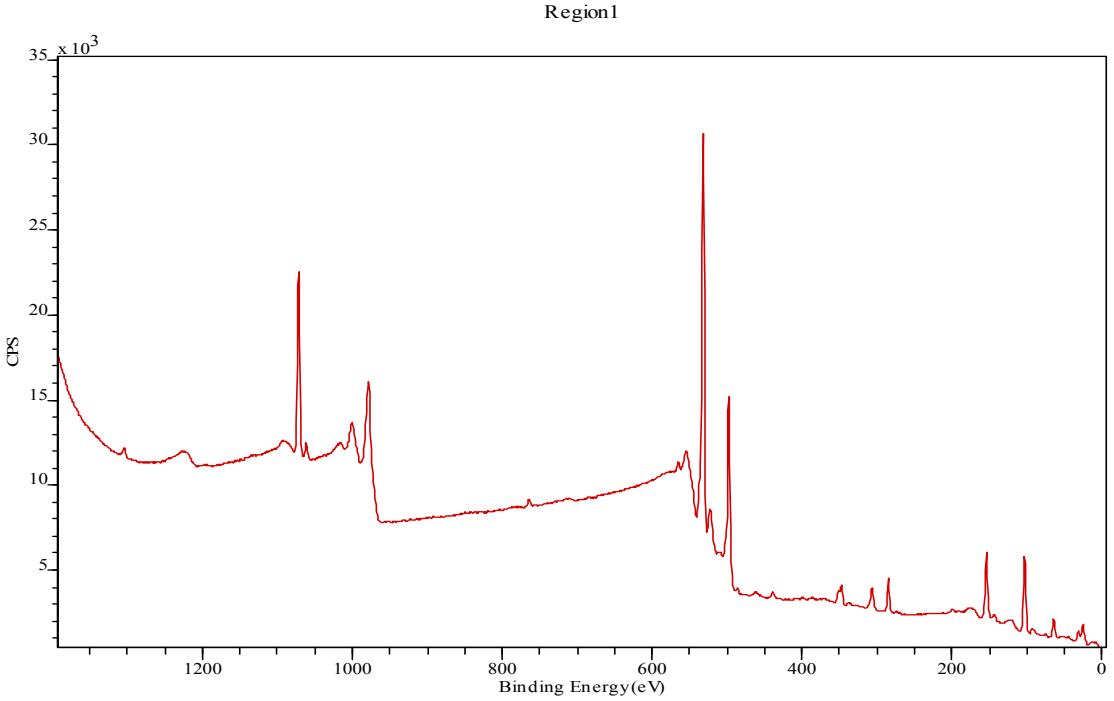

Figure 37. XPS spectrum of CdTe glass sample sandblasted at IMS.

Figure 38 illustrates where XPS examinations were performed on the CdTe module that had cracked in field. Table 7 summarizes the quantification of these spectra.

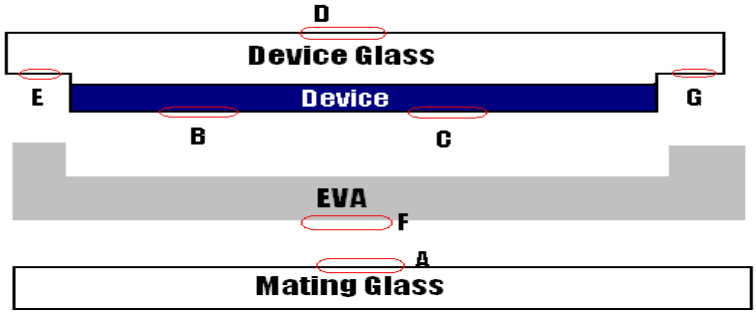

Figure 38. Location of XPS examinations in CdTe field fractured module.

	Sample							
Element	A	B	C	D	E	F	G	H
C	67.5	54.2	44.5	25.8	75.9	71.8	82.9	10.9
Si	12.5	11.6		19.8	9.2		4.4	27.2
O	19.4	29.0	30.6	42.8	13.6	16.2	11.1	49.2
Sn		2.4	5.5	0.6		0.7		
Cd		0.6	7.0			1.2		
Te		2.2	3.4			0.5		
Na	0.55			1.3	1.0	0.3	1.1	6.8
Cl			9.1			9.1		0.2
N				1.7				
Ca				0.7	0.3		0.5	1.8
Mg				4.4				4.0
Al				2.8				
Ti								0.2

Table 7. Quantification of XPS for CdTe field fractured sample.

The presence of a relatively large amount of C on these “glass or device”(except sample F) surfaces is due to thin residual layer of EVA on either the glass or device after sample preparation. Most of the materials observed are expected from the EVA, glass or the device. However, a major contamination of Cl was noted in this module. The Cl was only detected in the device region and not always there. Cl was not detected in the delete region.

As above, the presence of a relatively large amount of C on these “glass/device” surfaces is due to thin residual layer of EVA on either the glass or device after sample preparation. Most of the materials observed are expected from the EVA, glass or the device. However; a major contamination of Cl was noted in this module. The Cl was only detected in the device region and not always there. Although the number of samples is limited it appears Cl is more common in the device region near the junction box rather than other locations in the device region. Again, Cl was not detected in the delete region.

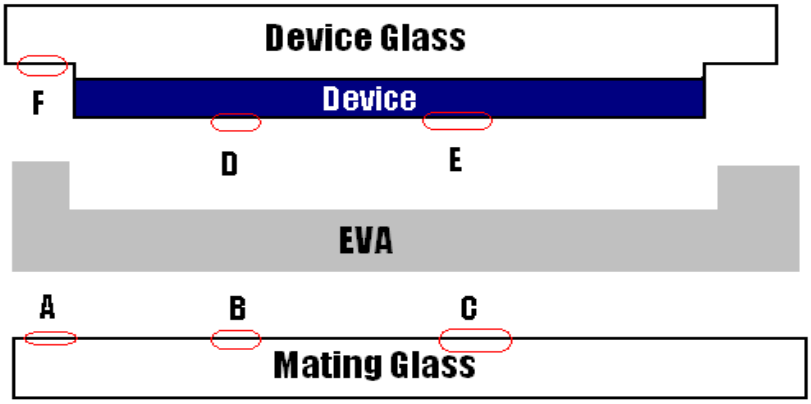

Figure 39. Location of XPS samples in 250 hour accelerated aged CdTe module.

	Sample						
Element	A	B	C	D	E	F	H
C	58.1	77.6	68.4	62.3	51.7	80.5	10.9
Si	13.7	7.1	11.6	3.8		7.0	27.2
O	25.8	13.9	17.9	20.3	24.2	11.7	49.2
Sn				2.3	5.9		
Cd				3.2	5.0		
Te				8.1	5.7		
Na	1.7	0.9	1.6			0.5	6.8
Cl					7.5		0.2
Ca	0.7	0.5	0.5			0.3	1.8
Mg							4.0
Ti							0.2

Table 8. Quantification of XPS for CdTe module with 250 hours accelerated aging.

The surface of the EVA after separating from the mating glass was studied extensively by XPS in these two samples. Samples were typically taken in three locations as indicated in Figure 40. In the device region both near and away from the junction box, in the deleted region, and near the device/delete interface.

Both survey spectra and high-resolution XPS spectra of the C1s peak were obtained. Cured but unused EVA as supplied by STR was also examined as a reference material. Figure 41 is a high-resolution spectrum of the C1s XPS peak of the reference EVA. The calculated values (in atomic percent) of the various states of C are in good agreement with previous studies.

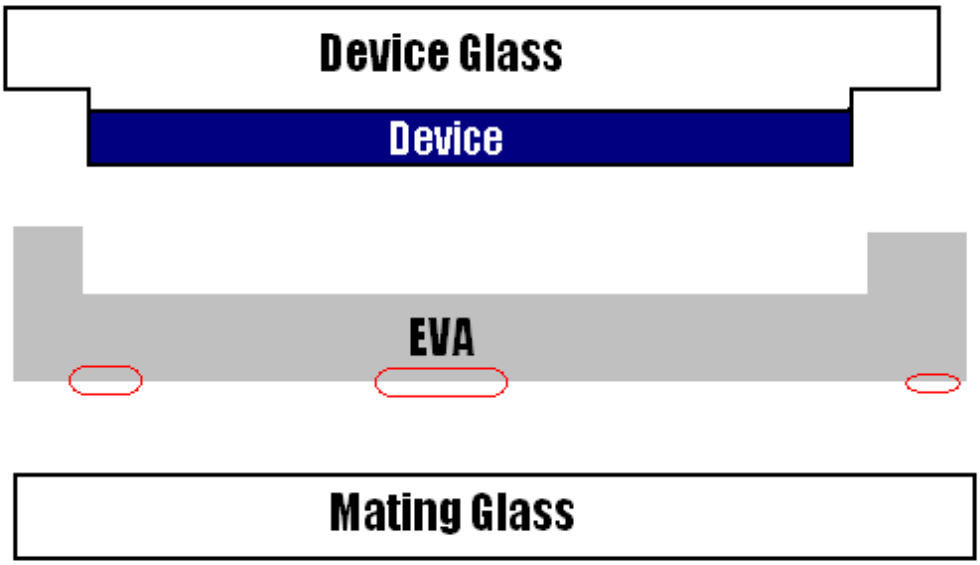

Figure 40. Location of samples for XPS examination of EVA.

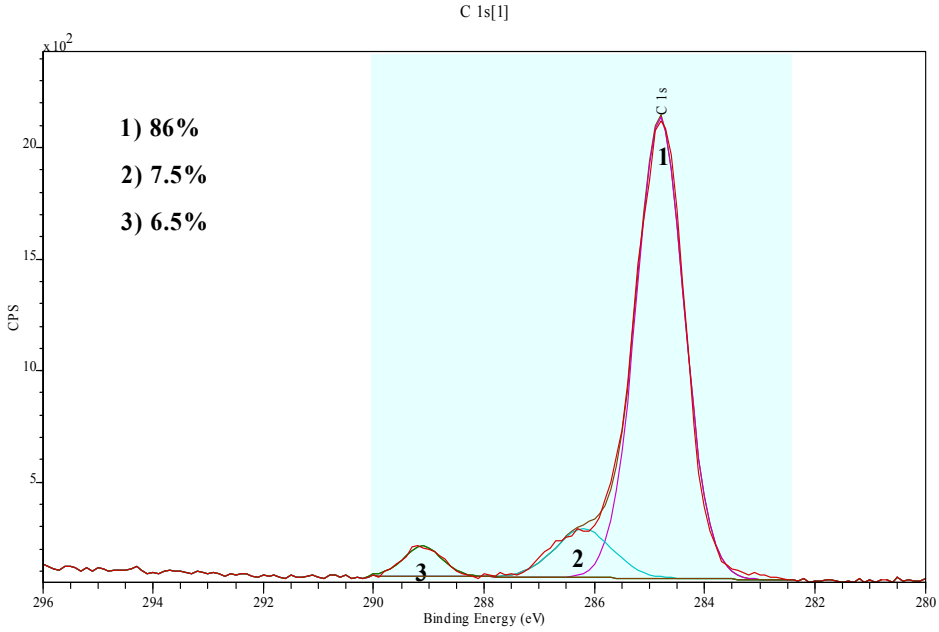

Figure 41. High-resolution XPS spectra of reference EVA.

Figures 42 and 43 are typical XPS survey spectra obtained from the CdTe modules.

Figures 44 and 45 are high-resolution spectra of the C1s peak in the indicated module. In both of these modules a trend in the high-resolution spectra of the C1s peak was noted from the interior to the edge of the device.

The high-resolution XPS spectra of the C1s peak in the delete region of both modules closely resemble the reference spectrum of cured but unused EVA as shown in Figure 46.

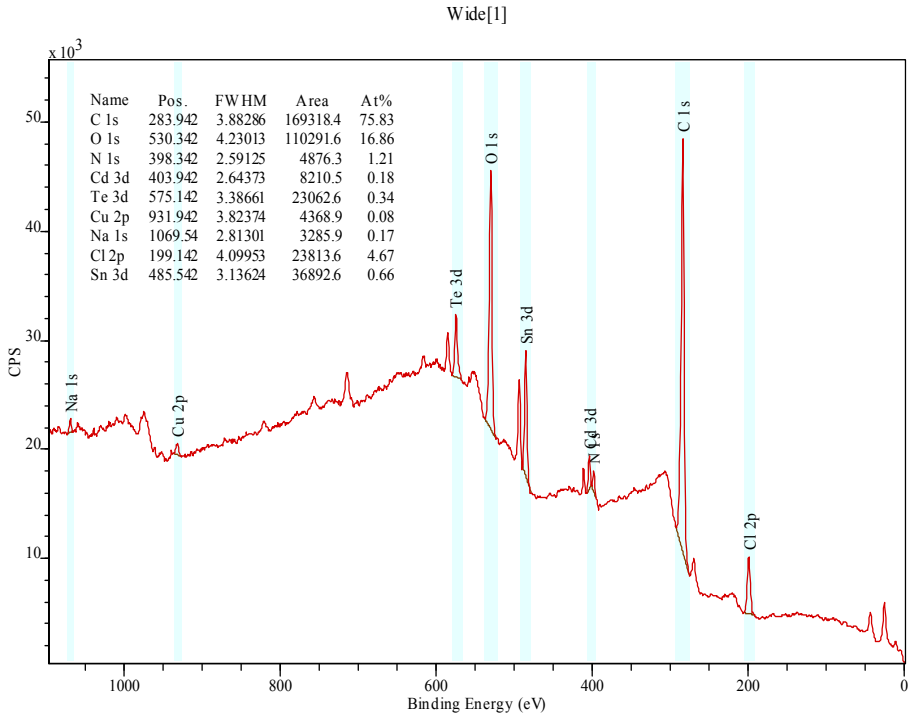

Figure 42. CdTe fractured module, device region near junction box.

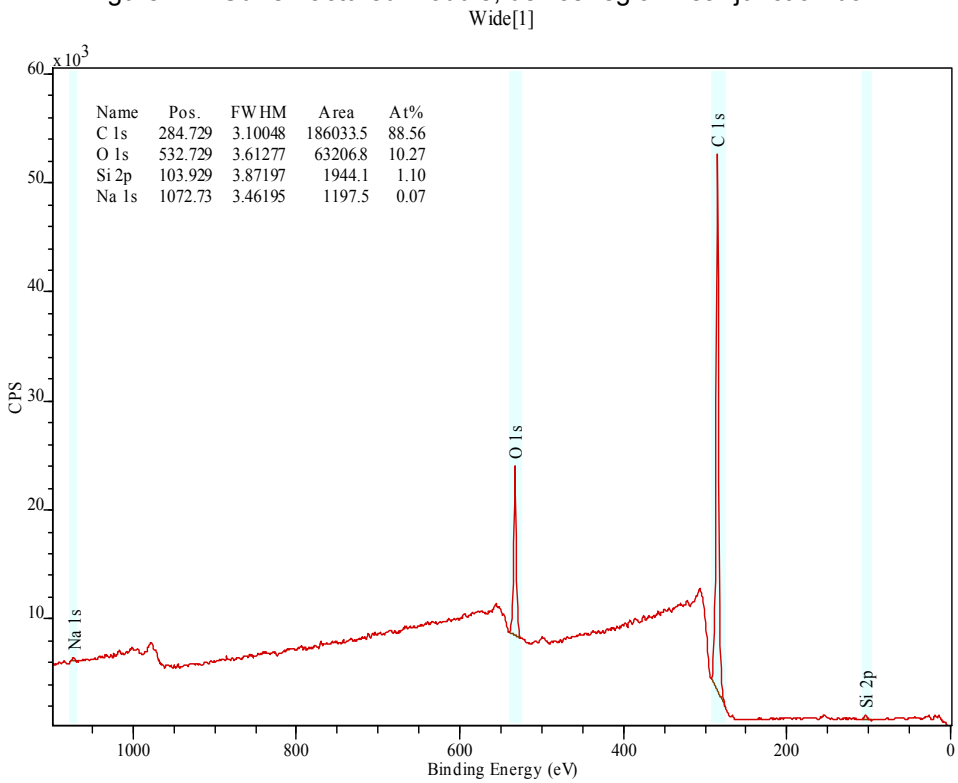

Figure 43: CdTe fractured module, delete region.

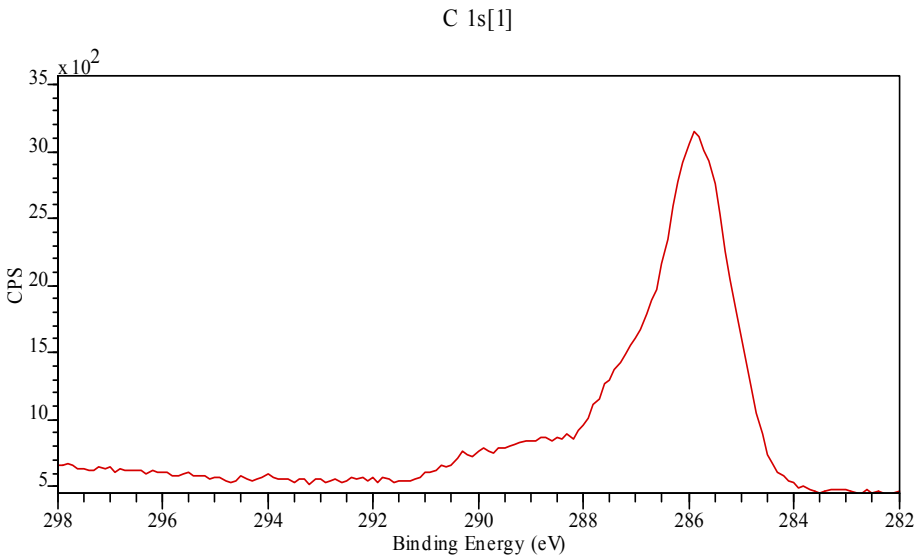

Figure 44. C1s region of CdTe fractured module, device region near junction box.

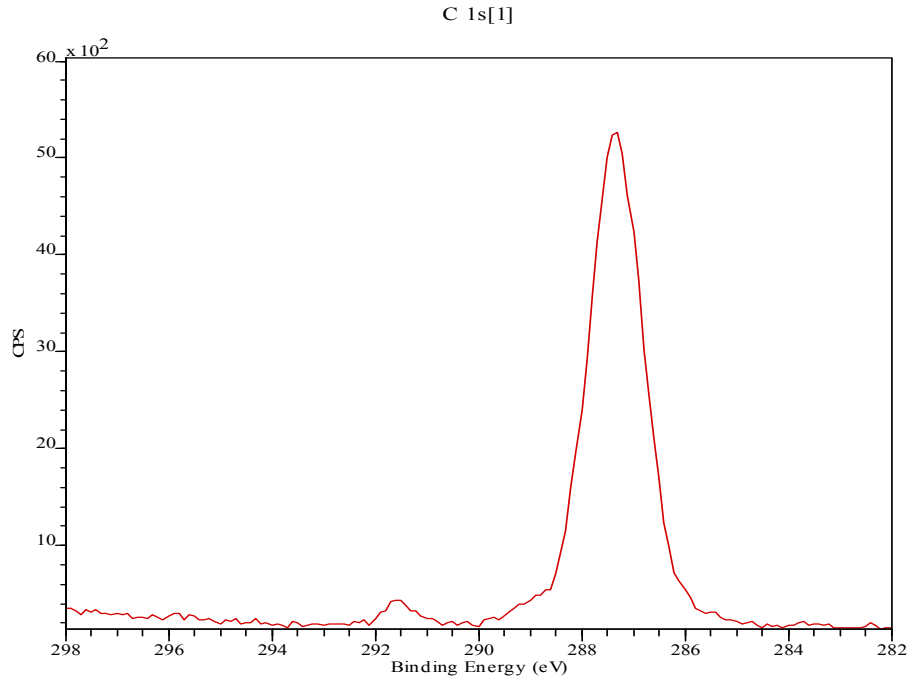

Figure 45. C1s region of CdTe 250 hour accelerated aging module, delete region.

In both the field fractured sample and the aged module we noted a change in the detailed C1s structure as the region of interest moved towards the interior of the device. Figures 47 and 48 show this change for the field fractured device and aged module respectively.

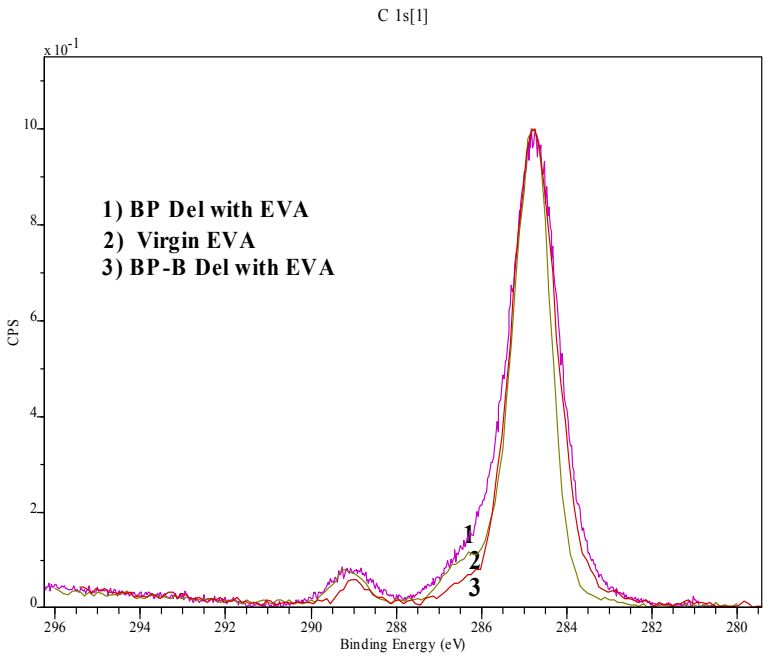

Figure 46. Comparison of C1s peak in deleted region of both devices and reference EVA.

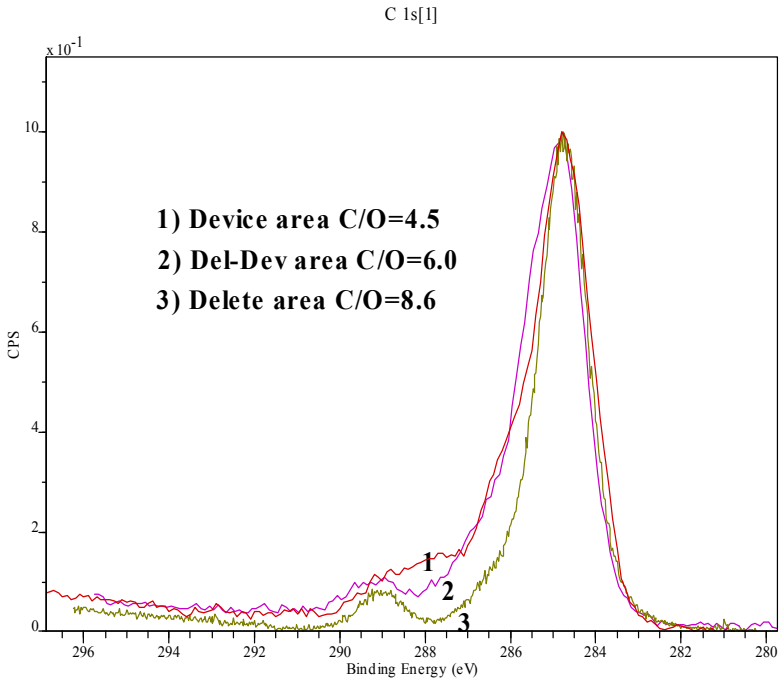

Figure 47. CdTe fractured module C1s spectra.

As indicated on these graphs there is also an associated increase in the amount of oxygen measured in the survey spectra as indicated by the decrease in the C/O ratio for the interior of the device versus the edge. Component analysis of a typical high resolution C1s XPS peak for EVA in the device region is indicated in Figure 49.

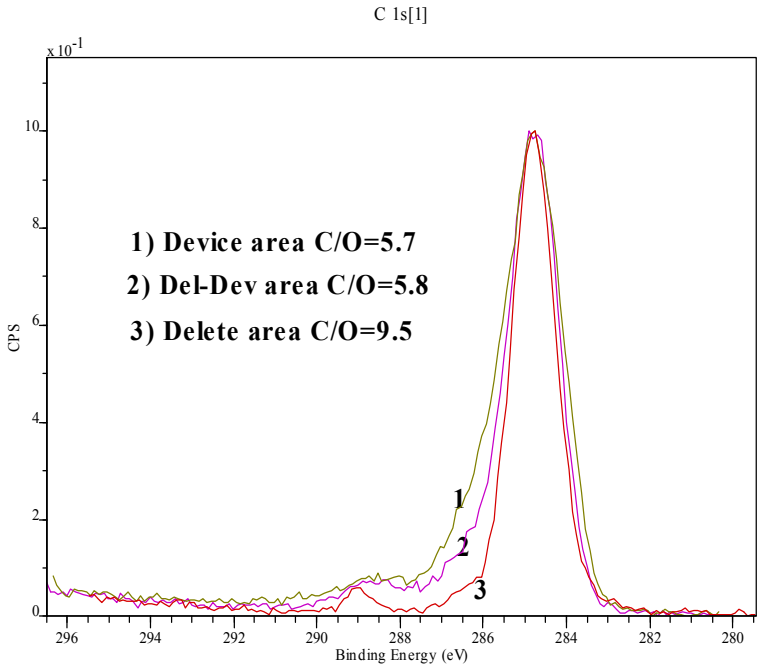

Figure 48. CdTe accelerated aging module.

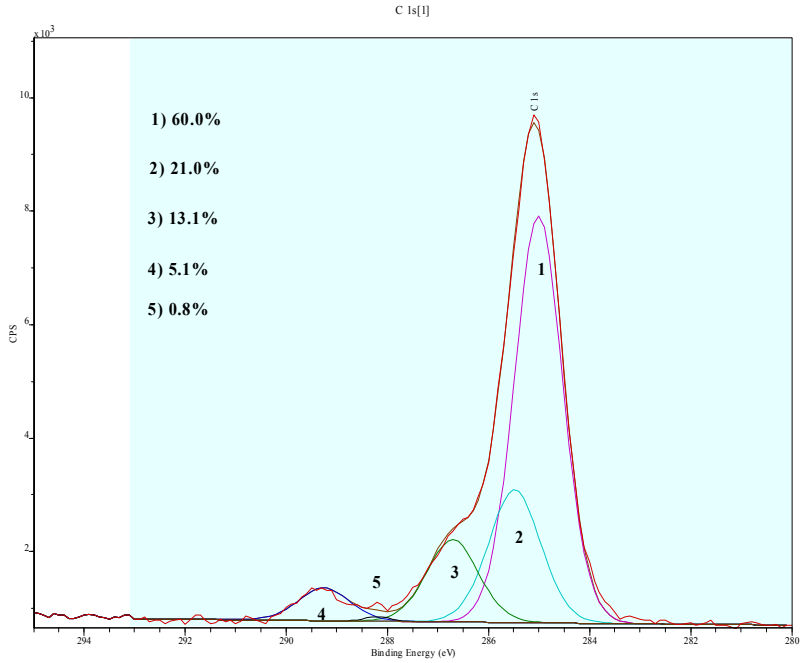

Figure 49. Typical component analysis of C1s spectrum in device region.

The measured shifts and concentrations of the various states are in good agreement with that previously reported by Klemchuk[72] for EVA in used photovoltaic modules.

As with the XPS of the glass or device surfaces we did find occasional significant amounts of Cl on the EVA (see Figure 42 for example). As with the XPS of the glass or device, Cl was not found in the EVA in the delete region of either device but was found in the device region and may have a preference for the device region near the junction box.

Although IMS measured a change in the EVA in these two devices no causal relation between these changes and device performance can be established from this study. More controlled experiments are necessary to confirm a connection between the two.

Conclusions

The conclusions based on the IMS literature study have mirrored the industry belief that moisture is a large contributor to the premature failure of the thin film devices. UCONN-IMS postulates the following probable failure mechanism:

1. Water migrates through EVA to glass/EVA interface.

2. Water rapidly degrades soda-lime glass surface (both the EVA and glass corrosion product also probably swell) leading to delamination.

Therefore, water must be prevented from reaching the EVA/glass interface.

Furthermore, a major indication at the conclusion of Tasks 2 and 6 is that soda lime glass that has been utilized in the fabrication of thin-film devices appears poorly suited to the fabrication of photovoltaic modules from the perspective that it is not especially stable when exposed to voltage and moisture. The literature indicated a migration of sodium ions to the TCO surface of the modules and, inevitably, delamination of the TCO layer from the glass. This problem appears to be delayed if moisture can be eliminated at the surface of the glass.

Given the instability in the glass, it appears that enhancing EVA adhesion to the glass likely will not play a substantial role in improving the reliability of the photovoltaic modules. It appears that the moisture vapor transmission through the bulk encapsulant must be minimized in order to extend the service life of the modules.

TASK 7: LONG-TERM EXPOSURE TESTING OF "FASTER-CURING" AND "FLAME-RETARDANT" EVA BASED ENCAPSULANT SYSTEMS

The SFC and FR formulations were originally developed under the 1988 BP Solarex PVMaT subcontract. Although the encapsulants met specific performance requirements set forth by BP Solarex, the materials suffered from pertinent shortcomings, primarily related to the manufacturing of these encapsulant formulations.

In an effort to address these shortcomings, both SFC and FR formulations were reformulated. Work on the SFC formulation focused on minimizing the liquid content of the material without sacrificing the curing kinetics performance. With the FR encapsulant, a new curing package was developed to improve crosslink density over the previous formulation.

Both encapsulant formulations were then successfully extruded on STR's production equipment. Following the extrusion trial, PV modules were then laminated with the manufactured encapsulant materials and subjected to specific IEC-qualification testing to determine the integrity of the encapsulant packaging and long-term testing on a tracker in Arizona.

IEC Qualification Testing

During Phase II, modules made with the FR formulation were subjected to testing designed to evaluate the ability of the encapsulant material to provide adequate encapsulation to the PV device; the specific tests involved in this evaluation is a precursor to IEC qualification testing. The results of are summarized below.

Experimental

Seven (7) modules laminated with each encapsulant formulation were made and tested by STR's PV manufacturer team member BP Solar. Out of the seven modules made with either the SFC or FR EVA materials, one (1) module was designated as a control and, therefore, not subjected to testing. The other six (6) modules are subjected to three (3) different testing pathways (two modules for each pathway).

Initially, all 14 modules (seven for each encapsulant formulation) were evaluated by the following.

- STC (standard testing condition) Electrical Performance: modules were measured for V_{oc} (open-circuit voltage), I_{sc} (short-circuit current), P_{max} (power at maximum power point), and FF (fill factor).

- IR Scan: a forward bias was applied to the module until the current equals two (2) times the short-circuit current (I_{sc}), and the back of the module inspected by an infrared (IR) camera. "Hot" and/or "cold" spots were mapped.

- Visual Inspection: modules were inspected noting defects.

- Electrical Insulation: dielectric breakdown and electrical current leakage were measured for modules in dry and wet conditions (i.e., submerged in water). Electrical insulation in dry conditions was performed at 3 kV, whereas wet insulations measurements were done at 1 kV.

Following the initial module characterization and measurements, six modules were subjected to three different tests.

- Thermal Cycling Without Bias (TC, duration: 100 days): modules were thermally cycled 500 times between +85°C and –40°C. After the first 200 cycles, intermediate STC electrical performance testing would be done on the modules.

- Thermal Cycle/Humidity Freeze (TC/HF, duration: 20 days): modules were thermally cycled between +85°C and –40°C 50 times and then followed by 10 humidity/freeze cycles. A humidity/freeze cycle involves 20 hours at 85°C and 85% relative humidity and then 24 hours at –40°C. Prior to the start of the 10 humidity/freeze cycles, STC electrical testing, IR Scan, visual inspection, and electrical insulation tests are performed on the modules.

- Damp Heat (DH, duration: 52 days): sample modules were subjected to 85°C and 85% relative humidity for 1250 hours. After 100 hours of damp heat, intermediate STC electrical performance testing would be measured.

Two modules, along with the check module, would go through each of the above testing pathways. Following the completion of each test, a final module characterization would be performed on the modules (STC Electrical Performance, IR Scan, Visual Inspection, and Electrical Isolation).

BP Solar had trouble manufacturing larger sized modules with the SFC formulation and was not able to start module testing at the same time as the FR formulation.

Results and Discussion

– Initial Module Characterization

Table 9 shows STC electrical measurements for the seven modules laminated with the FR EVA. All experimental modules had very similar performance compared to a typical module after lamination.

Table 10 summarizes results from the Visual Inspection and IR Scan. Results from the inspection and scan did not prevent modules from further testing and were not noted to be detrimental to the module quality. The front print pattern discoloration noted during the visual inspection refers to blemishes on the cell surface.

All experimental modules, including the control, passed the initial dry electrical isolation test but failed wet isolation. All modules laminated with the FR EVA did not contain the backsheet, as this packaging component prevents FR EVA-laminated modules from passing the various flammability ratings. The wet insulation failure was due to a lack of a dielectric barrier coupled with a higher conductivity in the FR encapsulant. Either the

FR encapsulant must be formulated to be less conductive or must be utilized with a dielectric barrier layer to protect the FR material.

S/N	Test Module Designate	Initial Electrical Parameters after Light Soak			
		V_{oc} (V)	I_{sc} (A)	P_{max} (W)	FF
2975580	Check	43.92	4.91	158.43	0.73
1376156	Control	43.84	4.99	156.44	0.72
1376151	TC-A	43.81	4.95	156.26	0.72
1376152	TC-B	43.96	5.01	157.29	0.71
1376153	TC/HF-A	43.92	5.00	158.12	0.72
1376154	TC/HF-B	43.78	4.98	157.42	0.72
1376155	DH-A	43.99	5.03	156.96	0.71
1376157	DH-B	43.85	4.99	156.53	0.71

Table 9. Initial electrical parameters of FR-laminated modules.

S/N	Test Module Designate	Notes	
		Visual Inspection	IR Scan
1376156	Control	EVA has a grainy appearance on sides and bottom of the module. Severe bubbling at the top edge of the module. Backsheet does not extend to the top of the module. Scrim fibers are exposed on the top back of the module. Several small areas of discolored front print pattern.	Many warm and cool areas. One cool corner, possibly a cracked cell.
1376151	TC-A	EVA has grainy appearance around entire edge of module. Many small areas of discolored front print pattern.	Many warm and cool areas. Several cool corners, possibly cracked cells.
1376152	TC-B	EVA has grainy appearance around entire edge of module. Top edge of serial number label is stained black. Many small areas of discolored front print pattern. Bottom edge of the bottom bus bar is stained black.	Many warm and cool areas. Many of the cells have a cool area across the center, possibly a tab soldering problem.
1376153	TC/HF-A	Entire matrix is shifted to the left of center. EVA has grainy appearance	Many warm and cool areas. Several of the cells have a cool area

		around entire edge of module. Top edge of serial number label is stained black. Many small areas of discolored front print pattern.	across the center, possibly a tab soldering problem.
1376154	TC/HF-B	EVA has grainy appearance around entire edge of module. Many small areas of discolored front print pattern. Three yellow stains on top bus bars.	Many warm areas.
1376155	DH-A	EVA has grainy appearance around entire edge of module. Many small areas of discolored front print pattern. Three yellow stains on top bus bars. Backsheet has 2 tears on left side running in the top-to-bottom direction.	Many warm and cool areas. Several of the cells have a cool area across the center, possibly a tab soldering problem.
1376157	DH-B	EVA has a grainy appearance around entire edge of module. Several small areas of discolored front print pattern.	Many warm areas.

Table 10. Module visual inspection summary.

- Thermal Cycle (TF)

After the experimental FR modules reached 200 thermal cycles, testing was paused to measure electrical performance at STC. Table 11 shows the measured electrical parameters and percent change in these parameters from the initial characterization. STC electrical parameters are also shown for the Check and Control modules as a reference; note that these two modules did not undergo thermal cycling and were measured at the same time as the two thermal-cycled modules.

The thermal-cycled modules had changes in all electrical parameters less than or equal to 1.0%. According to BP Solar, any changes less than 5% are allowed. Furthermore, the measurement error is ~1%. Since the STC electrical performance fell within the measurement error, the observed changes were not significant.

Both the Control and Check modules also showed changes in the electrical parameters when tested. Like the thermal-cycled modules, the measured percent change for the

Control and Check modules were not considered significant. In general, these changes were less compared to the experimental modules.

– Thermal Cycle/Humidity Freeze (TC/HF)

Following 50 thermal cycles between +85°C and –40°C, the electrical parameters of the experimental modules were measured at STC. Table 12 shows the results; the experimental modules are also compared to Check and Control modules measured at the same time as the experimental modules. No significant electrical degradation was observed in all modules.

S/N	Test Module Designate	Electrical Parameters after 200 TC							
		V_{oc} (V)	Change (%)	I_{sc} (A)	Change (%)	P_{max} (W)	Change (%)	FF	Change (%)
1376151	TC-A	43.78	-0.1	4.93	-0.4	155.62	-0.4	0.72	0.1
1376152	TC-B	43.91	-0.1	4.98	-0.5	155.70	-1.0	0.71	-0.4
2975580	Check	43.88	-0.1	4.91	0.0	157.69	-0.5	0.73	-0.3
1376156	Control	43.83	0.0	4.97	-0.4	156.10	-0.2	0.72	0.2

Table 11. Electrical performance after 200 TC.

A visual inspection and IR scan was performed on the experimental modules. No visible changes compared to the initial state were observed following the 50 thermal cycles in both modules. Changes were also not observed during the IR scan.

Electrical insulation tests done following thermal cycling revealed failures for wet isolation. Both experimental modules passed the dry isolation test. This trend was similar to all experimental modules initially characterized.

S/N	Test Module Designate	Electrical Parameters after 50 TC/ Before 10 HF							
		V_{oc} (V)	Change (%)	I_{sc} (A)	Change (%)	P_{max} (W)	Change (%)	FF	Change (%)
1376153	TC/HF-A	43.91	0.0	4.96	-0.9	156.43	-1.1	0.72	-0.1
1376154	TC/HF-B	43.87	0.2	4.95	-0.6	156.41	-0.6	0.72	-0.3
2975580	Check	43.88	-0.1	4.91	-0.1	156.97	-0.9	0.73	-0.8
1376156	Control	43.89	0.1	4.96	-0.6	155.56	-0.6	0.71	-0.1

Table 12. Electrical performance after 50 TC/before 10 HF.

– Damp Heat (DH)

After 1000 hours at damp heat (85°C/85% R.H.), electrical parameters of the experimental modules were tested at STC. Table 13 summarizes the electrical results. No significant electrical degradation was observed in all modules.

S/N	Test Module Designate	Electrical Parameters after 1001 hrs DH							
		V_{oc} (V)	Change (%)	I_{sc} (A)	Change (%)	P_{max} (W)	Change (%)	FF	Change (%)
1376155	DH-A	44.00	0.0	5.03	0.0	157.61	0.4	0.71	0.4
1376157	DH-B	43.87	0.0	4.97	-0.5	156.79	0.2	0.72	0.6
2975580	Check	43.91	0.0	4.90	-0.2	157.81	-0.4	0.73	-0.2
1376156	Control	43.84	0.0	4.96	-0.5	155.85	-0.4	0.72	0.1

Table 13. Electrical Parameters After 1001 hrs DH.

Conclusions

At the intermediate point of the three test pathways, modules laminated with the FR EVA show no significant electrical degradation. Failures are only being observed in wet electrical isolation testing. As mentioned above, the FR encapsulant must be formulated to be less conductive and/or utilize a dielectric barrier layer to protect the FR material. These options will be further investigated as module testing continues.

Long-term Field Testing

Eight modules laminated with the SFC and FR encapsulant formulations (four each) and manufactured as part of Phase I, Task 3, were received by the Photovoltaic Testing Laboratory (PTL) at Arizona State University on January 7, 2004. Six of these modules were installed on a two-axis tracker and the remaining two stored indoors to serve as control modules.

The installed modules, pictured in Figure 50, are on the top row of PTL tracker T1.

The module testing protocol will include electrical performance data (IV curves), translation of electrical performance data to Standard Test Conditions (STC), and visual inspection and photographs. The testing protocol will be performed by ASU on the day of installation and then after 7, 30, 90, and 180 days. During Phase III, the modules were tested on March 21, 2005 and again on September 21, 2005 (plus/minus 7 days).

Electrical performance is shown in Figures 51 - 56 for modules laminated with the SFC and FR formulations (exposure period 6APR04 – 21JUN07). As one can see, during the three-field exposure, in all critical performance areas, there has no been no module electrical degradation with either the FR or SFC encapsulant.

Figure 50. 2-axis tracker at ASU-PTL bearing SFC- and FR-laminated modules (top six modules).

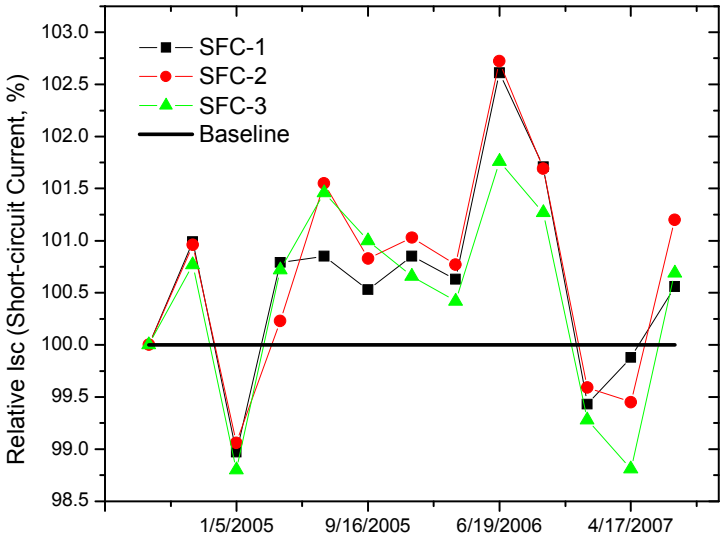

Figure 51. Relative Isc for SFC-laminated modules.

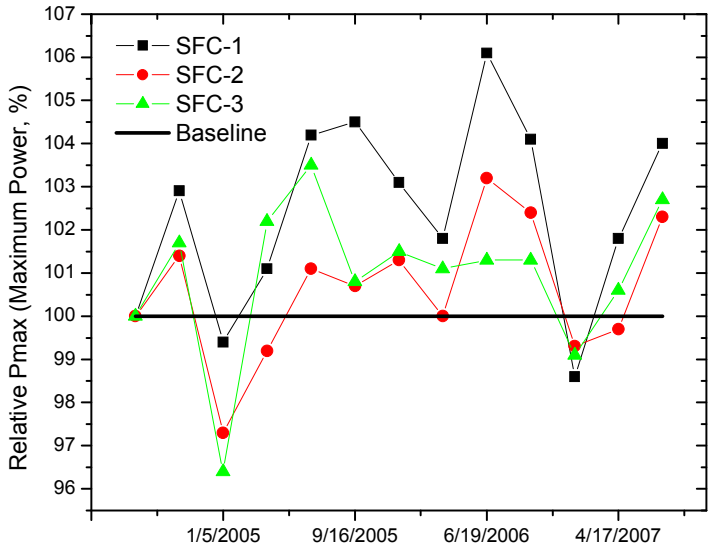

Figure 52. Relative Pmax for SFC-laminated modules.

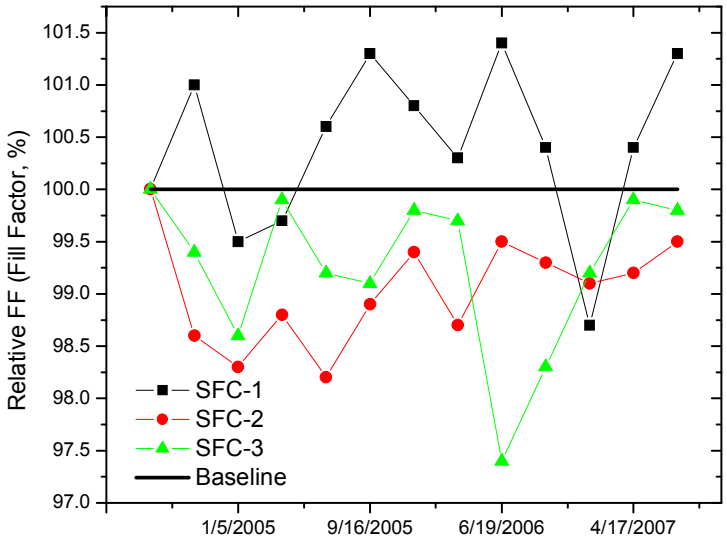

Figure 53. Relative Fill Factor (FF) for SFC-laminated modules.

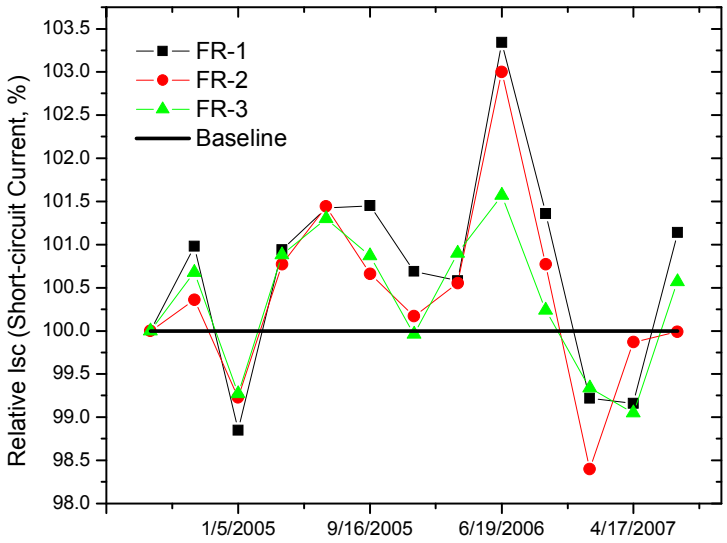

Figure 54. Relative Isc for FR-laminated modules.

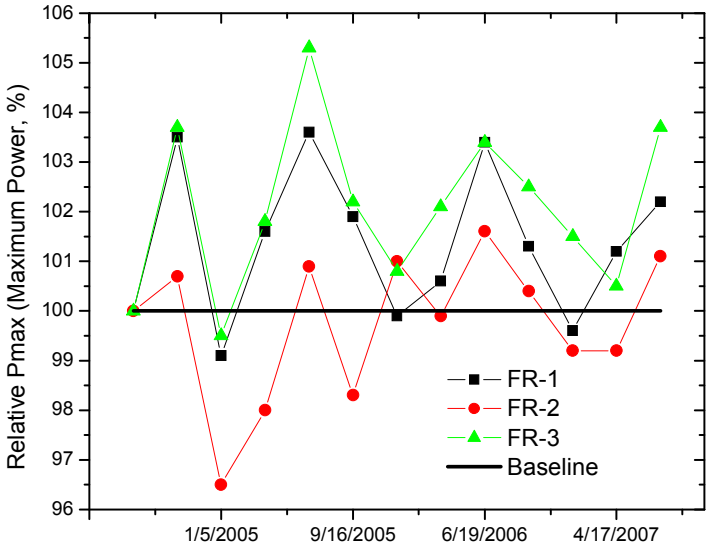

Figure 55. Relative Pmax for FR-laminated modules.

TASK 8: DESIGN OF FASTER-CURING EVA-BASED ENCAPSULANT SYSTEM PROCESS MODIFICATION

In addition to the improvements to the SFC encapsulant formulation, STR identified improvements in how the SFC encapsulant is manufactured. These improvements will reduce the overall costs of manufacturing a dimensionally stable (i.e., no shrinkage)

encapsulant sheet; minimizing shrinkage during lamination is a key factor in reducing lamination cycle times.

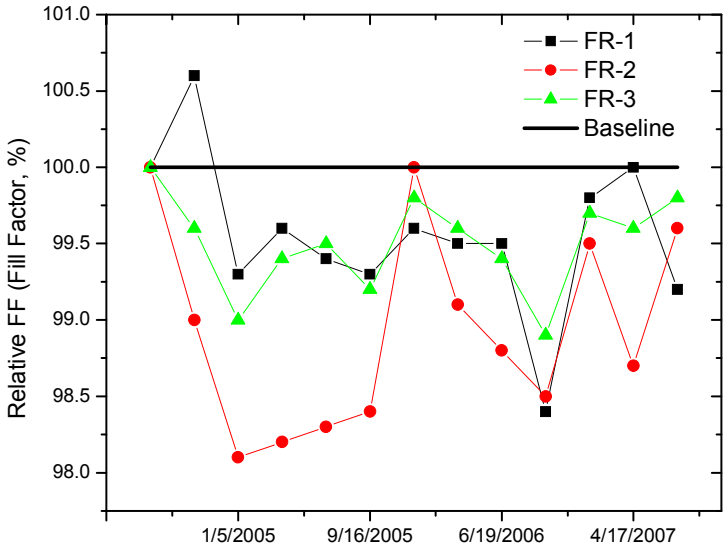

Figure 56. Relative Fill Factor (FF) for FR-laminated modules.

Part of the identified improvements to STR's manufacturing process of the SFC encapsulant is the installation of a tension management system/winder. This system, as designed, should minimize material usage during manufacture of an encapsulant sheet with enhanced dimensional stability.

Macro Engineering has been selected to design and fabricate the tension management system (TMS) for STR. Macro has designed and built the existing extrusion process equipment; therefore, the integration of the new equipment modifications, as well as control inputs/outputs from existing equipment pieces, should be accomplished much easier.

Design Considerations and Initial Site Visit

An engineering team from Macro visited STR on 4MAY05 for their initial visit. Space where the TMS will be installed was the major issue under consideration. Supporting infrastructure; structurally, electrically (power sourcing), and electronically (inputs and outputs for control of the modification equipment pieces); were also important factors under discussion during the visit.

Existing equipment dimensions and support structures, (e.g., beams, posts, etc.) were measured and identified. A portion of the initial engineering drawing has been included in this report (Figure 57).

The tension management system will occupy approximately 30 inches of floor real estate along the length of the extrusion line. The rest of the system will be located 85 inches above the ground floor. The elevated parts of the system will have dimensions of 36” x 18” x 58”.

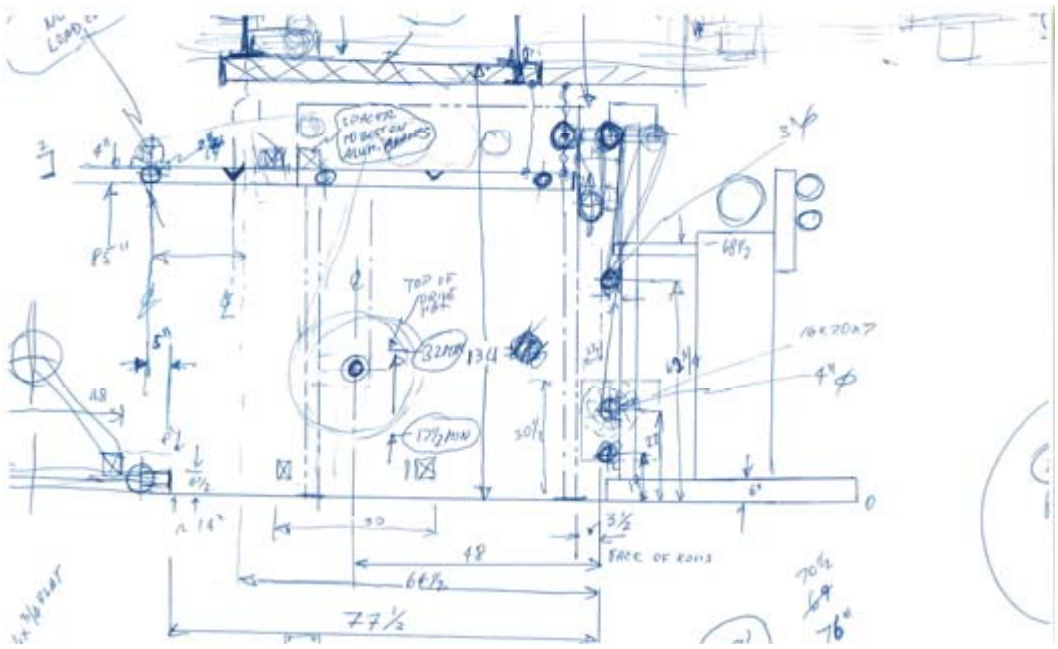

Figure 57. Part of the initial engineering drawing generated during Macro’s initial site visit. Structural infrastructure was being considered to support the elevated parts of the TMS.

There are four (4)-inch support beams, which run parallel to ground, that will attach to the system. In addition to these beams, two (2) vertical support poles will also need to be installed. Each pole will be located on either side of the TMS in the width direction (58”).

Because the equipment modification piece is handling continuous polymer sheet, sheet tension must be accurately controlled. Tension will be monitored via a torque controller and load cell. A motorized unit attached the load cell will extend 24 inches into the aisle beside the extrusion line. Some desks and cabinets, therefore, must be removed to accommodate the load cell equipment.

It was discussed during the site visit whether to employ an optical sensor along with the load cell to control tension properly. This sensor would focus on the position of the sheet passing through the process; the position would be used as another input to determine tension control. As the final design of the tension management system is completed, a decision on the optical sensor implementation will be made.

The final consideration, to be designed and resolved during preparation of the final form of the tension management system, is a “bypass” mode where the existing extrusion

process can operate when the TMS is no being employed. Roll sheet idlers will need to be positioned appropriately to ensure that the extrusion process can run independently from the added equipment piece.

Final Design

From the initial site visit, Macro presented a final, CAD-format design of the TMS. The specifications from the final design proposal (Figures 58 and 59) were received on 18MAY05 and accepted after a review of the design at the actual installation site by STR engineers.

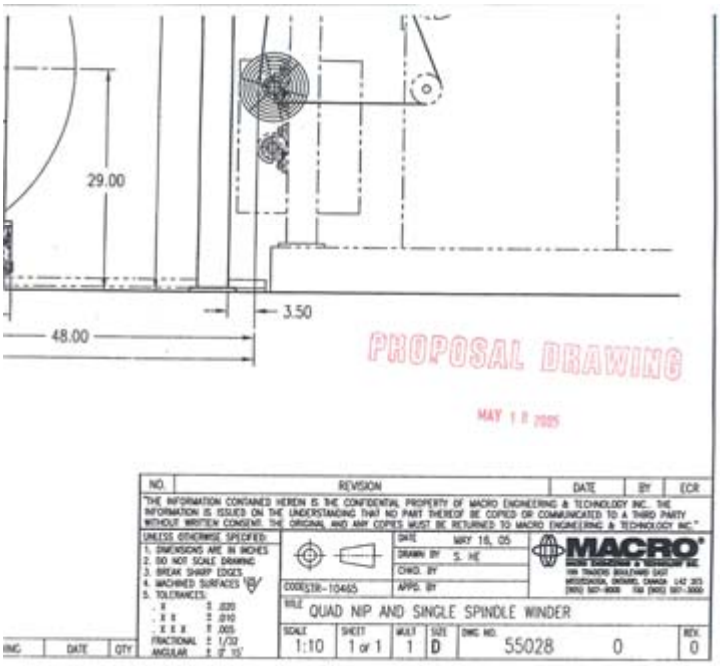

Figure 58. Part of engineering drawing from the final design proposal.

From the initial site visit, there were two (2) issues that needed further thought in terms of implementation. The first issue was use of an optical sensor to control tension.

STR engineers were initially hesitant about utilizing the optical sensor and preferred a torque motor. In discussions with Macro prior to issuing of the final design proposal, STR and Macro agreed to use the sensor with the stipulation that if the TMS performance is not satisfactory, Macro will replace the optical sensor with the torque motor at no cost.

The second issue was a bypass mode on the TMS when it is not being used. Macro designed and placed the proper equipment in the final design to allow for the bypass mode.

The TMS can be fabricated within eight (8) to 10 weeks of receipt of purchase order.

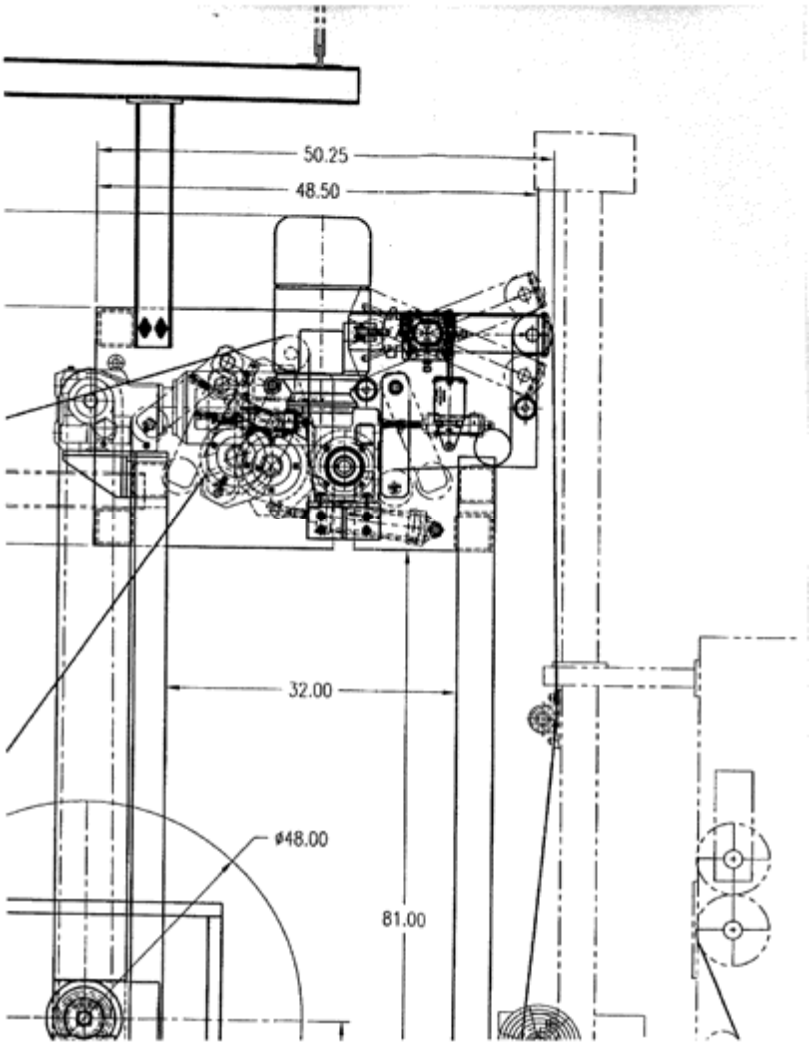

Figure 59. Part of TMS engineering drawing from the final design proposal.

PHASE III

INTRODUCTION

The activities with the three encapsulant-types developed under Phase I and II were completed in the last Phase. Phase III work consisted of three tasks.

- Task 9: implement super fast-cure encapsulant manufacturing process modifications with modules tests with materials made by new process,
- Task 10: reformulate and evaluate new flame-retardant encapsulant, and
- Task 11: complete module testing of selected thin-film-specific encapsulants.

The major development efforts during Phase III involved the reformulated flame-retardant (FR) EVA-based encapsulant. As discovered during Phase II, FR encapsulant X122-11-2P/FR had poor wet electrical insulation resistance, allowing modules to fail this critical evaluation during internal testing by STR's module manufacturer team member.

In response, STR teamed with PN Solutions to develop an alternative FR technology that provides similar performance as the previous FR technology strategy, but does not compromise the electrical insulation properties of the base polymer resin. Verifying the new FR encapsulant addresses the shortcomings of the pervious material and meeting the set performance criteria.

Work with the thin-film-specific and the faster-curing encapsulant mainly dealt with manufacturing trials at both STR and our PV module manufacturers' facilities and subsequent module testing. The primary goals for the modules tests of the faster-curing and thin-film-specific encapsulants was to validate that modules laminated with these materials would pass the respective IEC qualification testing sequence.

TASK 9: IMPLEMENTATION OF FASTER-CURING EVA-BASED ENCAPSULANT SYSTEM PROCESS MODIFICATIONS

STR has identified additional improvements in how the super fast-curing (i-SFC) encapsulant is manufactured. The improvements shall reduce the overall costs of manufacturing a dimensionally stable (i.e., no shrinkage) encapsulant sheet; minimizing shrinkage during lamination is a key factor in reducing lamination cycle times.

Part of the identified improvements to STR's manufacturing process of the i-SFC encapsulant was the installation of a tension management system/winder (TMS). This system, as designed, shall minimize material usage during manufacture of an encapsulant sheet with enhanced dimensional stability. The TMS was designed and submitted to STR during Task 8, Phase II.

In Task 9, the TMS design would be finalized and built, and our PV module manufacturing team member would evaluate materials from the new manufacturing system.

Installation and Manufacturing Trial

There were two issues that had to be resolved prior to installing the TMS: a) utilization of either an optical sensor or torque motor, and b) programming a bypass mode into the TMS when it is not in use.

The TMS manufacturer Macro delivered the equipment piece with a torque motor in place.

Once the TMS was physically installed, Macro sent their engineer to address the bypass mode on the TMS, as well as finish programming the operating software that controls the TMS.

The bypass on the TMS was easily achieved by ensuring that the line speed input signal from the upstream process is routed to the TMS and then back whether the TMS is operating or not.

The Macro also completed programming the TMS control software. Tweaks and changes to the control software were made while the TMS was operating.

Once the control software was completed to satisfaction, a full manufacturing trial was started.

We found that the EVA roll quality was comparable to our standard commercial products – no roll scoping was detected. The paper separation was also acceptable during the trial. At first, hard wrinkles would intermittently appear as the paper went through the TMS. Slight adjustments to the nip pressure of the TMS associated with paper payoff alleviated these hard wrinkles.

Furthermore, there were no occurrences of cuts and other damage to the paper occurring. This is of vital importance as the paper is recycled for later use.

During the trial, the TMS was able handle production speeds that were actually 38% faster than typical production specifications, vastly exceeding our through put target of at least 85% relative to production.

Encapsulant shrinkage was equal to normal production levels with our standard product.

At the conclusion of the trial, we found that the TMS exceeded our performance requirements and is qualified for customer production.

Rolls from the trial were then sent to our PV module manufacturing partner for module qualification/testing.

Lamination Trials

The i-SFC encapsulant was shown previously to properly laminate modules within a six-minute lamination cycle. Therefore, the primary objective of the current trial was to ensure that the new manufacturing method (utilizing the TMS) did not affect encapsulant handling and module laminate quality.

All modules laminated during the trial appeared to have adequate EVA cure. Furthermore, all i-SFC-laminated modules were defect-free – no voids, bubbles, or blemishes due to the encapsulant were observed in any of the modules.

To confirm the gel levels obtained with the i-SFC encapsulant, a dummy module (i.e. no cells) was constructed in such a way to extract an EVA sample for gel content analysis (solvent extraction method). Samples were taken from six locations in the module. Table 14 shows results from the gel content analysis.

Module Location	Gel Content (%)
A	63
B	79
C	76
D	82
E	62
F	60

Table 14. EVA gel content as a function of module location.

Based on the above results, it was decided to submit i-SFC-laminated modules through internal testing.

IEC Internal Testing

Introduction

Modules laminated with the i-SFC were evaluated according to an internal testing sequence (Q6000) to determine if the encapsulant will allow modules to pass the IEC 61215 crystalline module qualification.

Experimental

Five (5) modules were made and tested by STR's PV module manufacturer team member; 4 modules were produced with the i-SFC, and the fifth was laminated using the current encapsulant and serves as a control.

Each module was initially characterized for electrical performance and electrical insulation resistance (dry and wet) prior to environmental testing. Two modules, along with the control, were subjected to two different tests.

- Thermal Cycle./Humidity Freeze (TC/HF): modules were thermally cycled between +85°C and –40°C 50 times and then followed by 10 humidity/freeze cycles. A humidity/freeze cycle involves 20 hours at 85°C and 85% relative humidity and then 4 hours at –40°C. Prior to the start and at the end of the 10 humidity/freeze cycles, electrical testing at STC (standard testing conditions) and dry/wet electrical insulation resistance tests were done on the modules.

- Damp Heat (DH): sample modules were subjected to 85°C and 85% relative humidity for 1250 hours. At the conclusion of the test period, STC electrical performance and dry/wet insulation resistance were measured.

Results and Discussion

– Initial Module Characterization

Table 15 shows STC electrical measurements for the 5 modules tested. As one can see, the 4 experimental modules with the i-SFC had similar performance compared to the control module.

Table 16 lists the initial dry and wet electrical insulation resistance. All modules must measure at least 40 Mohms/m^2 or higher in order to pass. Once again, the i-SFC-laminated modules have similar performance to the control.

S/N	Test Module Designate	Initial Electrical Parameters after Light Soak			
		V_{oc} (V)	I_{sc} (A)	P_{max} (W)	FF
6383958	Control	43.75	5.09	161.61	0.73
6383914	TC/HF-A	43.64	5.05	161.61	0.73
6383921	TC/HF-B	43.72	5.05	160.17	0.73
6352200	DH-A	43.86	5.06	161.19	0.73
6383913	DH-B	43.68	5.05	161.57	0.73

Table 15. Initial module electrical characterization.

S/N	Test Module Designate	Initial Electrical Insulation Resistance	
		Dry Insulation Resistance (1kV) Mohm/m^2	Wet Insulation Resistance (1kV) Mohm/m^2
6383958	Control	> 1000	73
6383914	TC/HF-A	> 1000	71
6383921	TC/HF-B	> 1000	72
6352200	DH-A	> 1000	71
6383913	DH-B	> 1000	72

Table 16. Initial wet/dry electrical insulation resistance.

– Thermal Cycle/Humidity Freeze

Following 50 thermal cycles between +85°C and –40°C, the electrical parameters of the experimental modules were measured at STC. Table 17 shows the results. No electrical significant electrical degradation was observed in the i-SFC-containing modules. These modules had changes in all electrical parameters less than or equal to 1.0%. Any changes less than 5% are allowed. Furthermore, the measurement error is ~1%. Since the STC electrical performance fell within the measurement error, the observed changes were not significant.

In addition to the above, the i-SFC modules had similar performance to the control.

Dry and wet electrical insulation resistance for the two experimental, i-SFC modules was > 1000 Mohm/m^2 and 85 Mohm/m^2, respectively, greater than the 40 Mohm/m^2 minimum.

Electrical properties and insulation resistance were measured again at the conclusion of the 10 HF cycles. For module TC/HF-A, dry and wet electrical insulation resistance was > 1000 Mohm/m^2 and 82 Mohm/m^2, respectively; module TC/HF-B had readings of 578 Mohm/m^2 and 76 Mohm/m^2. Table 18 shows STC electrical parameters after 10 HF cycles, demonstrating that modules with the i-SFC encapsulant had no module

degradation and similar performance to the current encapsulant utilized by the module manufacturer.

S/N	Test Module Designate	Electrical Parameters after 50 TC/ Before 10 HF							
		V_{oc} (V)	Change (%)	I_{sc} (A)	Change (%)	P_{max} (W)	Change (%)	FF	Change (%)
6383914	TC/HF-A	43.83	0.4	5.02	-0.4	161.75	0.4	0.73	0.4
6383921	TC/HF-B	43.75	0.1	5.02	-0.5	159.96	-0.1	0.73	0.4
6383958	Control	43.99	0.6	5.05	0.3	161.69	0.0	0.73	-0.9

Table 17. Electrical Parameters after 50 TC/ Before 10 HF.

S/N	Test Module Designate	Electrical Parameters after 10 HF							
		V_{oc} (V)	Change (%)	I_{sc} (A)	Change (%)	P_{max} (W)	Change (%)	FF	Change (%)
6383914	TC/HF-A	43.80	0.4	5.10	1.0	166.25	2.5	0.74	1.8
6383921	TC/HF-B	43.89	0.4	5.16	2.1	165.58	3.4	0.73	0.9
6383958	Control	43.95	0.5	5.09	1.0	165.71	2.5	0.74	1.0

Table 18. Electrical Parameters after 10 HF.

– Damp Heat (DH)

After 1250 hours at damp heat (85°C/85% R.H.), electrical parameters of the experimental and control modules were tested at STC. Table 19 summarizes the electrical results, where no module degradation was observed in all modules.

Both experimental modules passed the electrical insulation resistance tests. Module DH-A had dry and wet electrical insulation resistance of > 1000 Mohm/m^2 and 54 Mohm/m^2, respectively; and DH-B had measurements of 605 and 58.

S/N	Test Module Designate	Electrical Parameters after 1001 hrs DH							
		V_{oc} (V)	Change (%)	I_{sc} (A)	Change (%)	P_{max} (W)	Change (%)	FF	Change (%)
6352200	DH-A	43.93	0.2	5.09	5.1	165.62	2.8	0.74	2.1
6383913	DH-B	43.73	0.1	5.11	1.3	164.78	2.0	0.74	0.6
6383958	Control	43.79	0.1	5.10	1.4	164.94	2.1	0.74	0.6

Table 19. Electrical characterization after 1001 hrs DH.

Conclusions

Based on the results from the Q6000 testing, the i-SFC encapsulant should allow modules to pass the IEC 61215 qualification sequence. Modules with the encapsulant passed the most rigorous environmental tests and had similar performance as the current EVA-based encapsulant.

TASK 10: CONTINUED FORMULATION IMPROVEMENTS TO FLAME-RETARDANT ENCAPSULANT

The original FR encapsulant developed under the BP Solarex subcontract obtained low levels of crosslinking. This shortcoming was corrected under the current PVMR&D contract. This FR encapsulant iteration allowed modules to pass the Class B flammability under UL 1703. However, modules laminated with the encapsulant consistently failed wet hi-pot testing.

It appeared that an additive component of the FR encapsulant formulation was compromising the electrical insulation performance of the base polymer. Removing this component would improve wet electrical isolation, but require a new strategy in flame-retarding the encapsulant.

STR worked with PN Solutions in developing a new phosphorous-based FR compound. Besides not requiring the need to load the encapsulant with a high amount of fillers, thereby compromising the electrical insulation, this FR technology can allow a much higher light transmission through the encapsulant, giving the possibility to utilize an FR encapsulant in front of the cells instead of solely on the back.

FR Reformulation Effort, X125-47 Series

Six (6) iterations of the FR encapsulant were evaluated via the flame impingement test with the PN additive. These iterations had similar levels of the active FR technology, but different EVA-based resins were utilized. Figures 60-65 show results from the flame test that simulates the UL-1703 flammability procedure.

Out of the formulations evaluated, Compound B, X125-47-1, and X125-47-2 had the best performance. As one can see, the formulations did not allow flame penetration, even after 15 minutes of constant impingent from the 1,900°C flame.

Figure 66 shows light transmission of the better performing FR formulations. X125-47-1 and X125-47-2 are close to the Control, but still not high enough to be utilized in front of the cells.

Based on the results from the flame impingement testing, the developed FT technology with PN Solutions should allow modules to pass at least the Class B flammability rating. One formulation will be selected for extrusion trials and subsequent testing in production-sized modules.

Figure 60. Flame impingement test: Compound A.

Figure 61. Flame impingement test: Compound B.

Figure 62. Flame impingement test: Compound EV2.

Figure 63. Flame impingement test: Compound EV4.

Figure 64. Flame impingement test: Compound X122-47-1.

Figure 65. Flame impingement test: Compound X122-47-2.

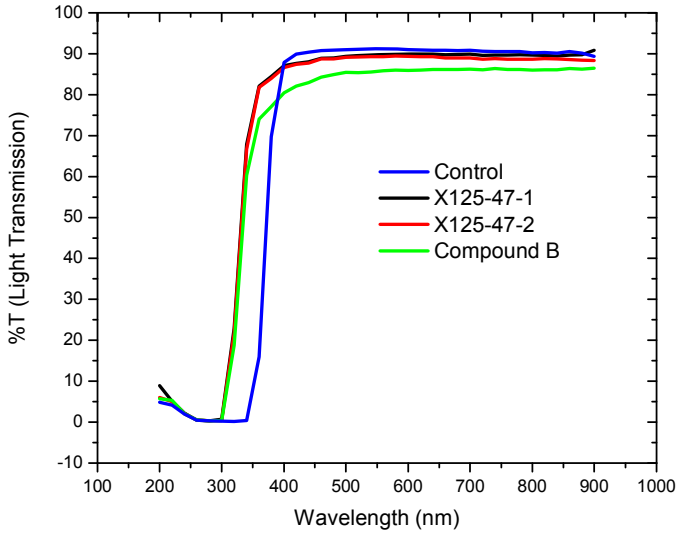

Figure 66. Light transmission of FR encapsulant formulations and Control.

Manufacturing Trial

The manufacturing trial of the FR encapsulant was conducted on October 24, 2006. The encapsulant widths were manufactured according to a 72-cell polycrystalline module.

The FR formulation X125-47-1P/FR utilizes the same base EVA resin as STR's typical EVA-based encapsulants. Coupled with the fact that the FR functional additive system melt mixes with the base resin and is at a much lower weight percentage compared to the two previous FR encapsulant generations, we did not expect any significant process differences with the FR EVA.

As the trial began, this was the case. Process temperatures were the same as typical production materials. Furthermore, the FR encapsulant could be produced at common extrusion speeds, although, for most of the trial, a slightly lower speed was used to ensure that any process upsets could be identified quickly.

During the extrusion trial, some bubbling within the encapsulant was observed. This bubbling was due to the slight hygroscopic character of the formulation. Glass/glass laminates made with the as-made product showed that the bubbles did not affect lamination quality (i.e., bubble-free).

The observations we made during the trial indicated that the FR formulation could be extruded in a high-volume way, deeming the trial a success. Rolls from the trial were then sent to our manufacturing partner for module qualification and testing.

Lamination Trials and Flammability Testing

The FR encapsulant X122-47-1 was laminated into a standard 160 W module construction. The lamination cycle was 4 minutes evacuation, 8 minutes press at 152°C. Laminates were checked for quality prior to flammability testing according to UL-1703. Due to available resources, only Class B testing could be done.

X122-47-1 was able to be processed successfully in a conventional production module construction. During the extrusion trial, small bubbles were formed within the encapsulant sheet due to the hygroscopic nature of the FR compound. Laminations of small glass/glass plates with X122-47-1 demonstrated that these bubbles should not pose a problem during module lamination. Indeed this was the case, as all modules were bubble-free. In addition, X122-47-1 adhered well to all surfaces within the module construction.

Modules were the subjected to flammability testing. As expected, the X122-47-1 allowed the polycrystalline modules to pass the Class B rating test. Depending on the module substrate used, a glass scrim coupled to the encapsulant is optional. For weaker module substrates, the glass scrim should be used to maintain contact of the cell backside materials to the substrate.

Conclusions

Based on the results from the lamination trials and flammability testing, the X122-47-1 should proceed to IEC 61215 module qualification. Internal module testing can be done first to ensure external qualification success and uncover potential problems that modules containing the X122-47-1 could have during any of the IEC 61215 testing sequences.

At the soonest convenience, modules with the FR encapsulant should be evaluated for Class A rating. The flammability tests show that the formulation provides enough protection to handle a larger flammable source.

TASK 11: FINAL OPTIMIZATION EFFORTS FOR THIN-FILM-SPECIFIC ENCAPSULANTS

Encapsulant moisture sensitivity was a major design consideration in developing thin-film-specific encapsulants, particularly for glass/glass module constructions where the PV device is vapor-deposited onto the glass superstrate.

From the initial development effort on thin-film-specific encapsulants, several material strategies and formulations were considered. After a secondary screening process where glass adhesion and moisture vapor transmission rate were heavily considered, X125-37 was chosen for continued testing.

Amorphous silicon-based glass/glass modules were made with X125-37 and subjected to damp-heat (85% RH, 85°C) exposure; visual observations were made on the integrity of the device. No device degradation was observed at the glass/PV device interface or at the device (back)/encapsulant interface. No encapsulant delamination was observed as well.

In addition to the modules, plates specially designed to measure encapsulant adhesion to the back of the PV device and glass were constructed, laminated, and exposed to damp-heat. Adhesion measurements were taken before and after exposure.

Against glass, X125-37 adhesion strength was so strong before and after damp-heat (average peel strength was 117 N/cm) that the pulling substrate failed during adhesion testing. Little adhesion degradation was observed for both glass and device backside after 500 hours damp-heat.

The adhesion results confirm that X125-37 shall adequately protect the module and PV device. Furthermore, we expect that modules manufactured with the formulation shall successfully pass a full IEC 61215 qualification testing sequence.

Manufacturing and Lamination Trials

Based on the above results, X125-37 was chosen to be manufactured for module qualification testing by our thin-film PV manufacturing partner. The trial was conducted on November 20, 2006, over a span of two days. The first day was taken to set-up the extrusion temperature profile of the new material and to understand, in a practical fashion, the most effective process parameters.

We found during the process set-up that due to the lower melt index and high melt point of the formulation, a reverse extrusion profile was necessary. This type of profile kept the pressure constant throughout the extruder, which is critical for consistent encapsulant sheet thickness.

The higher process temperatures needed for X125-37 resulted in extrusion temperatures that were approximately 2.5 times greater than typical production parameters.

Once the process parameters were verified and shown to produce consistent product, X125-37 for our thin-film manufacturing partner was made.

Rolls from the trial were then sent to our manufacturing partner for module lamination trials, which ran on January 11, 2007. A 15-minute lamination cycle at 150°C was used to manufacture the glass/glass modules.

At the beginning of the lamination trial, only glass/glass modules without the PV device were manufactured in order to verify the process. Due to the nature of the encapsulant,

the lamination platen temperature had to be increased by 10°C to properly melt and wet the encapsulant to the glass surfaces.

We also found that the material contained an excess amount of stress, leading to encapsulant shrinkage. This observation was consistent with the extrusion conditions during the encapsulant's manufacturing trial in November 2006. The shrinkage lead to a decrease of 0.125 inches in the encapsulant width during processing.

To ensure that the shrinkage fully took place during lamination, glass/glass laminates that were previously processed were subjected to additional temperature of 150°C for 1 hour. These laminates did not show any additional signs of shrinkage; therefore, it was determined that the encapsulant will undergo further relaxation at a later time (i.e., during environmental testing).

Seven modules were made for environmental testing with the X125-37 encapsulant and sent to ASU PTL for IEC testing.

IEC Module Testing

ASU PTL conducted three specific testing sequences on six of the seven modules; the seventh module was kept as control reference. The sequences were selected because they specifically evaluate the integrity and effectiveness of the encapsulant and module packaging. The testing sequences were:

- Damp-heat: 1000 hours exposure. I-V measurements done before and after testing.
- Thermal Cycle (TC)/Humidity Freeze (HF): 50 TC cycles followed by 10 HF cycles. I-V measurements done prior to and after TC and once again at the conclusion of HF.
- Thermal Cycle: 200 cycles. I-V measurements done before and after testing.

S/N	Test Module Designate	Initial Electrical Parameters			
		V_{oc} (V)	I_{sc} (A)	P_{max} (W)	FF (%)
STR 0133	TC200	63.5	1.09	47.9	69.2
STR 0119	TC200	63.8	1.11	49.1	69.5
STR 0117	DH-A	63.7	1.07	47.3	69.3
STR 0114	DH-B	64.0	1.10	48.8	69.1
STR 0120	TC50/HF10	64.0	1.10	48.8	69.1
STR 0113	TC50/HF10	63.7	1.10	48.4	69.0

Table 20. Initial electrical parameters for a-Si modules prior to environmental exposure testing.

Results and Discussion

Tables 21 through 24 summarize the results from the environmental testing. In most test sequences, significant reductions were observed in maximum power (Pmax) and Fill Factor (FF). No electrical degradation was found after 50 TC.

From the test data, it appears that the module performance degradation could be due to an interaction between the PV device back contact and the encapsulant, although no interaction could be visually observed in previous tests.

In environmental conditions with and without moisture, module electrical properties were severely compromised. The modules must be further examined via chemical surface analysis to determine the exact failure mechanism occurring in the a-Si-based construction.

S/N	Test Module Designate	Electrical Parameters after 1000 hrs DH							
		V_{oc} (V)	Change (%)	I_{sc} (A)	Change (%)	P_{max} (W)	Change (%)	FF (%)	Change (%)
STR 0117	DH-A	62.4	-2.04	1.13	5.60	40.9	-13.53	57.9	-16.45
STR 0114	DH-B	62.8	-1.88	1.16	5.46	43.3	-11.27	59.1	-14.47

Table 21. Results after 1000 hours in damp-heat on a-Si modules.

S/N	Test Module Designate	Electrical Parameters after 50 TC/ Before 10 HF							
		V_{oc} (V)	Change (%)	I_{sc} (A)	Change (%)	P_{max} (W)	Change (%)	FF	Change (%)
STR 0120	TC50/HF10	64.1	0.16	1.10	0	48.8	0	69.1	0
STR 0113	TC50/HF10	63.9	0.31	1.08	-1.82	47.7	-1.45	69.0	0

Table 22. Results after 50 TC on a-Si modules.

S/N	Test Module Designate	Electrical Parameters after 10 HF							
		V_{oc} (V)	Change (%)	I_{sc} (A)	Change (%)	P_{max} (W)	Change (%)	FF	Change (%)
STR 0120	TC50/HF10	62.2	-2.81	1.14	3.64	42.2	-13.52	59.3	-14.18
STR 0113	TC50/HF10	62.1	-2.51	1.09	-0.91	39.8	-17.77	58.5	-15.22

Table 23. Results after 10 HF on a-Si modules.

CONCLUSIONS

Despite the positive initial results with the X125-37 encapsulant, full-blown electrical testing of modules going through specific environmental exposures showed that the formulation was not an effective thin-film-specific encapsulant. The mechanism responsible for the module degradation must be characterized to determine the exact shortcomings of the X125-37. Although this characterization is not part of the scope of this subcontract, subsequent work on the X125-37 and this specific material strategy should include and start with surface analysis of the above a-Si modules.

S/N	Test Module Designate	Electrical Parameters after 200 TC							
		V_{oc} (V)	Change (%)	I_{sc} (A)	Change (%)	P_{max} (W)	Change (%)	FF (%)	Change (%)
STR 0133	TC200	61.6	-2.99	1.18	8.26	42.4	-11.48	58.4	-15.97
STR 0119	TC200	62.7	-1.72	1.11	0	39.8	-18.94	56.9	-18.13

Table 24. Results after 200 TC on a-Si module.

REFERENCES

[1] A. Abete, F. Scapino, F. Sperino, R. Tommasini, " Ageing Effect on the Performance of A-SI Photovoltaic Modules in a Grid Connected System: Experimental Data and Simulation Results", IEEE 2000, 0-7803-5772-8/00.

[2] D.L. King, J.A. Kratochvil, W.E. Boyson, "Stabilization and Performance Characteristics of Commercial Amorphous-Silicon PV Modules," IEEE 2000, 07803-5772-8/00.

[3] C.R. Wronski, " Amorphous Silicon Photovoltaics: Order From Disorder," IEEE 2000, 0-7803-5772-8/00.

[4] D.L. King, J.A Kratochvil, W.E. Boyson," Stabilization and Performance Characteristics of Commercial Amorphous-Silicon PV Modules," Sandia National Laboratories, DOE contract DE-ACO4-94AL85000.

[5] M.A. Quintanna, et. al. , "Commonly Observed Degradation in Field-Aged Photovoltaic Modules," Report on DOE contract DE-AC04-94AL85000.

[6] C.R. Osterwald, "Accelerated Stress Testing of SnO_2:F Films on Soda-Lime Glass, Thin Film Module Reliability National Team Meeting, Golden CO, Sept 4, 2002.

[7] M.A. Quintana, D.L King, T.J. McMahon, C.R. Osterwald, " Commonly Observed Degradation in Field-Aged Photovotaic Modules", Sandia National Laboratories, Report from DOE Contract DE-AC-04-94AL85000.

[8] G Jorgensen, G. Barber, S. Glick, T. McMahon, "Measurements of Backsheet Moisture Permeation and Encapsulation-Substrate Adhesion.

[9] T.J. McMahon, G.J. Jorgensen, "Electrical Currents and Adhesion of Edge-Delete Regions of EVA-to-Glass module Packaging (pre-print), NCPV Program Review Meeting, Lakewood, CO 14-17 October 2001.

[10] G. Jorgensen, et. al., " Measurements of Backsheet Moisture Permeation and Encapsulant-Substrate Adhesion" , NCPV Program Review Meeting Lakewood, CO 14-17 October 2001.

[11] C.R. Osterwald, T.J. McMahon, and J.A. delCueto, " Electrochemical Corrosion of SnO2:F Transparent Conducting Layers in Thin Film Photovoltaic Modules", NREL Preprint, February 2002.

[12] G. Mon, L. Wen, J. Meyer, R. Ross Jr., A. Nelson," Electrochemical and Galvanic Corrosion Effects in Thin-Film Photovoltaic Modules" IEEE, 1988 document 0160-8371/88/0000-0108.

[13] M.A. Quintana, D.L. King, T.J. McMahon, and C.R. Osterwald, " Commonly Observed Degradation in Field-Aged Photovoltaic Modules", Sandia National Laboratories, Report from DOE Contract DE-AC-04-94AL85000.

[14] D.E. Carlson, "Accelerated Corrosion Testing of Tin Oxide Coated Glass'", BP Solar, Thin Film Module Reliability National Team Meeting, Golden CO, Sept 4, 2002.

[15] C.R. Osterwald, T.J. McMahon, and J.A. delCueto, " Electrochemical Corrosion of SnO2:F Transparent Conducting Layers in Thin Film Photovoltaic Modules", NREL Preprint, February 2002.

[16] N. G. Dhere, S. M. Bet, H. P. Patil, " High-Voltage Bias Testing of Thin-Film PV Modules," Proc. 3rd World Conference of Photovoltaic Energy Conversion (WCPVSEC-3), Osaka, Japan, May 12-16, 2003.

[17] N.G. Dhere, M.B. Pandit, A.H. Jahagirdar, et. al., " Overview of PV Module Durability and Long Term Exposure research at FSEC" , US DOE contract # DEFC0400AL66793H.

[18] H. Elgamel, " Overview of FSI Moisture Testing", First Solar, TFRMT Meeting, Golden CO, Sept 4, 2002.

[19] J. Wohlgemuth, "Validity of Damp Heat Testing," Thin Film Module Reliability National Team Meeting, Sept 4, 2002.

[20] S. Voss, "CIS Field Stability and Accelerated Environmental Testing," Thin Film Module Reliability National Team Meeting, Golden CO, Sept 4, 2002.

[21] B. Marion, " Field Occurrences of Humidity and Temperature," TFRMT Meeting, Golden CO, Sept 4, 2002.

[22] G. Jorgensen, et. al., "Adhesion after Damp Heat," TFRMT Meeting, Golden CO, Sept 4, 2002.

[23] G. Jorgensen, " Basics of Polymer Permeability", Moisture Ingress and High –Voltage Isolation Workshop, March 22, 2001.

[24] J. Wohlgemuth and H. Yu, " Advancing Encapsulation Technology to Achieve High Performance and Reliability," Moisture Ingression and High Voltage Isolation Symposium, Golden CO, March 22-23, 2001.

[25] E. Kanto, "Flexible Laminate Materials Laminate Materials Comparisons," Thin Film Module Reliability

National Team Meeting, Golden CO; Sept 4-5, 2002
[26] K. Terwilliger, G. Barber, G. Jorgensen," Water Vapor Transmission Rates (WVTR) of Soft Backsheets and EVA," Thin Film Module Reliability National Team Meeting, Golden CO: September 4-5, 2002.
[27] F. Mannarino, J. Coyne, R. Davis," Low MVTR Films and Coatings for Backsheets," Thin Film Module Reliability National Team Meeting, Golden, OC; Sept 4-5, 2002.
[28] K. Terwilliger, G. Barber, G. Jorgensen," Water Vapor Transmission Rates (WVTR) of Soft Backsheets and EVA," Thin Film Module Reliability National Team Meeting, Golden CO: September 4-5, 2002.
[29] F. Mannarino, J. Coyne, R. Davis," Low MVTR Films and Coatings for Backsheets," Thin Film Module Reliability National Team Meeting, Golden, OC; Sept 4-5, 2002.
[30] A.K. Plessing, P. Pertl, S. Degiampietro, A. Skringer, B. Erler, ' New Film Materials and RTD Activities," Thin Film Module Reliability National Team Meeting, Golden CO; September 4-5, 2002.
[31] F. Jeffrey, B. Scandrett, D. Grimmer, D. Peter, " Iowa Thin Film Technologies," Thin Film Module Reliability National Team Meeting, Golden CO, Sept 4-5, 2002.
[32] US Patent 6, 337,381, "Siloxane and Siloxane Derivatives as Encapsulants for Organic Light Emitting Devices," January 2002.
[33] US Pa6yttent 5,895,228, " Encapsulation of Organic Light Emitting Devices Using Siloxane or Siloxane- Derivatives" April 1999.
[34] US Patent 6,087,198, " Low Cost Packaging for Thin Film Resonators and Thin Film Resonator-Based Filters," July 2000.
[35] US Patent 5,831,759, "Electro-Optic Modulator with Passivation Layer," November 1998.
[36] US Patent 5,541,445, " High Performance Passivation for Semiconductor Devices", July 1996.
[37] US Patent 5,217,566, "Densifying and Polishing Glass Layers," June 1993.
[38] US Patent 6,531,565, " MVTR Resin produced with Post-Titanated Cr/Si/Ti Catalyst," March 2003.
[39] US Patent 6,346,581 " Modified Cycloolefin Addition Polymer and Curable Resin Composition Containing the Same," February 2002.
[40] US Patent 6,531,565 " MVTR Resin Produced with Post-Titanted CR/SI/Ti Catalyst, March 2003.
[41] US Patent 6,524,720 " Moisture Barrier Film", February 2003.
[42] US Patent 6,403,231, " Thermoplastic Film Structures Having Improved Barrier and Mechanical Properties", June 2002.
[43] US Patent 6,403,222, " Wax-modified Thermosettable Compositions," June 2002.
[44] US Patent 6,524,720, "Moisture Barrier Film," February 2003.
[45] M.K. Akkapeddi, et. al., "Miscible Blends of Nylon 6 and TDAI, an Oligomeric Aromatic Nylon, with Improved Melt Flow and Moisture Resistance Properties," Product literature AlliedSignal Inc, 2003.
[46] W.W. Yau, D. Gillespie, " A TRISEC and 3DTREF Approach to Polymer Blend Design," Product Literature, Chevron Chemical Company LLC, 2003.
[47] US Patent 6,395,856 " Silicone Oligomers and Curable Compositions Containing Same," May 2002.
[48] Symmorphix Literature, " Wide-Are PVD Process for 'Symmorphous' metal Oxide 85/85 Barrier Film Applications'" presented at Thin Film Module Reliability National Team Meeting, Golden CO, Sept 4-5, 2002.
[49] P.E. Burrows, G.L. Graaff, M.E. Gross, et, al, " Gas Permeation and Lifetime Tests on Polymer-Based Barrier Coatings" SPIE Annual Meeting, August 30 , 2000.
[50] P.E. Burrows, M.S Weaver et.al.,"Plastic Organic Light Emitting Displays", Research report, Universal Display Corporation, Ewing, NJ partially funded by Battelle Memorial Institute, Vitex Systems, and DARPA, www.vitexsystems.com 2003.
[51] A. Sharma, H. Jain, A.C. Miller, "Surface Modification of a Silicate Glass During XPS Experiments," Surface and Interface Analysis 2001; 31 369-374.
[52] http://WWW.nes.coventry.ac.UK/research/cmbe/225che6.htm, " 225 CHE Solid-State Inorganic Chemistry."
[53] G. Little, " Moisture Ingress Workshop," Moisture Ingress and High-Voltage Isolation Workshop, March 22, 2001.
[54] C. Cording, " Bringing Innovation to Glass Technology," Moisture Ingression Workshop, September 4-5, 2003.
[55] N.G. Dhere, N.R. Raravikar, A. Mikonowicz, C. Cording, " Effect of Glass Sodium Content on Adhesional Strength of PV Modules," Proc. 29th IEEE Photovoltaic Specialists' Conference, New Orleans, LA, May 2002.

[56] D.M. Dobkin, " Gettering and Transport of Mobile Ion Contamination", http://www .batnet.com /enigmatics / semiconductor_processing /selected_shorts/Gettering.html.
[57] G.L. Schnable, R.B. Comizzoli, W. Kern, L.K. White, " A Survey of Corrosion Failure Mechanisms in Microelectronic Devices," RCA Review, Vol . 40 December 1979.
[58] D. Ast, et.al., " Low-Cost Glass and Glass-Ceramic Substrates for Thin-Film Silicon Solar Cells," NREL Final Subcontract Report, January 25, 2001.
[59] K. W. Jansen, A.E. Delahoy, " A Laboratory Technique for the Evaluation of Electrochemical Transparent Conductive Oxide Delamination from Glass Substrates," Thin Solid Films 423, 2003 153-160.
[60] G.L. Schnable, R.B. Comizzoli, W. Kern, L.K. White, " A Survey of Corrosion Failure Mechanisms in Microelectronic Devices," RCA Review, Vol . 40 December 1979.
[61] Amorphous Silicon Solar Cells: Efficiency and Stability Issues, Pouya Valizadeh, Electrical Engineering and Computer Science Department, University of Michigan, Course report of EECS512 (Amorphous semiconductors): Fall 2001.
[62] TrueSeal, PIB Insulating Glass Sealant Technical Data Sheet, F-8047E 02/02.
[63] K. Shas, et.al. , "Gas Permeability and Medical Film Products," Medical Plastics and Biomaterials Magazine, September 1998.
[64] Eval Company of America, Technical Bulletin No.110 , Rev. 07-00.
[65] B. Lipsitt, " Metallocene Polyethylene Films as Alternatives to Flexible PVC for Medical Device Fabrication", Medical Plastics and Biomaterials Magazine, September 1997.
[66] D. Zagory, "An Update on Modified Atmosphere Packaging of Fresh Produce," Packaging International 117, April 1998.
[67] Plastics for Barrier Packaging, Business Communications Co., Inc., September 2000.
[68] J.I. Hanoka, " Advanced Polymer PV System," Evergreen Solar, Inc. NREL PVMaT 4A1 Final Report, September 1995-December 1997.
[69] H. Schmidhuber, k. Krannich, " Why Using EVA for Module Encapsulation if there is a Much Better Choice?" 17th European Photovoltaic Solar Energy Conference and Exhibition, Munich 2001.
[70] G. Nisato, P.C.P Bouten, P.J. Slikkerveer, et. al. " Evaluating High Performance Diffusion Barriers: the Calcium Test", Vitex Systems Web Site 2003.
[71] R.T. Tucker, "Results to Date: Development of a Low-temperature, Super Fast-cure Encapsulant," 20th European Photovoltaic Solar Energy Conference, Barcelona, Spain, 2005.
[72] P. Klemchuk, M. Ezrin, G. Lavigne, W. Holley, J. Galica, S. Agro, "Investigation of the Degradation and Stabilization of EVA-based Encapsulants in Field-aged Solar Energy Modules," Polymer Degradation and Stability, 55 (1997) 347-365.

REPORT DOCUMENTATION PAGE

Form Approved
OMB No. 0704-0188

PLEASE DO NOT RETURN YOUR FORM TO THE ABOVE ORGANIZATION.

1. REPORT DATE *(DD-MM-YYYY)*	2. REPORT TYPE	3. DATES COVERED *(From - To)*
April 2008	Subcontract Report	22 Oct 2002 - 15 Nov 2007

4. TITLE AND SUBTITLE
Development of New Low-Cost, High-Performance, PV Module Encapsulant/Packaging Materials: Final Technical Progress Report, 22 October 2002 - 15 November 2007

5a. CONTRACT NUMBER
DE-AC36-99-GO10337

5b. GRANT NUMBER

5c. PROGRAM ELEMENT NUMBER

6. AUTHOR(S)
R. Tucker

5d. PROJECT NUMBER
NREL/SR-520-43019

5e. TASK NUMBER
PVB75301

5f. WORK UNIT NUMBER

7. PERFORMING ORGANIZATION NAME(S) AND ADDRESS(ES)
Specialized Technology Resources, Inc.
Enfield, CT 06082

8. PERFORMING ORGANIZATION REPORT NUMBER
ZDO-2-30628-10

9. SPONSORING/MONITORING AGENCY NAME(S) AND ADDRESS(ES)
National Renewable Energy Laboratory
1617 Cole Blvd.
Golden, CO 80401-3393

10. SPONSOR/MONITOR'S ACRONYM(S)
NREL

11. SPONSORING/MONITORING AGENCY REPORT NUMBER
NREL/SR-520-43019

12. DISTRIBUTION AVAILABILITY STATEMENT
National Technical Information Service
U.S. Department of Commerce
5285 Port Royal Road
Springfield, VA 22161

13. SUPPLEMENTARY NOTES
NREL Technical Monitor: Brian Keyes

14. ABSTRACT *(Maximum 200 Words)*

The primary objectives of this subcontract were to work with U.S.-based photovoltaic (PV) module manufacturers representing crystalline silicon, amorphous silicon, copper indium diselenide (CIS), and other state-of-the-art thin-film technologies to develop and qualify new low-cost, high-performance PV module encapsulant/packaging materials, as well as the module production processes that use the packaging materials. The manufacturers assisted in identifying candidate materials' deficiencies while undergoing development, and then ultimately in the qualification of the final, optimized materials designed to specifically meet their requirements. Upon completion of this program, new low-cost, high-performance PV module encapsulant/packaging materials were qualified, by one or more end-users, for their specific application. This document reports on progress toward these objectives and goals for the second phase of the three-phase subcontract.

15. SUBJECT TERMS
PV; crystalline silicon; amorphous silicon, copper indium diselenide (CIS); manufacturer; module; thin-film; solar cell; low cost; high performance; encapsulant/packaging materials; qualification;

16. SECURITY CLASSIFICATION OF:			17. LIMITATION OF ABSTRACT	18. NUMBER OF PAGES	19a. NAME OF RESPONSIBLE PERSON
a. REPORT	b. ABSTRACT	c. THIS PAGE			19b. TELEPHONE NUMBER (*Include area code*)
Unclassified	Unclassified	Unclassified	UL		